NTNU – Trondheim
Norwegian University of
Science and Technology

Comparison of conversion pathways for lignocellulosic biomass to biofuel in Mid-Norway

Heidi Ødegård Berg

Master of Energy and Environmental Engineering
Submission date: June 2013
Supervisor: Terese Løvås, EPT
Co-supervisor: Arne Fredrik Lånke, Rambøll Energi
Rajesh S. Kempegowda, EPT

Norwegian University of Science and Technology
Department of Energy and Process Engineering

NTNU

Norwegian University
of Science and Technology

Department of Energy
and Process Engineering

EPT-M-2013-19

MASTER THESIS

for

Stud.techn. Heidi Ødegård Berg

Spring 2013

Comparison of conversion pathways for lignocellulosic bio mass to bio fuel in Mid-Norway

Komparativ studie av konverteringsprosesser for lignocellulosisk biomasse til biodrivstoff i Midt-Norge

Background and objective

Biogas production from organic waste has a great potential both as a waste management strategy and as an energy source. Biogas can be used for both electricity production and as fuel for the transport sector. The end use of the biogas determines the final composition of the gas and sets certain demands to both the production process and the composition of the organic source. Biogas can be produced from many rather different types of sources; agricultural waste, domestic waste, waste from food industry, sewage sludge etc. Furthermore, biomass can be converted into gas by biological processes such as anaerobic digestion or by thermochemical processes such as gasification.

The purpose of the master thesis is to investigate and compare two conversion pathways for bio mass to energy in the shape of liquid bio gas. In both scenarios, end use takes place in the transport sector. Two possible pathways are

1 Anaerobic co-treatment of lignocellulosic bio mass with regionally abundant and favorable raw materials, followed by conversion to liquid bio gas
2 Thermochemical gasification of lignocellulosic bio mass, followed by conversion to liquid bio gas

The following tasks are to be considered:

1 Briefly describe existing and possible future value chains for lignocellulosic raw materials and waste products in Mid-Norway. Define a realistic market scenario and a corresponding estimate of available bio mass resources.
2 Describe the conversion pathways
3 Estimate plant size based on the defined market scenario and knowledge of cost aspects
4 Calculate and illustrate the energy flow
5 Roughly estimate production cost
6 Briefly discuss possible bi-products from each process and their markets
7 Discuss pros and cons of the processes

-- ” --

Within 14 days of receiving the written text on the master thesis, the candidate shall submit a research plan for his project to the department.

When the thesis is evaluated, emphasis is put on processing of the results, and that they are presented in tabular and/or graphic form in a clear manner, and that they are analyzed carefully.

The thesis should be formulated as a research report with summary both in English and Norwegian, conclusion, literature references, table of contents etc. During the preparation of the text, the candidate should make an effort to produce a well-structured and easily readable report. In order to ease the evaluation of the thesis, it is important that the cross-references are correct. In the making of the report, strong emphasis should be placed on both a thorough discussion of the results and an orderly presentation.

The candidate is requested to initiate and keep close contact with his/her academic supervisor(s) throughout the working period. The candidate must follow the rules and regulations of NTNU as well as passive directions given by the Department of Energy and Process Engineering.

Risk assessment of the candidate's work shall be carried out according to the department's procedures. The risk assessment must be documented and included as part of the final report. Events related to the candidate's work adversely affecting the health, safety or security, must be documented and included as part of the final report. If the documentation on risk assessment represents a large number of pages, the full version is to be submitted electronically to the supervisor and an excerpt is included in the report.

Pursuant to "Regulations concerning the supplementary provisions to the technology study program/Master of Science" at NTNU §20, the Department reserves the permission to utilize all the results and data for teaching and research purposes as well as in future publications.

The final report is to be submitted digitally in DAIM. An executive summary of the thesis including title, student's name, supervisor's name, year, department name, and NTNU's logo and name, shall be submitted to the department as a separate pdf file. Based on an agreement with the supervisor, the final report and other material and documents may be given to the supervisor in digital format.

☐ Work to be done in lab (Water power lab, Fluids engineering lab, Thermal engineering lab)
☐ Field work

Department of Energy and Process Engineering, 14. January 2013

Olav Bolland
Department Head

Terese Løvås
Academic Supervisor

Research Advisors: Arne Fredrik Lanke, Rambøll A/S, Trondheim

Preface

This master thesis was designed in collaboration with Rambøll Energi and is part of the Sintef Gasbio project. It has been written at the department of Energy and Process Engineering (EPT) at the Norwegian University of Science and Technology (NTNU) in Trondheim, Norway.

I would like to give special thanks to my advisor Terese Løvås for the continuous support and encouragement. I will also thank my co-advisor Arne-Fredrik Lånke for giving me the opportunity to participate on conferences and seminars relevant for my work, and my second co-advisor Rajesh S. Kempegowda for taking time of his schedule to sit down with me to give explanations or to share his point of view.

I would also like to give thanks to Anders Kiær for helping me with proof reading and for contributing to rewarding discussions.

I would like to thank my family and friends for their continuous support throughout my studies.

10.06. 2013, Trondheim Norway.

Heidi Ødegård Berg

Abstract

This work investigates one biochemical and one thermochemical biomass-to-liquid biofuel conversion pathway in terms of lignocellulose conversion to liquid Fischer-Tropsch diesel. The focus has been on comparing the two conversion pathways in terms of identifying their energy flows and respective feed to fuel ratios. The conversion pathways investigated comprise two-stage conversion sequences including biomass-to-gas conversion and gas-to-liquid conversion, exerted by anaerobic digestion or gasification followed by Fischer-Tropsch synthesis.

A systematic documentation of available technologies regarding the two conversion pathways is performed by literature study. The pathways are modeled in Aspen Plus supplied with FORTRAN declarations. Mass flows and composition for the two pathways are collected from simulations and energy flows are identified by heating value and energy balance calculations. The energy flows are presented graphically and by ESankey-diagrams, and the resulting energy utilities and feed to fuel ratios are presented graphically and in tabular form.

The key finding is that for the application to Fischer-Tropsch processes, the biochemical conversion pathway is less energy effective in terms of gas-to-liquid conversion. This result is observed both in terms of energy utility for the pathway and might indicate that biochemical pathways are more energy consuming than conventional thermochemical gas-to-liquid conversion. However, results on feed to fuel ratio indicate that the biochemical conversion of lignocellulose to Fischer-Tropsch diesel is competitive when compared to thermochemical conversion.

Sammendrag

I denne studien har to systemer for henholdsvis biokjemisk og termokjemisk omdannelse av biomasse til flytende biodrivstoff i form av lignocellulose-til-Fischer-Tropsch diesel blitt sammenlignet. Hovedfokus er rettet mot å identifisere energistrøm gjennom de to systemene og å evaluere energiutnyttelsen av biomassen i det ferdige biodrivstoffproduktet. De to systemene som har blitt undersøkt er to-trinns omdannelses-systemer. Trinn en består av ett biomasse-til-gasstrinn som utføres med anaerob utråtning for biokjemisk system og gasifisering for termokjemisk system. Trinn to utgjør gass-til-flytende biodrivstoff og består av Fischer-Tropsch syntese for begge systemer.

En systematisk kartlegging av aktuell teknologi for de to systemene er blitt utført ved hjelp av et litteraturstudium. For system-modelleringer har programvaren Aspen Plus blitt brukt. Enkelte beregninger gjort i programvaren er supplert med deklarasjoner skrevet i FORTRAN. Massestrømmer og deres komposisjon er samlet inn fra simuleringer gjort i Aspen Plus, og disse er blitt benyttet i brennverdi og energistrømberegninger. Energistrøm for de to systemene er presentert grafisk og i ESankey-diagrammer. Brennverdier og energiutnyttelse er presentert grafisk og ved hjelp av tabeller.

De viktigste resultatene er at det biokjemiske systemet er mindre energieffektivt når det gjelder gass-til-flytende omdanning. Dette resultatet er hentet fra energistrømanalysen for systemet og gir en mulig indikasjon på at det biokjemiske systemet er mer energikrevende enn konvensjonelle termokjemiske systemer når det gjelder gass-til-flytende omdanning. På den annen side indikerer resultatene for energiutnyttelse at den biokjemiske omdannelsen av lignocellulose til flytende Fischer-Tropsch diesel er konkurransedyktig satt opp mot konvensjonell termokjemisk omdannelse.

Table of Contents

Appendix

List of Figures

Appendix

List of Tables

Appendix

1. Introduction

It is of great concern that the environment in which we sustain our way of living is subject to abnormal change. The impetus of these climatic changes is the tremendous discharge of carbon dioxide related to human activities, involving the exploitation of fossil fuels, of which a large fraction is related to the transport sector. A part of the solution to a reduction in the discharge of climatic gases could be the transition from fossil fuel utilization into biofuel utilization. *Biofuel* is the term denoted to liquid or gaseous fuels derived from biomass and comprise fuels like biogas, bioethanol and biodiesel, and a transition from fossil fuels to biofuels is assumed to reduce emissions of climatic gases immediately. To achieve such a transition in Norway one must ensure to make biofuels publicly available and, moreover, the vehicle fleet must be able to utilize biofuels.

The biofuel production and distribution is still on the threshold to commercial application both on national and international levels. In Norway there are no established bio refineries devoted solely to biofuel production today, but the commercial interest is there. On the demand side, Avinor is currently investigating the possibility to transform Norway`s airplane fleet into using biofuels as a jet fuel, and a report on the issue was recently published. On the supply side, Biokraft AS is a pioneer company established in the region of Mid-Norway that plans to produce biogas from locally available biomass resources with the intention to upgrade it to biofuel. The company has been on the threshold to implementation for several years, but has been facing challenges that delay their plant start-up. One of the major challenges related to the implementation of bio refineries on a large scale is the economic considerations related to them. Economical sustainability is vital for the startup of biofuel production projects. The economic sustainability is related to the maturity of relevant technology applied to the plant, the energy utilization of the plant and a stabile demand for the plant end product. Satisfactory energy utilization is linked to good biofuel production plant energy efficiency and a high quality biofuel product.

This work aims to address the energy utility of two biomass-to-biofuel conversion pathways and to compare them with respect to biofuel calorific value, energy conversion, energy demand and energy losses. The work is restricted to address the use of lignocelluloses as biomass feedstock and Fischer-Tropsch diesel as biofuel end product. System one comprises an anaerobic treatment of lignocellulosic biomass followed by conversion to liquid Fischer-Tropsch Diesel and system two comprises fluidized bed gasification of lignocellulosic biomass followed by conversion to liquid Fischer-Tropsch Diesel. The conversion systems include 5 sub processes each that are identified in this work. They consist of biomass pretreatment, anaerobic digestion, biomass gasification, gas conditioning and Fischer-Tropsch synthesis. A theoretical study of different technologies available for these processes is performed, and the systems design is based on this study. The two pathways are modeled in Aspen Plus simulation software supplied with FORTRAN declarations, and necessary operation data are obtained from theoretical studies. Mass flows for the two systems are collected

from simulations and energy flows are identified by heating value and energy balance calculations performed in excel. The energy flows are presented in ESankey-diagrams. Heating values and energy utility are presented graphically and in tabular form.

This work is limited to evaluate the utilization of lignocellulosic biomass in the production of Fischer-Tropsch Biodiesel. The energy flow is limited to identify the energy contained in mass flows and is based on a simple conservation of energy principle. Thermal energy flows and exergy is not taken into consideration. The Aspen Plus models are simplified expressions of complicated process systems and may produce results that differ from energy flows and biofuel calorific values obtained in actual bio refineries. The access to relevant operation parameters is limited for some parts of the system, and this may result in uncertainty in the accuracy on results obtained.

In chapter 2 the lignocellulosic biomass is presented as a biomass feedstock denoted to biofuel production. Important biomass characteristics that affect the utilization of the feedstock in biofuel conversion systems are emphasized. In chapter 3 a general biomass-to-biofuel conversion is presented and the chapter includes a theoretical study of anaerobic digestion and gasification technologies. Chapter 4 includes a theoretical study of biomass pretreatment, gas conditioning and the Fischer-Tropsch conversion process. Chapter 5 introduces and explains the model setup in Aspen Plus, and chapter 6 presents the results from simulations performed in Aspen Plus. Chapter 7 analyses the results obtained and chapter 8 gives a conclusive remark and suggestions regarding further work.

2. The Biomass Feedstock: Lignocellulose

Biomass constitutes plant material derived from the reaction between carbon dioxide, water and sunlight to produce carbohydrates via photosynthesis. The solar energy driving the photosynthesis is stored in the chemical bonds of the biomass components. By applying efficient biochemical or thermochemical processing of the biomass, the energy product can be utilized, producing carbon dioxide and water (McKendry, 2001). The term biomass has been used to describe any material of recent biological origin by different sources (Crofcheck, 2010), and has been claimed to be the most profitable renewable energy source after hydropower, with respect to total energy and carbon reduction costs. Biomass can be generated from both natural and anthropogenic sources and comprises natural constituents originated from growing land-and water based vegetation produced by photosynthesis or processed by animal and human food digestion. Biomass can also be anthropogenic products derived from processing of the above natural constituents (Tran, 2012).

Biofuel is the term denoted to solid, liquid or gaseous fuels derived from biomass. Today, the most integrated biofuel is bioethanol derived from energy crops, as its properties make it possible to blend bioethanol into commercial fossil fuels. However, the sustainability of using energy crops as a feedstock has been put up to question because it competes with arable land for food production. An alternative to biofuel production from energy crops are the use of a woody biomass feedstock commercially known as lignocellulose. The lignocellulose can be processed biochemical or thermochemical, generating a product that can be converted into biofuels (S. van Loo, 2008). The use of lignocellulose as a feedstock is eliminating some of the major issues of bioethanol production because woody materials derived from woodlands like forests do not compete with aerable land for food production.

Lignocellulose Definition

Lignocellulosic biomass includes plants with high fiber content (Crofcheck, 2010). They consist mainly of cellulose, hemicellulose and lignin, and some inorganic materials and extractives. Lignocellulosic biomass includes (McKendry, 2001):

- Woody material (hardwoods like birch and softwoods like spruce and pine)
- Herbaceous material (grass and straw)
- Aquatic plants (microalgae, macroalgae)
- Manure (cattle, pig, poultry)

The choice of plant species to be converted into liquid biofuels depends upon the regional availability, storage and transportation costs related to them. The composition of lignocellulose is a

determining factor when identifying the suitability of application to different biofuel process technologies.

Lignocellulose Composition

Lignocellulose is made up of three different substances, namely cellulose, hemicellulose and lignin. In addition trace elements like potassium and sodium are present. The composition of the lignocellulosic material varies between the species and affects the properties of the lignocellulosic material. Cellulose is a linear polysaccharide polymer of glucose ($C_6H_{12}O_6$) (Crofcheck, 2010). It is the main constituent of most lignocellulosic material and the organic compound most abundant on the planet Earth. Cellulose represents 40-45% of the dry weight of wood. Hemicellulose consists of various sugars other than glucose that encloses the cellulose fibers and represents 20-35% of the dry weight of wood. Lignin is a complex amorphous non-sugar polymer with high molecular mass that gives strength to the wood-fiber. It accounts for 15-30% of the dry weight of wood (Tran, 2012), (M. Crocker, 2012). Typical lignin, hemicellulose and cellulose composition for wood, straw and grass biomass feedstock are given in Table 2-1.

The distribution of these constituents, especially cellulose and lignin, are determining factors when evaluating the biomass suitability of application to biofuel conversion. The complexity of lignin makes it unsuitable for some biochemical process technologies because lignin is not easily decomposed. Also hemicellulose may promote problems for biochemical conversion processes. It can, however, be converted by applying a thermochemical conversion process. However, pretreatment technologies applied prior to the anaerobic digestion break down hemicellulose and make the glucose available for anaerobic microorganisms as will be seen in chapter 4.1.

Biomass Feedstock		Lignin (%)	Cellulose (%)	Hemi-cellulose (%)
Wood	Hardwood	27-30	35-40	25-30
	Softwood	20-25	45-50	20-25
Straw	Wheat Straw	15-20	33-40	20-25
Grass	Switchgrass	5-20	30-50	10-40

Table 2-1: General Lignin, Cellulose and Hemicellulose composition for wood, straw and grass biomass feedstock (McKendry 2001).

Lignocellulose Properties

During biochemical and thermochemical biomass processing, particular material properties are of interest to us because they affect the utility of the processing. From literature review of two recent works written by Mc Kendry (McKendry, 2002) and C. Crofcheck (Crofcheck, 2010) it is found that the most important material properties constitute:

- Moisture content
- The calorific value (CV)
- Fixed Carbon and volatiles proportions
- Ash/residue content
- Alkali metal concentration
- Cellulose/lignin ratio

The properties listed above vary between different lignocellulosic species and must be analyzed separately for each species. The biomass feedstock composition analyzed in terms of volatile content, fixed carbon, ash and moisture is called the *proximate analysis*, whereas an analysis of the vol-% of carbon, hydrogen, oxygen, nitrogen and sulfur compounds is called the *ultimate analysis* (Tran, 2012). The proximate and ultimate analysis is used to investigate the biomass feedstock suitability as a biofuel and is illustrated for three types of lignocellulosic biomass feedstock in Table 2-2.

		Proximate analysis					Ultimate analysis						
Biomass Feedstock		Moisture (%)	VM (%)	FC (%)	Ash (%)	LHV ($MJkg^{-1}$)	C (wt%)	H (wt%)	O (wt%)	N (wt%)	S (wt%)	Alkali metals (K, Na) (%)	Source
Wood	Hardwood	20	82	17	1	18,6	51,6	6,3	41,5	0,0	0,1	4,8	P. McKendry, 2001
	Softwood	20	82	17	1	18,6	51,6	6,3	41,5	0,0	0,1	-	P. McKendry, 2001
Straw	Wheat Straw	16	59	21	4	17,3	48,5	5,5	3,9	0,3	0,1	11,8	P. McKendry, 2001
	Barley Straw	30	46	18	6	16,1	45,7	6,1	38,3	0,4	0,1	11,8	P. McKendry, 2001
Grass	Switchgrass	0	73,75	21,57	5,76	-	47,27	5,31	41,59	0,51	-	-	C. Crofcheck, 2010

Table 2-2: General Proximate and Ultimate analysis for wood, straw and grass biomass feedstock (P. McKendry 2011, C. Crofcheck 2010).

Table 2-2 illustrates that the biomass characteristics vary among different species of lignocellulose. The columns represent wood properties and the rows represent different lignocellulosic species and will be commented in the last section of chapter 2. The relative importance of the different properties varies to some extent with different conversion technologies applied. Therefore, also the cellulose-to-lignin ratio is listed above. This ratio becomes important when biochemical processes like fermentation or anaerobic digestion is applied to the biomass. The reason why is that these processes are unable to decompose lignin, implying that a low cellulose-to-lignin ratio means a low decomposition rate of the material. This issue will be further evaluated in chapter 3. In the following sections, the properties evaluated in proximate analysis as listed above are explained and

evaluated in separate sections. One section at the end is devoted to ultimate analysis consideration.

Moisture Content

Some biomass-to-biofuel conversion processes are sensible to biomass moisture content. Biomass gasification processes for example require a biomass feedstock with moisture content of 10 to 15 vol-% to operate efficiently, as will be discussed in chapter 6.2. Thus, the biomass moisture content is a measure of interest and can be divided into two types. These are the *intrinsic* moisture content, describing the biomass moisture content without the influence of weather condition effects, and the *extrinsic* moisture content describing the influence of weather conditions during biomass harvest on the biomass moisture content (McKendry, 2001). Of highest interest is the real moisture content of the biomass, thus taking the extrinsic moisture into consideration. Raw biomass feedstock may contain approximately 50 vol-% of moisture. In order to reduce the moisture content drying pretreatment must be applied to the biomass prior to conversion processes like gasification (McKendry, 2001). Different types of pretreatment processes will be identified in chapter 4.

Heating Value

In this work the conversion pathways for two different cases will be analyzed in terms of energy. The energy will be measured in terms of heating value. The *calorific value* (CV) of a material is a measurement of the energy content released when the material is combusted in air. It can be expressed in two forms, either as the higher heating value (HHV), which corresponds to the gross calorific value (GV) of the material, or as the lower heating value (LHV), which corresponds to of the net calorific value (NCV) of the material. The HHV represents the total amount of energy released when the biomass is combusted in air. It includes the latent heat contained in the biomass moisture, usually present as water vapor, and is thus representing the maximum amount of energy that is potentially recoverable from the biomass. The LHV also represents the total amount of energy released when the biomass is combusted in air, but without taking into consideration the latent heat contained in the water vapor. The latent heat contained in the biomass cannot be used efficiently and the LHV is the preferred definition to use (McKendry, 2001). It will be used as a measure of fuel energy content throughout this work.

Proportions of fixed carbon and volatile matter

In addition to the heating value it is of interest to know the composition of the biomass feedstock. The chemical energy stored in the biomass can be measured by two properties, namely the *fixed carbon* and the biomass *volatile matter* content. The volatile matter content (VM) of the biomass is the proportion driven off as a gas, per definition by heating to 950 ^{o}C for 7 min. The fixed carbon content (FC) is the material remaining after the volatiles are released, without taking ashes into consideration. The FC and the VM is used to predict the theoretical energy yields obtainable by converting the biomass into useful energy. (McKendry, 2001). It is an important concept to keep in

mind when the gasification technologies are introduced in chapter 3. The concept is further being used in chapter 5, where the plant models developed in Aspen Plus are presented.

Ash and alkali metal content

The ash and alkali content are non-volatile fractions of the biomass other than fixed carbon (char). It tends to deposit on process equipment walls or appear as small particulates in gas phases. At high temperature it can also melt and stick to char and un-combusted volatile matter forming clusters of material that may damage or prevent process equipment from proper operation, which is often referred to as *agglomeration* in biomass processing literature (McKendry, 2002). As such, high contents of alkalis and ash is not wanted in our biomass feedstock.

Ultimate Analysis

The *ultimate analysis* of the lignocellulose gives information about the carbon, hydrogen, oxygen, nitrogen and sulfur content of the species, which is the main components that the biomass is made up of. In this work the ultimate analysis is used to predict the gas yield and composition of the product gas obtained from gasification process. The issue is evaluated further in chapter 5.

Birch as a Biofuel Production Feedstock

Table 2-2 above illustrates that wood in general contain more volatile matter and less ash and alkalis than straw and grass , here not taking algae and manure into consideration. The general net calorific value (LHV) is higher for wood species compared to straw and grass, and wood is therefore an interesting option for application to biofuel conversion. Recall that biomass composition in terms of cellulose, hemicellulose and lignin is important characteristics of the wood as a biofuel production feedstock, and that especially small amount of lignin is preferable for some processes. Table 2-1 above shows that the biomass composition in terms of these compounds varies between hardwoods and softwoods. *Softwood* species are evergreen trees like spruce and pine, whereas *hardwood* species are seasonal trees like birch and oak. There is a tendency towards the larger distribution of cellulose and less lignin for the softwood species compared to the hardwood species in Table 2-1, although the difference is small. However, testing of softwood and hardwood species in both thermochemical and biochemical processes for liquid biofuel conversion performed by R. Gonzalez et.al and T.D. Foust et.al indicates the opposite. R. Gonzalez et.al states that thermochemical processes can process almost any wood species, and that the restrictive process is the biochemical one (R. Gonzalez, 2011). T.D. Foust et.al suggests that hardwood species are more suited for biochemical pathways because of more stable overall conditions.(T.D.Foust, 2009). In Mid-Norway, one of the most usual hardwood species is birch. It is not harvested for other purposes than firewood and is assumed to have a good potential as a biomass feedstock for biofuel production in the region (Lånke, 2013). For these reasons it is chosen as the biomass feedstock input for both biochemical and thermochemical pathways. Table 2-3 presents the birch wood characteristics in terms of proximate analysis.

	Proximate analysis					Ultimate analysis					
Biomass Feedstock	Moisture (%)	VM (%)	FC (%)	Ash (%)	LHV ($MJkg^{-1}$)	C (wt%)	H (wt%)	O (wt%)	N (wt%)	S (wt%)	Alkali metals (K, Na)
Birch	22.00	10.35	89.43	0.22	14.83	43.62	6.34	44.9	0.09	0.05	-

Table 2-3: Proximate and Ultimate Analysis of Birch species (Kempegowda 2013).

The data is obtained from a research performed by post doc R.S. Kempegowda and used in the models developed in chapter 5 (Kempegowda, 2013).

3. Introduction to Biochemical and Thermochemical Conversion

Biomass can be converted into useful energy carriers like biofuels by many different conversion pathways, and only two of them are considered in this work. Both follow the general conversion pathway as described in Figure 3-1 below.

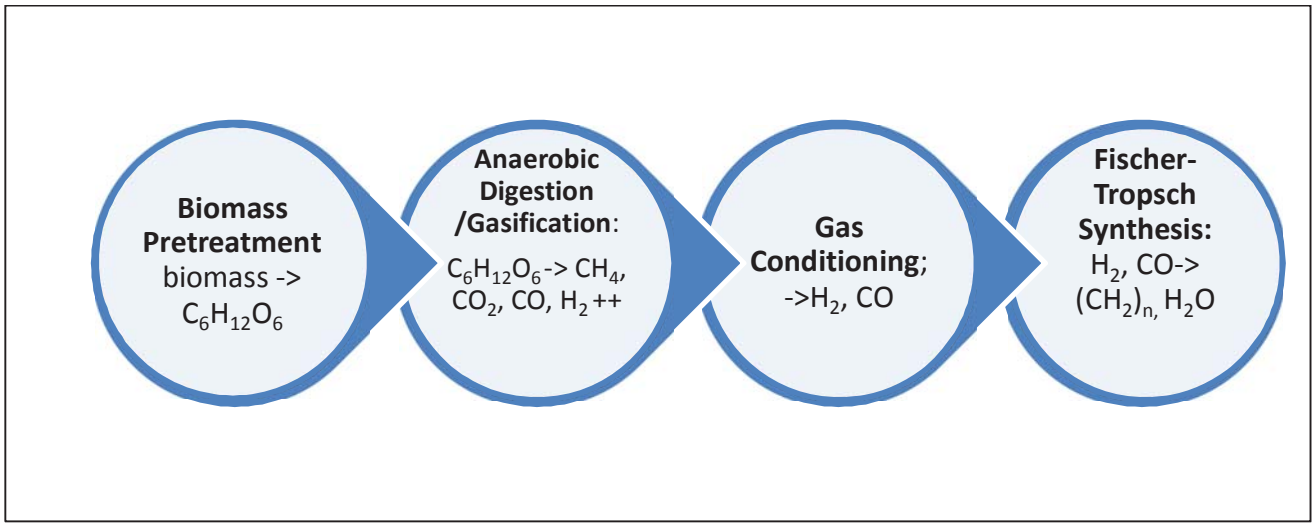

Figure 3-1: Conversion Pathway, biomass to liquid biofuel via Fischer Tropsch synthesis.

Figure 3-1 illustrates that the production of liquid biofuels involves several steps. The energy content in the biomass must be made available to the gas conversion process in order to optimize gas conversion. This done by biomass pretreatment represented by the first box in Figure 3-1, which convert biomass into simple sugars ($C_6H_{12}O_6$). The biomass is thereafter converted to a gas represented by the second box in Figure 3-1. Before the gas can be converted into liquid biofuel, it must keep syngas standard, meaning that it must consist of only hydrogen (H_2) and carbon monoxide (CO). Therefore, gas conditioning, represented by the third box must be applied to the gas before Fischer-Tropsch synthesis converts it to the liquid Fischer-Tropsch diesel $(CH_2)_n$ and water, represented by the fourth box in the figure. The second and fourth boxes are representing the main processes of the two conversion pathways and the second box will be given most emphasis in this work.

This work investigates one biochemical and one thermochemical conversion pathway. *Biochemical* conversion describes the decomposition of biomass by microorganisms or enzymes into simple sugars and acids. In this work the biochemical conversion pathway is represented by anaerobic digestion for production of methane-rich biogas. *Thermochemical* conversion describes the thermal degradation of biomass and includes pyrolysis, liquefaction, combustion and gasification (S. van

Loo, 2008). In this work, the gasification technology is chosen as the thermochemical conversion pathway.

The general biochemical or thermochemical conversion pathways consists of five process steps, namely a biomass pretreatment process, a biomass-to-gas conversion process (anaerobic digestion or gasification), a gas cleaning process, a gas upgrading process and a the Fischer-Tropsch synthesis (gas-to-liquid process in Figure 3-2). The general biomass-to-biofuel conversion plant is illustrated in Figure 3-2.

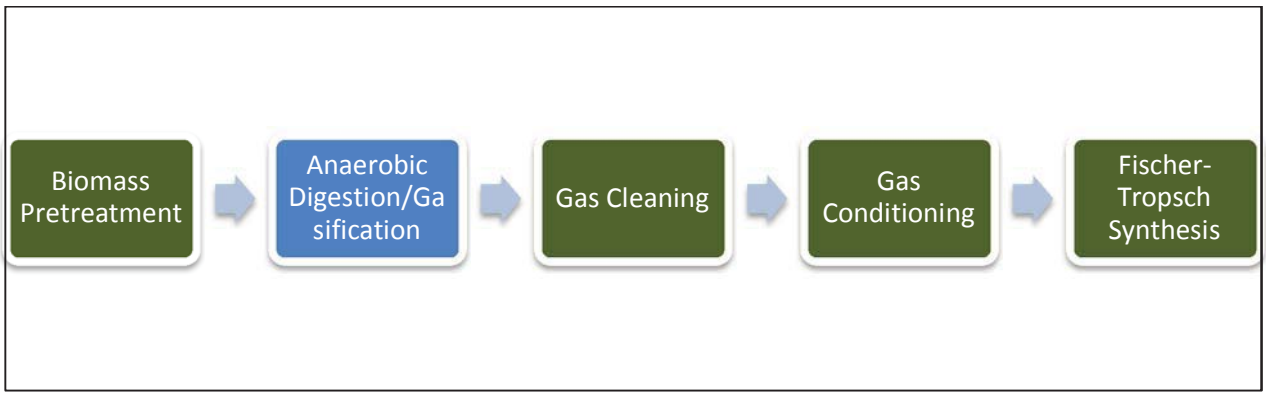

Figure 3-2: The General Biomass-to-biofuel Conversion Plant.

In the current chapter and the next, different technologies concerning the five steps presented in Figure 3-2 will be evaluated. It is stressed that the *biomass-to-gas* conversion processes are weighted the most in this work and will be evaluated separately in this chapter, emphasized with the blue colored box in Figure 3-2. The rest of the processes, emphasized with green colored boxes in Figure 3-2 are investigated in chapter 4.

3.1. Biochemical Conversion: Anaerobic Digestion

Anaerobic digestion represents catabolic processes that occur in the absence of free molecular oxygen. During anaerobic digestion, microorganisms break down organic material and release gases that are collected and designated as biogas. The biogas usually constitutes methane, carbon dioxide, water vapor and traces of ammonia and hydrogen sulfide. The high amount of methane makes the gas energy rich and it can be utilized as a fuel gas or combusted directly providing heat (A. Steinhauser, 2011). It can also be used as a source of liquid biofuels as is the case in this work. The anaerobic digestion as a process is complex and comprises several sub-processes and strains of bacteria that participate in the gas generation. These include *hydrolysis, acidogenesis, acetogenesis* and *methanogenesis*.

Hydrolysis is the first stage of anaerobic digestion, and involves the break-down of complex water-soluble organic molecules like long chain proteins, lipids (fats) and carbohydrates that can be found in cellulose and hemicellulose. These are broken down into short-chain molecules by enzymes. Carbohydrates are broken down into soluble sugars, proteins are broken down into amino acids and lipids are broken down into fatty acids. Short-chain molecules are easily digested by microorganisms. Hydrolysis thus makes the molecules in the material that is to be digested available to the microorganisms, and is an important stage in the anaerobic digestion. The time rate of hydrolysis varies between different compounds. Some complex organic molecules like cellulose, hemicellulose and lignin found in lignocelluloses decompose slowly and incompletely (Gerardi, 2003). To improve material decomposition, external pretreatment technologies can be invented prior to the anaerobic digestion with a purpose of starting the hydrolysis before anaerobic digestion is applied. Such pretreatment technologies can be pretreatment of the material with steam catalysts (McKendry, 2002), and a chapter is devoted to such technologies later in this thesis (chapter 4).

The next stage in the anaerobic digestion is acidogenesis and acetogenesis. *Acidogenesis* is the degradation of short-chain soluble sugars, amino acids and fatty acids by microorganisms. The products of this degradation are organic acids and gases. The organic acids constitute propionic acid, butyric acid, acetic acid and acetate (A. Steinhauser, 2011). The gases constitute hydrogen and carbon dioxide. The *acetogenesis* represent the reaction between the acidogenesis products and water to form acetate and more hydrogen. The hydrogen produced by acetogenesis reactions is essential for the methane formation, as will be made clear in the next section explaining the methanogenesis (Gerardi, 2003).

Methanogenesis is the last stage of anaerobic digestion and describes the production of methane as a result of the reduction of acids like acetate and the reaction of hydrogen and carbon dioxide to produce methane. In addition to methane, water vapor and carbon dioxide is formed. A more detailed description of the anaerobic digestion microbiology can be found in "*The microbiology of anaerobic digesters*" by M.H.Gerardi (Gerardi, 2003).

The microorganisms are living creatures that are sensitive to changes in their environment like temperature, pH and nutrient availability among others. Small changes in these parameters may decrease the microbiologic activity drastically, thereby decreasing the biogas yield. For larger parameter fluctuations, the microorganisms may even die, resulting in a complete stop in biogas production. Therefore, finding optimal process parameters and keeping them constant is important when operating an anaerobic digestion process.

3.1.1.Anaerobic Digestion Technologies

In Norway, biogas production started becoming practice around 2009, mainly from the organic material of sewage sludge and food waste. This happened as a response to the ban on land-filling of biodegradable wastes of which was effective from the 1st of july 2009. Since then, the development of biogas facilities in Norway has been following a slow pace compared to other countries in Europe like Germany and Sweden. However, research on the area shows that organic material like manure, straw and grass waste from agriculture and wood are well suited for biogas production – material of which can be found in large amounts in local communities all over Norway.

An anaerobic digestion system consists of one or several digester tanks with a gas collecting unit on top. The tank has an inlet section for feedstock input and two outlets, one for gas and one for residues. A general digester tank is illustrated in Figure 3-3. The figure is taken from a webpage for industrial wastewater treatment systems (Waste Water System, 2013). The reactor tank on the left shows the different layers in the digester tank. The feedstock input section is not shown, but is usually located in the mid-region of the digester. The reactor to the left is divided into four layers. The gases are collected and transported through a pipeline to the end user or to upgrading processes. The reactor to the right in Figure 3-3 illustrates the energy demanding equipment installed in the reactor. The reactor needs a heat supply to keep a constant temperature environment inside the digester. Stirring is required to enhance good mixing of the digesting sludge, which is important to make all sludge available to the microorganisms.

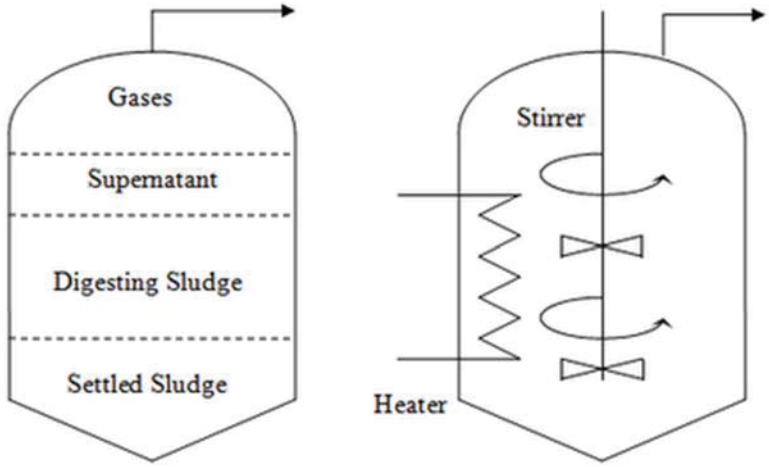

Figure 3-3: General Anaerobic Digestion Reactor (www.wastewatersystems.net 2013).

The microorganisms in the reactor are, depending on the feedstock type, most active in one of three temperature ranges, namely psychrophilic, mesophilic or thermophilic temperature range. The *psycrophilic* temperature range is about 15-30 ^{o}C, the *mesophilic* temperature range is about 30-42 ^{o}C and the *thermophilic* range is from 48-60 ^{o}C (Gerardi, 2003). The optimal temperature range is often narrow. P. Weiland states that mesophilic microorganisms are most active in the temperature range of 38-42 ^{o}C, implying that a stable temperature should be maintained in the reactor (Weiland, 2009). The operational temperature is related to residence time (the period of time the biomass is exposed for the anaerobic environment), and the lower the temperature, the lower the residence time. In this work mesophilic operational conditions are chosen due to the low

amount of energy required for reactor heating and the moderate residence time it promotes. The stable operational temperature is chosen to 30 ^{o}C and the residence time is set to 30 days. Other process parameters essential for the microbiological activity constitutes reactor pH, the carbon-to-nitrogen ratio and nutrient composition. These aspects have been disregarded to simplify the work. M. H. Gerardi provides a good introduction to the topic in "The microbiology of anaerobic digesters" (Gerardi, 2003).

The anaerobic digesters can be of several types, and P. Weiland suggests wet anaerobic digestion and dry anaerobic digestion to be the most general (Weiland, 2009). *Wet digestion* processes are characterized by total solids content lower than 10%. To obtain this concentration a mixing with water or liquid manure is necessary. The digestible slurry obtained is pumpable and must be fed continuously to the reactor tank(Weiland, 2009). *Dry digestion* processes are characterized by total solids content between 15-35 % of the feedstock, and can be operated continuously or on a batch basis. Batch operation involves the batch-vice loading of solid substrate in a gas-tight reactor tank (Weiland, 2009).

P. Weiland suggests that wet continuous digestion is the most common anaerobic digestion process and this is verified by the tremendous amount of research found on wet reactors. P. Weiland assumes that 90 % of all reactors implemented in Germany today are vertical continuously stirred wet tank fermenters (Weiland, 2009). However, batch operation allows for higher loading rates than the wet processes. The dry batch process is relatively new and research on the area is deficient. D. Brown et.al compared a liquid and a solid state reactor on 8 different lignocellulosic feedstock and found that the solid state (dry) reactor is more sensitive to lignin content in the biomass, which makes up a large fraction of the woody biomass composition (D.Brown, 2012). However they also found indications on the improved biogas yield from dry reactor operation on straw and grass (D.Brown, 2012). P. Weiland stated that the gas yield from solid dry processes where approximately equal to that of liquid wet processes (Weiland, 2009). For the application in this thesis, a dry batch-fed anaerobic digester is applied. This approach is chosen because it is thought to reduce the amount of energy spent on biomass pretreatment before anaerobic digestion.

Anaerobic digesters can be operated in series and in parallel. For dry batch reactors to obtain a constant gas production, a minimum of three reactors must be operated in parallel with different start-up times. In this work only one reactor is considered to simplify. The operational specifications regarding the anaerobic digestion process are summarized in table Table 3-1, and will be used throughout this work.

Operation Specifications	
Reactor Type	Dry Batch Reactor
Operation Temperature	Mesophilic, T=30^{o}C
Residence time	30 days

Table 3-1: Operation Specifications, anaerobic digesetion

3.2. Thermochemical Conversion: Gasification

Gasification is the conversion of biomass into a gaseous energy carrier in an oxidizing medium like air, oxygen, steam, carbon dioxide or a combination of the former (McKendry, 2002). In Europe, gasification is not a new technology. Foley et.al (1983) reviewed the early history of gasification and made clear that product gas was already in use in 1791 to drive an internal combustion engine (T.A. Milne, 1998)! The gasification of fossil resources like coal has been used for decades, whereas biomass gasification is relatively new. It was applied around 1920, but did not get its "boost" before the World War II made fossil resources scarce (T.A. Milne, 1998).

Gasification is easily confused with *combustion*, where oxidation is substantially complete in one process (McKendry, 2002). During gasification the intrinsic chemical energy of carbon in the biomass is converted into combustible gas in two stages, and the supply of oxidizing media is controlled in order to obtain a reducing environment rather than a highly oxidizing environment. This conserves most of the thermal energy, which would otherwise be released to the surroundings as heat by combustion (McKendry, 2002).

The gasification process can be divided into four steps: drying, pyrolysis, gasification and reduction (S. van Loo, 2008). First the moisture conserved within the biomass is removed trough a drying process. Secondly, continuous heating devolatilizes the biomass. Devolatilization is the release of all volatile matter contained in the biomass. When the volatile matter comes in contact with the gasification agent the gasification occurs. Gasification occurs as described by reactions (3-1) and (3-2):

$$\mathrm{C} + \tfrac{1}{2} O_2 \rightarrow CO \left(-268 \text{ MJkg/mol} \right), and \qquad \textbf{(3-1)}$$

$$\mathrm{C} + O_2 \rightarrow CO_2 \left(-406 \text{ MJkg/mol} \right). \qquad \textbf{(3-2)}$$

Here, reaction (3-1) represents the partial oxidation reaction and reaction (3-2) represents complete oxidation. The fourth and final phase is the reduction, where carbon and carbon monoxide reacts with water, hydrogen and carbon dioxide to form carbon monoxide, hydrogen, methane and water as described by reactions (3-3) to (3-6):

$$\mathrm{C} + H_2O \leftrightarrow CO + H_2 \left(+118 \text{ MJkg/mol } \right), \quad \textbf{(3-3)}$$

$$CO + H_2O \leftrightarrow CO_2 + H_2 \left(-42 \text{ MJkg/mol } \right), \quad \textbf{(3-4)}$$

$$CO + 3H_2 \leftrightarrow CH_4 + H_2O \left(-88 \text{ MJkg/mol } \right) \text{ and} \quad \textbf{(3-5)}$$

$$\mathrm{C} + CO_2 \leftrightarrow 2CO \left(\text{ MJkg/mol } \right). \quad \textbf{(3-6)}$$

Here, reaction (3-3) is the water gas reaction and reaction (3-4) represents the water gas shift reaction. Reaction (3-5) describes the methane formation reaction whereas reaction (6) is the Boudouard reaction (McKendry, 2002) (R.M. Swanson, 2010). It follows from this set of reactions (3-1) to (3-6) that the resulting product gas consists of hydrogen, carbon monoxide, carbon dioxide, water vapor and methane of different concentrations. The heats of reaction are given in parenthesis behind each reaction and are measured in Mjkg/mol. A positive sign implies that the reaction requires energy in order to be performed and it is then called endothermic. A negative sign implies that the reaction gives off heat when reaction is performed and it is then called exothermic. The heat of reaction is thus an indicator on whether the equation requires or release energy. The only endothermic reaction presented above is the water-gas-shift reaction (3-3). The Boduoard reaction (3-6) are endothermic for high temperatures (T>700 ^{o}C) and exothermic for low temperatures (T<700 ^{o}C) (Tran, 2012).

3.2.1. Gasification Technologies

Three different types of furnaces can be used for gasification. These are presented in Table 3-2 and are called fixed bed, fluidized bed and pulverized bed gasification technologies. The *fixed bed gasification* furnace is constructed as an up-draft, down-draft or cross-flow furnace. The *fluidized bed* can be either bubbling or circulating, and the *pulverized bed gasification* is called entrained flow gasification (S. van Loo, 2008).

Gasification Technologies					
Fixed Bed Gasification			Fluidized Bed Gasification		Pulverized Bed Gasification
Up-draft	Down-draft	Cross-flow	Circulating Bed	Bubbling Bed	Entrained Flow

Table 3-2: The different Gasification Technologies.

In this work a bubbling fluidized bed will be modeled and thereby the fluidized bed technology will be described in detail. The other furnace technologies will be given only briefly in the end of this chapter. This sub chapter is started by introducing a general combustion furnace for fluidized bed gasification, and is followed by an introduction to the circulating and bubbling bed technologies. The other technologies will be given short introductions thereafter.

The Fluidized Bed Gasification Furnace

A general fluidized bed gasification furnace is illustrated in Figure 3-4. It includes a primary air inlet, a secondary air inlet, a biomass feed inlet (*"fuel" in Figure 3-4*), a flue –and product gas outlet and a fixed plate perforated with holes for primary air and ash throughput (S. van Loo, 2008). The furnace is separated into a primary and a secondary gasification zone. In the primary gasification zone, primary air and biomass is fed into the furnace. Here it is exposed to high temperatures ranging from 700 °C to 1300 °C depending on the technology in use. The primary air supplies the furnace with the oxidizing agent and the gasification reactions starts to taking place. Solid residues like char and ash falls down through the fixed plate while the gas flows upwards to the second gasification zone (*red color, Figure 3-4*) (S. van Loo, 2008). In the second gasification zone, more oxidizing agent is supplied to the furnace through the secondary air inlet allowing for complete gasification of the biomass. Here the reduction reactions (3-3) to (3-6) take place and a product gas interspersed with fly ash and other particulates leaves the furnace at temperatures ranging from 700 °C to 1300 °C, depending on the gasification technology applied. The primary and secondary air inlet supplies the furnace with the gasification oxidizing agent. It does not necessarily have to be air. Oxygen, steam, carbon dioxide and

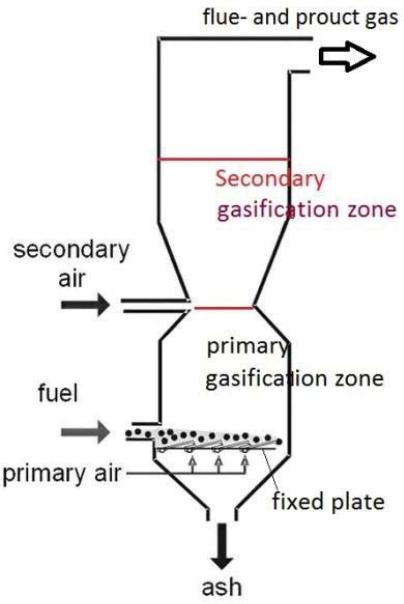

Figure 3-4: A General Fluidized Bed Gasification Furnace

combinations of these can also be used as an oxidizing agent. The choice of oxidizing agent affects the product gas quality but is often restricted due to economic limitations. An overview of the different oxidizing agents is given by K.Kim et.al and is illustrated in Table 3-3 (K.Kim, 2013):

Column one lists the oxidation agent options. Column two lists the general gasification product gas energy content in terms of heating value (MJ/Nm^3) for the respective oxidation agent. Nm^3 is an abbreviation for *normal cubic meters*, which denotes 1 m^3 gas at 0 ^oC and pressure 760 mmHg. Column three lists the economic feasibility related to the oxidation agents based on the evaluation given below.

Gasification Oxidizing Agent	Product Gas Heating Value [$MJNm^{-3}$]	Economic Feasability
Air	< 3	Good
Oxygen	3-5	Poor
Steam	10-15	Medium
Carbon dioxide	>15	Medium

Table 3-3: Options for Gasification Oxidation Agents, product gas quality and economic feasibility (K.Kim 2013).

Air is a cheap and common oxidization agent, but it contains lots of nitrogen, about 50%, that dilutes the product gas and lowers its heating value. By using oxygen as an oxidizing agent the product gas quality increases, reaching 3-6 MJ/Nm^3. However, the supply of oxygen is related to high operational costs. By using steam as an oxidizing agent the product gas heating value reaches 10-15 MJ/Nm^3. However, the endothermic steam reactions make it necessary to provide the system with an external heat supply. Steam as an oxidizing agent is thus only beneficial when the gasification system can be combined with industry providing excess heat and steam from its internal processes. The use of carbon dioxide as an oxidizing agent also requires external heat supplies due to its endotherm occurrence. It produces a product gas with high heating value which exceeds 15 MJ/Nm^3 (K.Kim, 2013).

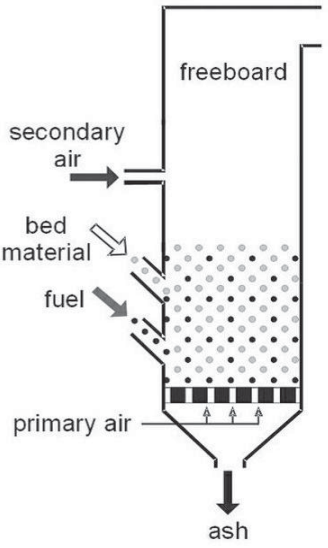

Figure 3-5: Bubbling Fluidized Bed Gasification Furnace. (S. van Loo 2008).

In fluidized bed gasification furnaces the fixed plate located at the furnace bottom is covered with a bed material, which usually consist of sand, silica, dolomite, olivine or some other grained and non-reactive material with high heat capacity (McKendry, 2002), (S. van Loo, 2008). The biomass feed inlet is located above the plate, letting the biomass feed mix with the bed material. The concentration of biomass feed is usually about 1-5 % of the biomass feed-bed material mixture (McKendry, 2002), (S. van Loo, 2008). When

primary air is flowing upwards trough the plate it fluidizes the bed, making a homogeneous mixture of bed material, biomass feed and gasification gases. The processes of drying, devolatilization, combustion and reduction occur in parallel (McKendry, 2002). A second air inlet is placed in the upper part of the furnace, making the hot gases pass through a secondary combustion zone before leaving the furnace. The secondary combustion zone prevents incomplete combustion. As stated in the introduction to this sub chapter one distinguishes between two types of fluidized bed technology: The Bubbling Fluidized Bed (BFB) and the Circulating Fluidized Bed (CFB). The two types are evaluated in the proceeding sections.

Bubbling Fluidized Bed Gasification

In a *Bubbling Fluidized Bed* (BFB) furnace the primary air velocity is high enough (1.0-2.0 m/s (S. van Loo, 2008)) to fluidize the bed, which promote a good mixing of biomass feed, bed material and gas bubbles as illustrated in Figure 3-5. The dots in the figure represents biomass feed (dark colored dots) and the bed material (light colored dots). The homogeneous nature of the mixture makes the process temperature isothermal and well distributed. The process temperatures usually range about 700-900 ^{0}C (McKendry, 2002). The furnace can also be operated at lower temperatures, in the range of 650-850 ^{0}C. The bubbling fluidized bed furnace can handle biomass feedstock of particle sizes up to 80 mm diameter and also possesses high flexibility in biomass moisture content and biomass type applied (S. van Loo, 2008).

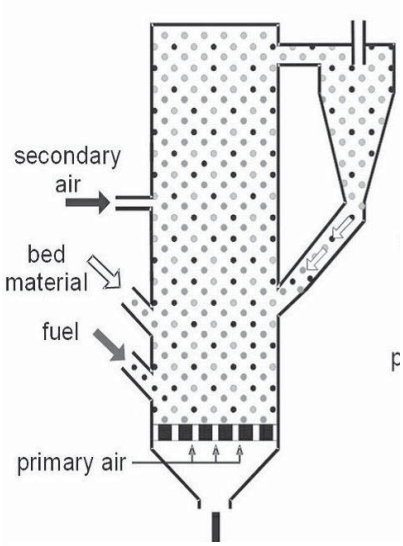

Figure 3-6: Circulating Fluidized Bed Gasification Furnace (S. van Loo 2008).

Circulating Fluidized Bed Gasification

In a *Circulating Fluidized Bed* furnace (CFB), the primary air velocity is high (5.0-10.0 m/s (S. van Loo, 2008)) and the bed material particle sizes are usually low compared to the BFB, making the homogeneous mixture of biomass feed, bed material and gas circulate through the furnace. The furnace is equipped with a cyclone, as illustrated in Figure 3-6 where the bed material is gathered and returned to the combustion zone on the fixed plate. The circulation results in a higher heat transfer rate between the hot bed material and the biomass feed, which require a higher bed temperature compared to the BFB. The furnace is operated at a temperature around 750-900 ^{0}C. The circulating fluidized bed technology allows for the use of biomass feedstock of high ash and moisture content. Compared to the bubbling fluidized bed it requires biomass particles of smaller size, up to 40 mm diameter. The circulation of bed material imposes high particulate and impurities content in the product gas that needs to be cleaned out of the gas (S. van Loo, 2008).

The major operational difficulty related to fluidized bed gasification is, according to Mc Kendry, the potential slagging when the bed material comes in contact with the ash contained in the biomass

feed (McKendry, 2002). *Slagging* is the formation of clusters of ash and bed material as a result of ash reaching its melting temperatures. The rather sophisticated gasification furnace design also imposes high investment and operational costs and advanced furnace operation. On the other hand, the fluidized bed gasification technology also provides flexibility in the choice of biomass feed due to the high heat capacity of the bed material (McKendry, 2002). Mixing of different biomass feedstock is possible, even though not at the same scale as is the case for fixed bed gasification systems (S. van Loo, 2008), which is the topic of the next section.

Fixed Bed Gasification

The general fixed bed gasification furnace is similar to the general fluidized bed furnace illustrated in Figure 3-4. The major difference is that in the fixed bed, the biomass is forced down into the furnace by gravity to form a bed, and there is no material to fluidize the bed. The biomass input is located at the upper part of the furnace and the gas outlet can be located on the furnace top, like in Figure 3-4, or at the lower furnace part. The primary air enters the furnace at the bottom and is flowing upwards through the bed as the biomass is gasified. The biomass becomes devolatilized and the solid matter consisting of char and ash falls down through a fixed perforated plate in the furnace bottom. Typical fixed bed gasification temperatures are in the range from 700 ^{o}C to 900 ^{o}C. The fixed bed technology is advantageous in its simplicity and its tolerance to low-quality biomass feedstock (high ash, moisture and impurities content). However, the simple furnace construction results in a low-quality product gas with high amount of impurities (R.M. Swanson, 2010). Three different fixed bed gasification technologies are identified in accordance with Table 3-2, namely down-draft, up-draft and cross-flow gasification furnaces.

In the *down-draft* gasification furnace the primary air inlet is located in the very furnace bottom. Gasification occurs and the hot product gas is transported downwards by ventilation air, leaving the furnace at the bottom holding a temperature of about 900-1000 ^{0}C (McKendry, 2002), (Neathery, 2010). The high temperature and the contact with the hot char in the furnace bottom make the product gas contain low concentrations of pyrolysis products. The particulate concentration is high and the process energy efficiency is low due to heat losses related to the high product gas temperature at the furnace outlet (Neathery, 2010).

In the *up-draft* gasification furnace the primary air inlet is also located at the lower part of the furnace The product gas is leaving the furnace in the top section with a temperature of about 200 ^{0}C (McKendry, 2002). The low product gas temperature provides higher process energy efficiency than for down-draft processes. The product gas is transported through the drying feed before leaving the furnace, which helps filtering the gas so that it contains only small amounts of particulates. However, the concentration of pyrolysis products like tar in the product gas is high due to its low temperature (Neathery, 2010).

In the cross-flow gasification furnace primary air is supplied from the furnace walls and product gases are withdrawn out on the opposite side at the same level, forming a hot zone around the primary air entrance where combustion and gasification occur. The product gas leaving at the

opposite side of the furnace is withholding a temperature of 900-1000°C. This gives the process low energy efficiency and a product gas containing a high concentration of pyrolysis products (McKendry, 2002).

Pulverized Bed Gasification

In a pulverized bed furnace, like the entrained flow gasification furnace illustrated in Figure 3-7, the biomass feed and the primary air is injected at the top of the gasification furnace, which is constructed as a pipeline. The biomass feed and oxidation agent mixture flows through the furnace at high temperatures of about 1000-1400 °C (M.J. Prins, 2006) and an operation pressure of 20-70 bar (Tran, 2012). The ash is collected and removed, whereas the resulting product gas leaves the pipeline-shaped furnace with a high temperature and low concentrations of impurities, especially tars – significantly lower than what is the case for both fixed bed gasification systems and fluidized bed gasification systems. The biomass feedstock input must be pulverized, which indicates particle sizes down to 1 mm in diameter (S. van Loo, 2008). This sets restrictions on the types of biomass used as a feedstock for the pulverized bed gasification technology. The technology is however interesting because of the simple furnace construction and the improved product gas properties obtained, and is a technology option undergoing extensive research and development at the time being.

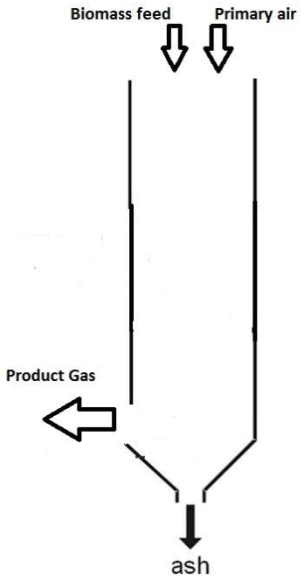

Figure 3-7: Entrained Flow Gasification Furnace.

Gasification Technologies Evaluation

The three gasification technologies evaluated in this chapter are summarized in Table 3-4. The table gives a rating of each technology from low too high for 6 technology features. Dark blue color indicates the least desirable technology feature and light blue indicate the most desirable technology feature. The properties are listed in column 2 to 7 and covers product gas tar content, product gas particles/dust content, product gas quality in terms of gas composition and calorific value, agglomeration potential in the gasification furnace, economic feasibility and process efficiency in terms of energy. The three gasification technologies are listed in row 2 to 4.

Gasification Technology	Product Gas Particulates/dust content	Product Gas Quality	Biomass Pretreatment Requirement	Economical Feasability	Process Efficiency
Fixed Bed	High	Low	Low	High	Low
Fluidized Bed	High	Medium	Medium	High	Medium
Pulverized Bed	Low	High	High	Low	High

Table 3-4: Gasification Technologies Evaluation regarding Fixed, Fluidized and Pulverized Gasification Technologies.

The fixed bed gasification technology generally possesses low investment and operational costs due to its simplicity and widespread commercial application (S. van Loo, 2008). It is flexible in biomass feedstock composition, but also produces a product gas of poor quality and with high ash content (R.M. Swanson, 2010).

The entrained flow gasification on the other hand produces a product gas of high quality with low ash and particulates content (McKendry, 2002). The operation is simple, but restrictions are set on biomass feedstock of which must be pulverized before application (S. van Loo, 2008). It has been getting a lot of attention recently due to its high efficiency and simple construction but it is still too expensive for commercial application (McKendry, 2002).

In this work, the choice of gasification technology falls upon the fluidized bed gasification. Generally it is flexible to biomass composition; in particular to moisture and ash content (McKendry, 2002). This reduces the scale of necessary biomass pretreatment prior to the gasification and allows for the use of a variety of lignocellulosic material as gasification feedstock. It also possesses high volumetric capacities and easy temperature control (McKendry, 2002). The bubbling fluidized bed has been chosen as gasification technology over the circulating fluidized bed due to its slightly increased flexibility in biomass feedstock particulate sizes and because it is related to lower particulate emissions than the circulating fluidized bed (S. van Loo, 2008)

For bubbling fluidized bed modeling a techno-economic NREL report made by R.M. Swanson et.al comparing an birch fed entrained flow reactor and a corresponding bubbling fluidized bed reactor by using Aspen Plus is used to decide the proper operational parameters (R.M. Swanson, 2010). The operational parameters used further in this work are presented in Table 3-5.

Spesification	Model Parameter	
Low-Temperature BFB	1134	K
Oxidation Agent O2/steam	30/40	-

Table 3-5: Model Spesifications, Bubbling Fluidized Bed (R.M. Swanson 2010).

Table 3-5 summarizes that for the thermochemical process, a low-temperature bubbling fluidized bed reactor operating at 1134 K and supplied with an oxidation agent consisting of oxygen and steam at a ratio of 30/40 is applied in the model developed in this work.

4. Biomass Pretreatment, Gas Conditioning and Gas-to-liquid biofuel Conversion

Chapter 3 was denoted to presenting available biomass-to-gas processes for both biochemical and thermochemical conversion pathways. Recall from table 3-2 that in addition to these processes biomass pretreatment, gas conditioning and Fischer-Tropsch synthesis must be applied. In chapter 4.1 available biomass pretreatment technologies are presented whereas chapter 4.2 presents available gas conditioning technologies. In chapter 4.3 available gas-to-biofuel conversion technologies are presented. An evaluation of the technologies is performed with respect to application in the biochemical and thermochemical pathways.

4.1. Biomass Pretreatment Technologies

Recall from chapter 3.1 that a major challenge associated with the anaerobic digestion of lignocellulosic material is making the cellulose available for the anaerobic microorganisms. Recent studies indicate that hemicellulose and lignin is resistant to anaerobic decomposition, and that improper lignocellulose degradation eventually inhibit biogas production (M.J. Taherzadeh, 2008), (A.T.W.M. Hendriks, 2008). Thus, biomass pretreatment is required before anaerobic digestion can be performed optimally.

A major challenge associated with the gasification of lignocellulosic material is related to the combustible properties of the material. Recent studies indicate that the raw lignocellulosic feedstock is associated with challenges regarding high moisture content, low energy density and thermal instability (M.J. Prins, 2006), (McKendry P. , 2002). High *moisture content* may decrease the energy efficiency of the gasification process due to lower biomass heating value. Low *energy density* implies that the energy gained per unit biomass (kg, Nm^3) is low compared to commercial fossil fuels. *Thermal instability* of the biomass may cause incomplete gasification and irregular temperature distribution in the gasification furnace. Biomass pretreatment can be applied to improve one or more of these combustible fuel properties, promoting more energy efficient operation.

The available biomass pretreatment processes are various. Table 4-1 gives an overview of the current pretreatment technologies for both conversion pathways. They are organized into four main categories; physical, thermal, chemical and biological pretreatment technologies. *Physical pretreatment* technologies include biomass drying, biomass milling and irradiation. *Thermal*

pretreatment technologies include steam pretreatment, steam explosion, liquid hot water pretreatment and torrefaction. *Chemical pretreatment* technologies include the use of acid, alkaline or oxidative catalysts. *Biological pretreatment* technologies include the addition of certain types of bacteria or fungi.

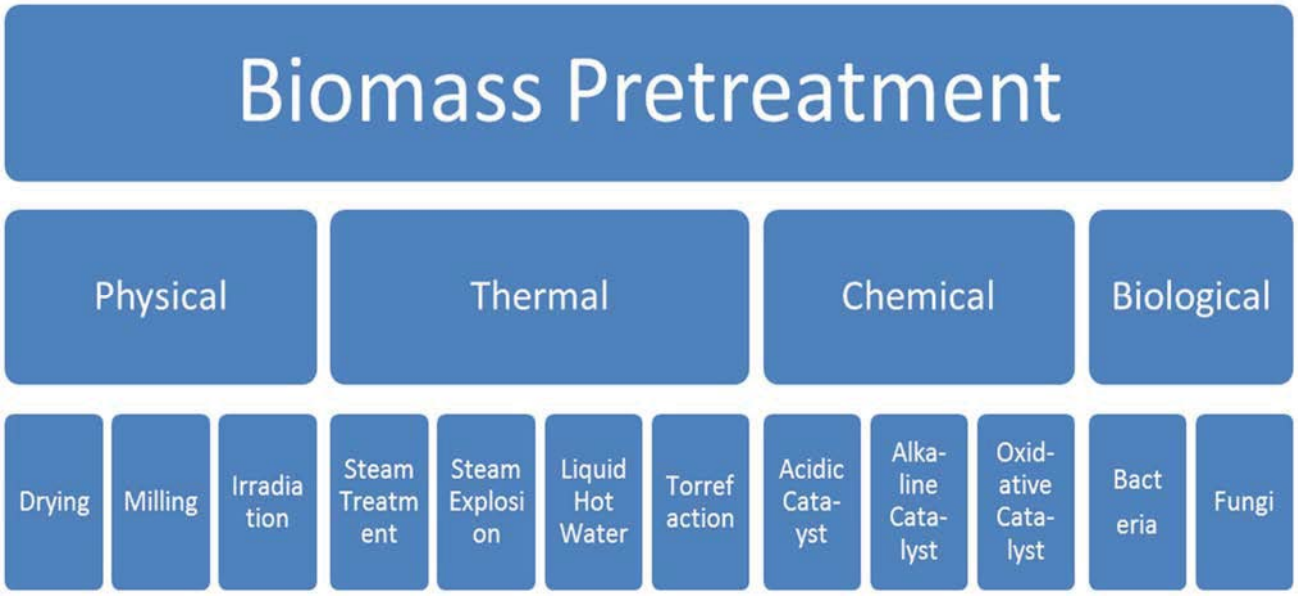

Table 4-1: Biomass Pretreatment Technologies.

In the following sections the pretreatment technologies are evaluated. The evaluation is summarized in two tables at the end of the chapter. For the biochemical plant the lignin removal, hemicellulose removal and the production of eventual inhibitors are emphasized in the evaluation. For the thermochemical plant, the moisture content, energy density and thermal instability are emphasized. Environmental and economic feasibility are emphasized in both evaluations. Based on this, one technology will be chosen for each plant to be used in the model analysis in chapter 5.

Physical Pretreatment

Drying

Biomass drying is most relevant for the gasification plant. Raw lignocellulosic biomass like birch may contain up to 50 % moisture, whereas the biomass moisture content should be 10 to 15 % to be prudent as a biomass feed in the gasification process (McKendry P. , 2002). The drying can be done both direct and indirect. Direct drying involves the use of a heat source like steam or process heat, or fan equipment. Indirect drying occurs naturally by moisture diffusion to the surroundings. The indirect drying involves no energy-requiring equipment and is thus slightly more economically feasible than the direct drying methods. Drying has a good effect on the biomass moisture content but does not affect energy density or thermal properties of the fuel.

Milling

Milling is relevant for both the anaerobic digestion and the gasification plants. Examples of milled material comprise grass or straw cut into smaller pieces, wood shavings and sawdust. By cutting the biomass into smaller pieces the hemicellulose becomes more available for anaerobic microorganisms, thus improving the biogas yield in the anaerobic digestion plant. The lignin degradability is not affected (M.J. Taherzadeh, 2008). The biomass particle size is reduced by milling, thus making the biomass feasible for fluidized bed gasification (chapter 3.2). The biomass bulk density may be improved by milling. The milling is not related to any inhibitory or toxic emissions (A.T.W.M. Hendriks, 2008). However it represents a demand for mechanical energy (M.J. Taherzadeh, 2008). Another form for milling where the biomass is both milled and compressed is known as biomass pelletizing. Biomass pellets have an improved bulk density but also an increased demand for mechanical energy.

Irradiation

Irradiation is relevant for the anaerobic digestion plant and represents the application of irradiation like gamma rays, microwaves or ultrasound to the biomass before it enters the anaerobic digester. Irradiation removes lignin from the biomass and the effect of irradiation pretreatment is proportional to the lignin content in the biomass. Irradiation involves no use of chemicals, which means that the pretreatment process possesses low toxic emissions and no additives with inhibitory effects on the anaerobic microorganisms. The decomposition of lignin release phenols that may inhibit some anaerobic microorganisms. The pretreatment process is expensive, representing a barrier for its implementation in the biochemical anaerobic digestion system (M.J. Taherzadeh, 2008).

Thermal Pretreatment

The thermal pretreatment technologies are usually applied to anaerobic digestion plants and consist of pretreatment with steam or liquid water at various conditions. The only exception is torrefaction, which is applied to gasification plants. The technologies are presented in the following sections.

Steam Pretreatment

During *steam pretreatment* the biomass is fitted in a vessel, and steam with high temperature ($T > 240^{o}C$, (A.T.W.M. Hendriks, 2008)) and high pressure ($p > 7$ bar, (K. Panther, 2006)) is applied for some minutes. The steam is then released from the treated biomass of which is quickly cooled down. The pretreatment process solubilizes and effectively removes the hemicellulose content in the biomass. It is not effective on lignin removal. It involves no toxic additives and is not related to high investment or operational costs as steam is easily provided by exothermic industrial processes. However, thermal treatment processes entails a risk of releasing furfurals and phenols which may impose inhibitory effects on the anaerobic microorganisms (A.T.W.M. Hendriks, 2008).

Steam Explosion

During *steam explosion* the biomass is fitted in a vessel, and steam with high temperature (T >240 ^{o}C, (A.T.W.M. Hendriks, 2008)) and high pressure (p > 7 bar, (K. Panther, 2006)) is applied for some minutes. The steam is then released from the treated biomass, and the biomass is exposed to a rapid pressure drop. The pressure drop removes most of the hemicellulose and also lignin. If the process is applied in symbiosis with established industry providing excess heat and steam there are low energy costs associated with the process. The steam explosion is associated with a risk of releasing inhibitors like furans and phenols (M.J. Taherzadeh, 2008).

Liquid Hot Water

Biomass pretreatment in *liquid hot water* involves cooking of the lignocellulosic material in liquefied hot water at high temperatures (160-220 ^{o}C, (M.J. Taherzadeh, 2008)) for time intervals varying from 2 to 20 minutes depending on the composition of the biomass feedstock. The pretreatment process removes most of the hemicellulose and it also removes some lignin. Besides the liquid water no further chemicals are used, resulting in low emission of toxics. The process is simple and involves few economic disadvantages if excess heat from local industry is available. Inhibitors like furfural and xylose can be released, but compared to the other thermal pretreatment processes presented here this process possesses less inhibitory effects (M.J. Taherzadeh, 2008), (A.T.W.M. Hendriks, 2008).

Torrefaction

Torrefaction is applied to improve the biomass properties as a gasification feedstock both regarding moisture content, energy density and thermal instability. It is a process where biomass is heated in a closed vessel at temperatures ranging from 200-300 ^{o}C in the absence of oxygen. (Tran, 2012). The torrefaction product is a solid bio-char, liquid bio-oil and some gas, where the concentration of the three products varies with torrefaction process parameters (W. Yan, 2009)).The solid fraction of the torrefaction product has a coal-like appearance and is illustrated in Figure 4-1. Torrefied biomass has improved properties as a fuel, including a higher heating value, hydrophobic nature, very low moisture content, higher porosity (higher reactivity) and less gas impurities enhancing a cleaner combustion (Tran, 2012). The process is not involving any toxic substances and the environmental feasibility is considered good. The heating process is energy consuming and may involve significant costs. The technology is not commercial and still at the research stage, which contribute to a low economic feasibility.

Figure 4-1: Milled raw wood sample above torrefied and milled wood sample (Tran, 2012).

Chemical Pretreatment

The chemical pretreatment processes consist of biomass treatment with acidic, alkaline or oxidative catalysts and are relevant for the anaerobic digestion plant.

Acidic Catalyst

Recall that the first step of anaerobic digestion is the hydrolysis. Chemical pretreatment with *acid catalysts* enhances the hydrolysis (chapter 3*)* of hemicelluloses. Some lignin is also decomposed, releasing phenols with inhibiting effects on anaerobic microorganisms. Biomass decomposition by acid catalysts may release monomers, furfural, and other volatile products which also provide inhibitory effects on anaerobic microorganisms. The addition of acids like nitric acid and sulfuric acids will reduce methane production in downstream processes as a result of reduction reactions forming hydrogen sulfide (H_2S) and nitrogen gas (N_2). The supply of catalyst is expensive, reducing the economic feasibility (A.T.W.M. Hendriks, 2008).

Alkaline Catalyst

Chemical pretreatment with *alkaline catalysts* makes the biomass swell and becoming more accessible to anaerobic microorganisms. Recent studies state indications that alkaline catalysts modify the crystalline state of the biomass, thus actually making it more thermodynamically stable and resistant to anaerobic digestion. The removal of lignin is resulting in phenol inhibitor formation. The supply of catalyst is expensive, reducing its economic feasibility (A.T.W.M. Hendriks, 2008).

Oxidative Catalyst

Chemical pretreatment with *oxidative catalysts* involves the addition of an oxidizing compound like oxygen or carbon dioxide to the biomass. Oxidative catalysts remove both hemicellulose and lignin effectively. Unlike the other chemical catalysts presented the oxidative catalysts usually do not possess inhibitory effects on the anaerobic microorganisms and they are not subject to toxic emissions. However, inhibitors like phenols and furfurals are formed in the process. The supply of catalysts is expensive, reducing the economic feasibility (A.T.W.M. Hendriks, 2008), (M.J. Taherzadeh, 2008).

Biological Pretreatment

Biological treatment is relevant for the anaerobic digestion plant. It can be performed by the addition of fungi, bacteria, microorganisms or enzymes to the biomass. They decompose both hemicelluloses and lignin effectively but the pretreatment process residence time is longer than for the other pretreatment technologies. The technology is performed in mild environmental conditions giving a low energy and chemical additives requirement. This results in low toxic emissions (M.J. Taherzadeh, 2008). The effective decomposition of lignin results in the release of inhibitory phenols, and the low treatment rate may lead to problems supplying the demanded

amount of biomass feedstock to the anaerobic digester. This has been “punished” by lowering its economic feasibility.

4.1.1.Summary and Evaluation of the Pretreatment Processes

The pretreatment processes presented in the previous sub-chapters are summarized in two tables. Table 4-2 summarizes the pretreatment technologies for the biochemical pathway; the anaerobic digestion. Table 4-3 summarizes the pretreatment technologies for the thermochemical pathway; the gasification process.

Pretreatment Technologies Evaluated for Anaerobic Digestion

	Pretreatment Technology	Lignin Removal	Hemicellulose Removal	Inhibitors	Toxics	Economic Feasability	Source
Physical	Milling	Poor	Medium	Low	Low	Medium	M.J. Taherzadeh, 2008, A.T.W.M. Hendriks, 2008
	Irradiation	Good	Poor	Medium	Low	Poor	M.J. Taherzadeh, 2008
Thermal	Steam Pretreatment	Poor	Good	Medium	Low	Good	A.T.W.M. Hendriks, 2008
	Steam Explosion	Medium	Good	High	Low	Medium	M.J. Taherzadeh, 2008
	Liquid Hot-Water	Medium	Medium	Low	Low	Good	M.J. Taherzadeh, 2008, A.T.W.M. Hendriks, 2008
Chemical	Acid Catalysts	Medium	Medium	High	Medium	Medium	A.T.W.M. Hendriks, 2008
	Alkaline Catalysts	Good	Medium	Medium	Medium	Medium	A.T.W.M. Hendriks, 2008
	Oxidative Catalysts	Good	Good	High	Low	Good	M.J. Taherzadeh, 2008, A.T.W.M. Hendriks, 2008
Bio.	Biological	Good	Good	Medium	Low	Medium	M.J. Taherzadeh, 2008

Table 4-2: Pretreatment technologies evaluation for the biochemical plant (M.J. Taherzadeh 2008, A.T.W.M. Hendrix 2008).

When evaluating the pretreatment technology options for the anaerobic digestion of lignocelluloses, the removal of lignin is the least important factor. Anaerobic microorganisms can usually not digest lignin, even not in its decomposed forms. The lignin decomposition also releases phenols, which impose inhibitory effects on the anaerobic microorganisms (McKendry P. , 2002). As such the removal of lignin is unwanted. Decomposition of hemicellulose and the economic feasibility are the most important factors. Decomposition of hemicellulose into cellulose and short-chain sugars is an important factor as the microorganisms can utilize these compounds effectively and convert them into raw biogas. Economic feasibility covers commerciality, supply costs and operational costs and is important to achieve a profitable system. Microorganism inhibitors decrease the rate of biomass-to-biogas conversion and needs to be weighed against the decomposition of hemicellulose. Toxic emissions are only significant for chemical pretreatment as can be read from Table 4-2 above.

By these considerations the thermal pretreatment processes are most feasible for the case of anaerobic digestion. From Table 4-2 it is seen that they possess overall low lignin decomposition

rates and toxic emissions, and good hemicelluloses decomposition rates and economic feasibility. The steam pretreatment process is evaluated as the best option because of the poor lignin removal and the good hemicelluloses removal rates. It also possesses good economic feasibility and medium release of inhibitors. The steam explosion (SE) and the liquid hot water (LHW) pretreatment processes both possess a medium lignin decomposition ratio. The SE have better hemicelluloses decomposition rates but also a high release of inhibitors as compared to the LHW, resulting in a slightly better weighed result for the LHW compared to the SE. The economic feasibility of the LHW is also better, making the LHW the second best option for the process of anaerobic digestion.

Based on the above given considerations, thermal steam pretreatment is evaluated as the most suitable lignocellulosic pretreatment technology for the implementation in a biochemical anaerobic digestion system.

Pretreatment Technologies Evaluated for Gasification

Gasification Pretreatment		Moisture Content	Energy density	Thermal Instability	Environmental Feasability	Economic Feasability	Source
Drying	Direct	Good Effect	No Effect	No Effect	High	Medium	McKendry, 2002
	Indirect	Good Effect	No Effect	No Effect	High	High	McKendry, 2002
Milling /pellet.	Milling	No Effect	Medium Effect	No Effect	High	Medium	McKendry, 2002
	Pelletizing	Medium Effect	Good Effect	Medium Effect	High	Low	McKendry, 2002
Torr.	Torrefaction	Good Effect	Good Effect	Good Effect	High	Low	Tran, 2012

Table 4-3: Pretreatment technologies evaluation for the thermochemical plant (Mc Kendry 2002, Tran 2012)..

When evaluating the pretreatment technology options for the gasification system one must base the evaluation on the gasification technology that is to be applied. In this case the gasification will be done in a bubbling fluidized bed gasifier (BFB). The BFB requires a dry (10-15% moisture) biomass feedstock input consisting of small particles (50 mm diameter). Therefore, drying and milling are important factors. Indirect drying can be uncontrollable and not sufficient by itself in the spring and autumn seasons due to high moisture content in air and rainy weather. A direct drying process should therefore be applied to dry the biomass to about 10% moisture.

Milling can be performed by a crusher that reduces particles to the required size. Pelletizing of the biomass can be feasible economically if the biomass is transported over long distances from harvest site to the gasification plant. Transportation distances are not evaluated in this thesis and is thus excluded, making pelletizing an option with low economic feasibility. Torrefaction is energy intensive and not commercially available at the time being. It would be considered if the gasification technology was based on an entrained flow gasifier that require a very dry biomass feedstock and pulverized biomass particles down to 1 mm diameter. Thus, a direct drying process and grinding is considered the best option for the gasification process.

Based on the above given evaluation, the pretreatment processes applied to the two plants in this work will consist of a steam pretreatment for the biochemical plant and a direct dryer using steam as heating media with a grinder for the thermochemical plant.

4.2. Gas Conditioning

Before the biogas or product gas can be converted to a liquid biofuel it needs to undergo both cleaning and upgrading processes which makes up the generic term gas conditioning. *Gas cleaning* represents the removal of unwanted contaminants from the gas. This can be done by physical removal of gas particulates like char, soot and ash by cyclones or filters for example. Gas upgrading represents the conversion of unwanted contaminants into wanted contaminants in the gas. This can be done by applying methane reforming reactions for example, which is the conversion of methane to carbon monoxide and hydrogen by the addition of steam. Typical biogas and product gas compositions are given in Table 4-4.

Biogas consists of methane (CH_4), carbon dioxide (CO_2), water (H_2O), hydrogen sulfide (H_2S) and cases trace-impurities like siloxanes, nitrogen, oxygen, ammonia and particles (T. Patterson, 2011), (A. Petersson, 2008). Product gas leaving a bubbling fluidized bed gasifier consists of water (H_2O), carbon monoxide (CO), carbon dioxide (CO_2), hydrogen (H_2) and methane (CH_4) (W. Torres, 2007). In literature the gas obtained by gasification is usually called syngas. Syngas is a gas consisting of carbon monoxide and hydrogen. The product gas must usually undergo gas conditioning before the composition is that of a syngas as can be seen from Table 4-4. Thus, the gasification gas is called a product gas in this work, and it represents the gas before gas conditioning is applied to it.

Acid gases like carbon dioxide, hydrogen sulfide and siloxanes may cause corrosion and wearing on downstream equipment (Johansson, 2008). These compounds must thus be removed by gas cleaning. Liquid biofuel conversion processes like the Fischer-Tropsch process that will be described in 4.3 require a clean syngas for its synthesis. Thus also methane, water, nitrogen, oxygen, ammonia and carbon dioxide must either be removed by gas cleaning or converted to hydrogen and/or carbon monoxide by gas upgrading, and only those assumed relevant for the model that is to be developed in chapter 5 is considered.

Gas Composition and acceptable impurities amounts	Biogas	Product gas (with steam/O_2 oxidizing agent)	LBF-Conversion Reqirements	Source
Methane (vol-%)	60-70	6-8**	-	A. Petersson 2008, **W. Torres 2007
Carbon dioxide (vol-%)	30-40	14-36**	< 25 ppmv*	A. Petersson 2008, *N. Johansson 2008, **W.Torres 2007
Carbon monoxide (vol-%)	-	43-52**		**W.Torres 2007
Hydrogen (vol-%)	-	14-32**		**W.Torres 2007
Nitrogen (vol-%)	0,2	0**	-	A. Petersson 2008, **W.Torres 2007
Oxygen (vol-%)	0	-	-	A. Petersson 2008, **W.Torres 2007
Hydrogen sulfide (ppm)	0-4000	-	< 4 ppmv*	A. Petersson 2008, *N. Johansson 2008,
Ammonia (ppm)	100	-	-	A. Petersson 2008, **W.Torres 2007
Siloxanes (ppm)	1	-	-	**W.Torres 2007
water (vol-%)	10-20	38-61**	< 1 ppmv*	A. Petersson 2008, *N. Johansson 2008, **W.Torres 2007

LBF: Liquid Biofuel

Table 4-4: Typical Gas composition for biogas and product gas and typical gas-to-liquid biofuel conversion requirements (A. Petersson 2008, W. Torres 2007, N. Johansson 2008).

4.2.1.Gas Cleaning Technologies

Gas cleaning technologies can be divided into two classes: primary and secondary gas cleaning technologies. *Primary gas cleaning* represents technologies applied directly into the biomass-to-gas conversion pathway (anaerobic digester/gasifier). *Secondary gas cleaning* represents the physical removal of unwanted compounds in the gas downstream of the biomass-to-gas conversion process.

Primary Gas Cleaning Technologies

The *primary* gas cleaning technologies are presented in Table 4-5 and can be divided into two categories. One is the dimensioning of the digester or gasification reactor. Dimensioning may encompass adjusting process temperature, the excess air demand and residence time in the reactor. The other is the addition of catalysts into the digester or the gasifier. Digester catalysts can be acidic, basic, iron based or nickel based and may comprise additional substrates to regulate the alkalinity/acidity in the digester or enzymes to increase microbiological activity which may increase the gas yield. Gasifier bed additives like olivine and limestone can be added to the fluidized bed to promote complete gasification and reduce tar formation and ash among others. Primary gas cleaning technologies are not applied in this work, and are therefore not considered in detail.

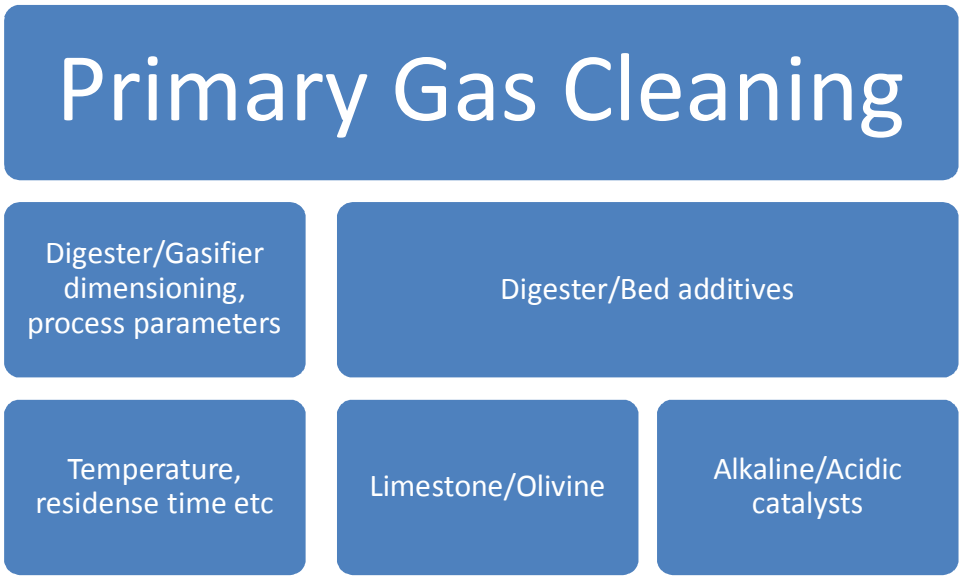

Table 4-5: Primary Gas Cleaning Technologies Overview.

Secondary Gas Cleaning Technologies

The *secondary* gas cleaning technologies are presented in Table **4-6** and are divided into four categories; absorption, adsorption, permeation and cryogenic technologies. Each category contains a variety of technologies, whereas only those considered relevant for this work are presented in the following sections.

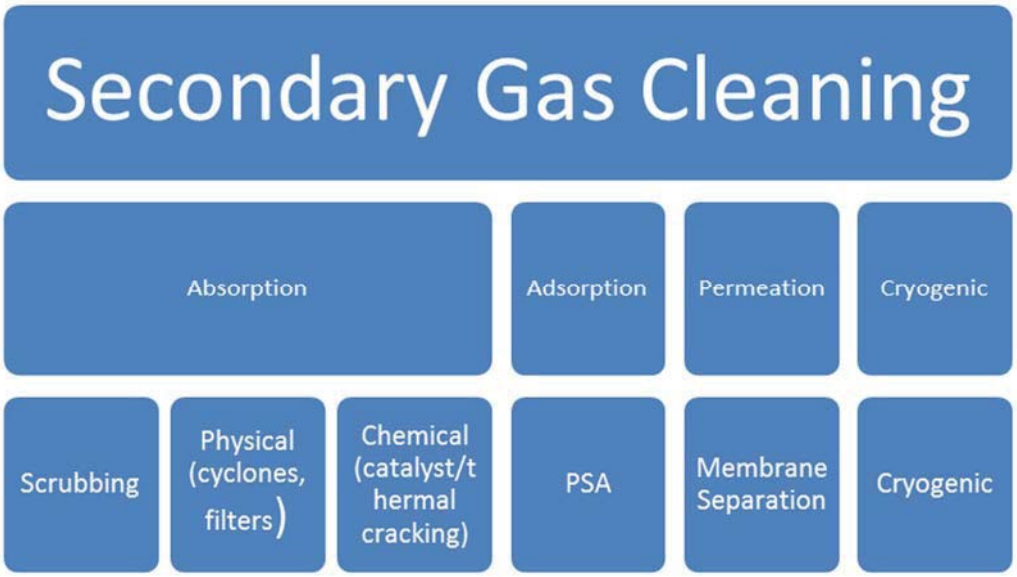

Table 4-6: Secondary Gas Cleaning Technologies.

Absorption

Recall from chapter 3.2.1 that the product gas resulting from gasification usually contain particulate impurities like char, soot, tar and bed material. These constituents may accumulate to prevent equipment from proper operation and they cause wear and tear on both furnaces and downstream equipment. *Absorption technologies* are suitable for removal of gas particulates. Absorption describes the adhesion or uptake of gas molecules by a volume. The volume can be water, filters, cyclones and chemical catalysts among others. The most applied technologies in anaerobic digestion and fluidized bed gasification systems are scrubbing, physical and chemical absorption. In physical absorption processes the absorbent is a non-reactive fluid or solid that is used to physically absorb specific gas molecules from the gas. Solid absorption is performed by cyclones and filters.

Cyclones

Cyclones are conical simple equipment assembled downstream of the gasification process. A simple cyclone is illustrated in Figure 4-2. The gas flows through the cyclone, and particulates, tar and trace elements are trapped by the cyclone while the gas continues its flow downstream the pathway (Neathery, 2010). The purpose of a cyclone is not to rinse the product gas for impurities contained in it. Rather, the cyclone reduces the amount of impurities, and is usually the first step in a product gas cleaning series consisting of different gas cleaning equipment.

Figure 4-2: Gas Cleaning Cyclone (Van Loo 2008).

Filters

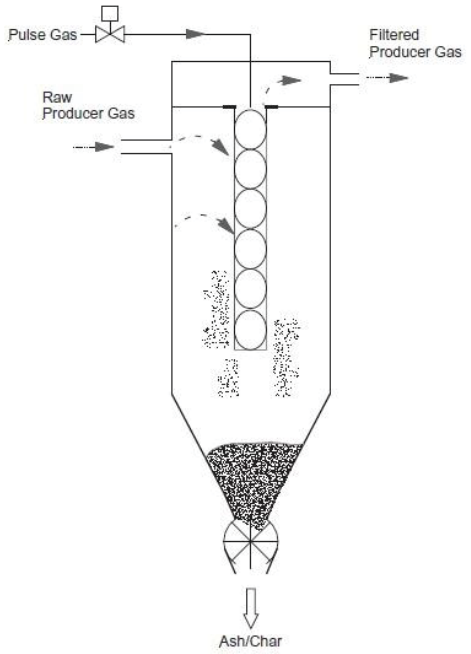

Figure 4-3: Baghouse Cloth Fabric Filter (Neathery, 2010).

There exists a variety of filter devices for product gas cleaning. A common filter type is the *Baghouse Cloth Fabric Filter* (Neathery, 2010). It is illustrated in Figure 4-3. The Baghouse Cloth Fabric Filter is used to capture particles with a diameter smaller than 5 µm in hot gas environments. The device consists of a filter tube fixed into a metal cage letting hot product gas passing through. The device is equipped with a pulse gas pipeline which is controlled manually. The raw product gas enters the filter tube on the upper left hand side as illustrated in Figure 4-3. The filter tube acts as a barrier for gas impurities and only let gas passing through. The impurities are trapped on the outside of the filter tube and form a filter cake. At various time intervals, a pulse gas is back-pulsed through the filter tube, making the filter cake fall down to the bottom of the device where it is removed from the system (Neathery, 2010). The clean product gas is carried by pipelines downstream to the next process plant step.to the supply costs related to the absorbent (T. Patterson, 2011).

The last absorption technology evaluated is the chemical absorption. In *chemical absorption* processes applied to anaerobic digestion processes the absorbent is amine-based chemicals. This improves the absorption of CO_2 and reduces the plant sizes necessarily implemented when compared to scrubbers and physical liquid absorption systems. However, the process requires some heat input in order to regenerate the amine solution prior to recirculation and its maintenance costs are high compared to the other technologies. The amine solvent takes up less methane than the other absorbents, thus reducing the methane losses and improving the environmental feasibility of the process (T. Patterson, 2011). In gasification systems thermal or catalyst cracking can be applied, amd the most common technologies are thermal cracking and catalyst cracking.

Adsorption

Both biogas and product gas may contain many unwanted gas compounds of which can be difficult to remove. Sometimes, only some specific gases needs removal and specific delicate gas cleaning equipment is required for the removal. Adsorption is suitable for these cases. Adsorption describes the adhesion of gas molecules to a surface. Pressure swing adsorption is one of the most common technologies. It can be applied to purify gas mixtures and are based on the ability of adsorbent materials to retain one or more gas components selectively under various pressure conditions. (T. Patterson, 2011). The adsorption technologies are complicated and are therefore not considered in this work. Instead, a technology doing pretty much the same in a simpler manner is considered, namely the permeation technology

Permeation

Permeation describes the gas cleaning technologies where the raw gas is flowing through a permeable membrane. A common permeation technology is membrane separation. During membrane separation, the gas is transferred through a semi-permeable membrane, only allowing specific gas molecules to passing through. CO_2 is effectively removed by the process, whereas H_2O and H_2S are partly removed. The technology possesses relatively low operational and maintenance costs, but is related to high methane losses (T. Patterson, 2011).

Cryogenic Technology

The last technology evaluated for gas cleaning is the cryogenic technology. The *cryogenic technology* uses the boiling points of different gases in the raw gas to separate them from the gas. It is not considered in this work do to its advance, but is a widely used technology for both gas cleaning and other gas conditioning features (T. Patterson, 2011).

4.2.2.Gas Upgrading Technologies

In this work, product *gas upgrading* represents the application of reactions that change the composition of the gas after gas cleaning is performed. Before the gas can be converted to liquid biofuel in the form of Fischer-Tropsch diesel it must be upgraded to syngas. Recall that syngas is defined as a gas consisting of only hydrogen and carbon monoxide in this thesis.

After gas cleaning the gas generally contain carbon dioxide, methane, carbon monoxide and hydrogen. Carbon dioxide and methane can be converted into hydrogen and carbon monoxide. The conversion of the gas constituents to syngas is called shifting. Methane is shifted to syngas by the methane steam reforming and methane partial oxidation. Carbon dioxide is shifted by applying the reverse water-gas-shift reaction. G. Jacobs describe how the removal of methane is done through two reforming reactions (4-1) and (4-2) (G. Jacobs, 2010).

Methane steam reforming by reaction (4-1):

$$CH_4 + H_2O \rightarrow CO + 3H_2 \left(+206\text{kJ/mol} \right), \qquad \textbf{(4-1)}$$

and methane partial oxidation by reaction (4-2):

$$CH_4 + \frac{1}{2}O_2 \rightarrow CO + 2H_2 \left(-36\text{kJ/mol} \right). \qquad \textbf{(4-2)}$$

In most cases it is beneficial to combine the two reactions in order to take advantage of the heat produced in equation (4-2) in equation (4-1)(G. Jacobs, 2010). G. Jacobs also describe how CO_2 can be removed by applying the reverse water-gas-shift reaction (4-3) (G. Jacobs, 2010):

$$CO_2 + H_2 \rightarrow CO + H_2O. \qquad \textbf{(4-3)}$$

Another option is to apply CO_2-hydrogenation, producing a hydrocarbon product and water by reaction (4-4):

$$nCO_2 + 3nH_2 \rightarrow CnH_{2n+1}OH + (2n-1)H_20, n \in 1:4. \qquad \textbf{(4-4)}$$

But equation (4-4) is rather a gas-to-LBF conversion reaction than a gas upgrading technology. The gas, now containing hydrogen and carbon monoxide has been upgraded to a syngas. Before it can be applied to a gas-to-LBF process, the hydrogen-to-carbon monoxide ratio (H2/CO-ratio) must be investigated because there are restrictions on it (G. Jacobs, 2010). The ratio is adjusted by applying the water gas shift reaction (4-5):

$$H_2O + CO \rightarrow CO_2 + H_2 \left(-41.4\ \mathrm{kJ/mol} \right). \qquad \textbf{(4-5)}$$

The syngas containing hydrogen and carbon monoxide can then be converted to a liquid biodiesel fuel by applying one of the gas-to-liquid biofuel conversion technologies presented in chapter 4.3.

4.2.3.Summary of the Gas Conditioning Technologies

For the biochemical process, the gas conditioning system contains a methane reforming reactor that shifts the methane rich raw biogas into a syngas containing hydrogen and carbon monoxide. For the thermochemical process, in which the product gas is expected to contain higher amounts of particulates and tar and lower amounts of methane than the biogas, a baghouse cloth fabric filter is applied to remove the solid particulate impurities.

For both biochemical and thermochemical cases, the gas is still expected to contain impurities like ammonia and hydrogen sulfide after the first gas conditioning stage. Therefore a membrane separation and a water gas shift reactor are applied in both processes. The water gas shift adjusts the hydrogen to carbon monoxide ratio to a ratio suitable for Fischer-Tropsch synthesis. This aspect will be explained in the next chapter 4.3. The membrane separator removes gas impurities from the shifted gas to make it a pure syngas containing only hydrogen and carbon monoxide.

4.3. Gas-to-Liquid Biofuel Conversion

The conversion of syngas to liquid biofuels can be performed by different technologies. Biomass can be converted into fuels like hydrogen, synthetic natural gas, ethanol and Fischer-Tropsch diesel. According to K.Kim et.al the Fischer-Tropsch diesel production from syngas obtained by gasification is a promising technology because the Fischer-Tropsch diesel characteristics are similar to those of conventional diesel (K.Kim, 2013). One important advantage is the high fuel energy density. FT-diesel is sulfur-free and low in aromatics concentration. A study reviewed by G. Jacobs and B. H. Davis suggests that the Fischer-Tropsch synthesis generally is related to low toxic emissions, and substantially lower than that of other gas-to-liquid biofuel conversion processes (G. Jacobs, 2010).

In this work, the Fischer-Tropsch synthesis is chosen as gas-to-liquid biofuel conversion technology. The Fischer-Tropsch synthesis is a catalyzed chemical synthesis conversion of *gaseous* hydrogen and carbon monoxide to *liquid* hydrocarbons and water by the following reaction (4-6) (M.J.A. Tijmensen, 2002):

$$nCO + (2n+1)H_2 \rightarrow C_nH_{(2n+2)} + nH_2O \left(-154\ \mathrm{kJ/mol}\right). \qquad \textbf{(4-6)}$$

The synthesis reaction (4-6) illustrates that the Fischer-Tropsch synthesis produce liquid hydrocarbons ($C_nH_{(2n+1)}$) and water from gaseous hydrogen and carbon monoxide. The subscript *"n"* denotes the number of moles for each constituent, and the hydrocarbons produced can be of different length depending on *n*. In order to produce a Fischer-Tropsch diesel product the hydrocarbon produced must be cracked, resulting in the formation of ethane, gasoline, diesel and waxes (M.J.A. Tijmensen, 2002), (R.S. Kempegowda, 2013). It is preferable to obtain long hydrocarbons in the synthesis reaction (4-6), because this generally leads to the formation of liquid hydrocarbons. To exemplify, gasoline (light crude) is in the range of C_5-C_9 whereas diesel (heavy crude) is in the range of C_{10}-C_{20}. Lighter hydrocarbons in the range of C_1-C_4 are driven off as fuel gas (C.N. Hamenlinck, 2004).

There exist three main types of Fischer-Tropsch synthesis (FT) reactors: the fixed bed FT –reactor, the fluidized bed FT-reactor and the slurry phase FT-reactor of which can be operated at high or low temperature. Low temperature operation is performed at temperatures ranging from 210 to 260 ^oC whereas high temperature operation is performed at temperatures ranging from 330 to 370 ^oC (C.N. Hamenlinck, 2004), (M.J.A. Tijmensen, 2002). The synthesis can be performed by different catalysts where iron catalyst or a cobalt catalyst is the ones most widely used (G. Jacobs, 2010). The choice of catalyst depends on the H_2/CO-ratio of the syngas and temperature. The cobalt-catalyst Fischer-Tropsch process is performed in a temperature range of 200-230^oC at 20 atm (G. Jacobs, 2010). The iron catalyst is performed in a temperature range of 230-270^oC at 20 atm (G. Jacobs, 2010). In this work, a low-temperature cobalt catalyst Fischer-Tropsch synthesis is adopted for

model simulations from a model developed by post.doc R.S. Kempegowda (R.S. Kempegowda, 2013).

A clean gas is essential for Fischer-Tropsch synthesis application. The Fischer-Tropsch catalysts are sensitive to chlorine and sulfur compounds which may inhibit their catalytic activity. Tar and alkaline metals can be deposited on the catalysts and lead to catalyst poisoning. Particles and acid gases like hydrogen sulfide cause fouling and impose corrosive effects in equipment (G. Jacobs, 2010). Thus the concentration of these compounds must be minimal. Typical syngas specifications for the application for Fischer-Tropsch synthesis are given in Table 4-7 as presented in (A. vanderDrift, 2004):

Compound	**Concentration Limit**
Sulfur compounds (H2S, COS, CS_2)	< 1 ppmv
Nitrogen compounds (NH_3, HCN)	< 1 ppmv
Halide compounds (HCl, HBr, HF)	< 10 ppbv
Alkali metals (Na, K)	< 10 ppbv
Particles (soot, ash)	Complete removal

Table 4-7: Typical Syngas Specifications for FT-synthesis. Source: A. vanderDrift, 2004

Table 4-7 illustrates that sulfur compounds, nitrogen, halides alkali metals and particles must be completely removed in practice. Also, the H_2/CO-ratio in the syngas input to the synthesis must be investigated. The ratio should not exceed 2:1 and not be less than 0.7:1 (G. Jacobs, 2010). The ratio is adjusted by the water-gas-shift equation as described in chapter 4.2. The requirements listed in Table 4-7 are taken care of in the upstream processes of gas conditioning as described in chapter 4.2.

4.4. Summary of the Biochemical and Thermochemical Pathways

To this point, two conversion pathways for the conversion of lignocellulose in the form of birch to liquid biofuel in the form of Fischer-Tropsch diesel have been identified. The two pathways each contain 5 separate processes, and the technologies chosen for each of these processes are based on the theoretical techno-economic evaluation performed in chapters 3 and 4. The processes are summarized in Table 4-8 and Table 4-9.

Table 4-8: Conversion Pathway Biochemical Plant.

Table 4-9: Conversion Pathway Thermochemical Plant.

Table 4-8 shows the conversion pathway for the biochemical plant whereas Table 4-9 show the conversion pathway for the thermochemical plant. As can be seen from the tables the evaluation resulted in identical biomass pretreatment processes, identical final gas conditioning step and Fischer-Tropsch synthesis for both processes. The evaluation also resulted in one dry batch anaerobic digester followed by methane reforming for the biochemical plant, and bubbling fluidized bed gasification with an integrated cyclone and a baghouse cloth fabric gas filter for the thermochemical plant.

5. Model Development in Aspen Plus

To this point, two pathways for the conversion of lignocellulose to liquid Fischer-Tropsch diesel have been identified. The two pathways each contain 5 separate processes, and the technologies chosen for each of these processes are based on the theoretical techno-economic evaluation performed in chapters 3 and 4, and the results of the evaluation where presented in tables 4-8 and 4-9 in chapter 4. The purpose of developing the pathways are to generate as much usable energy as possible to as low cost as possible, which leads to economic challenges being related to the energy consumed and utilized by the process pathways. Therefore, it is of interest to predict the net energy yield of the processes, considering the phase changes of the solid biomass input to a gaseous biofuel and thereafter a liquid biofuel. To being able to analyze these pathways in terms of energy utilization, two models have been developed in the simulation software Aspen Plus, supplied with declarations made in FORTRAN code.

Aspen Plus is a process-simulation software that enables easy process modeling. By developing a process model on a flow sheet and by specifying chemical components and operational conditions the software can simulate the process and hence predict its behavior. It is used in the chemical industry to improve or optimize process plants (aspentech). *FORTRAN* is an acronym for FORmula TRANslation, and is a programming language for numerical applications. One of its most important features is its portability, making it easily moved from one computer system to another (valhalla, 2001). It can be integrated in Aspen Plus to manipulate variables. Details on how it works are provided throughout this chapter.

To be able to develop a model for the entire plant, a simulation model developed in Aspen Plus by post doctor R. Kempegowda has been used as a simulation basis (Kempegowda). The model originally consisted of a separate pretreatment process, an entrained flow gasification process, two gas conditioning processes and a Fischer-Tropsch synthesis. For the biochemical plant developed in this work, the pretreatment process and the Fischer-Tropsch synthesis is adopted from R. Kempegowda whereas the gasification and gas-conditioning processes have been adjusted.

5.1. Model Description of Biochemical Plant

Figure **5-1** gives a simplified plant overview of the *biochemical* biomass-to-biofuel conversion plant that is developed in this work. The figure is applied to illustrate the basic concepts of the model that is developed and do not go into the model details. A detailed model description will be given in chapter 5.1.2. The biochemical scenario is a 873 ton per day 150 MW dry birch-fed anaerobic

digestion bio refinery that produces liquid hydrocarbons and fuel gas to be used as a biofuel feedstock. This amount of biomass is necessary to provide a 150 MW input basis and is based on birch calorific value. The 150 MW basis is chosen as an realistic estimate for medium to large scale application in Mid-Norway (Kempegowda). The plant is divided into six areas denoted by the nomenclature A100, A200, A300, A400, A500 and A600 respectively. The areas represent the separate processes of the plant and will be described in the following. The components in Figure **5-1** represents plant components like reactors and heat exchangers. The arrows in the figure represent mass flows and Table 5-1 shows a diagram that summarize the mass flow values obtained from simulations measured in ton/day. The values will be analyzed in chapter 6.

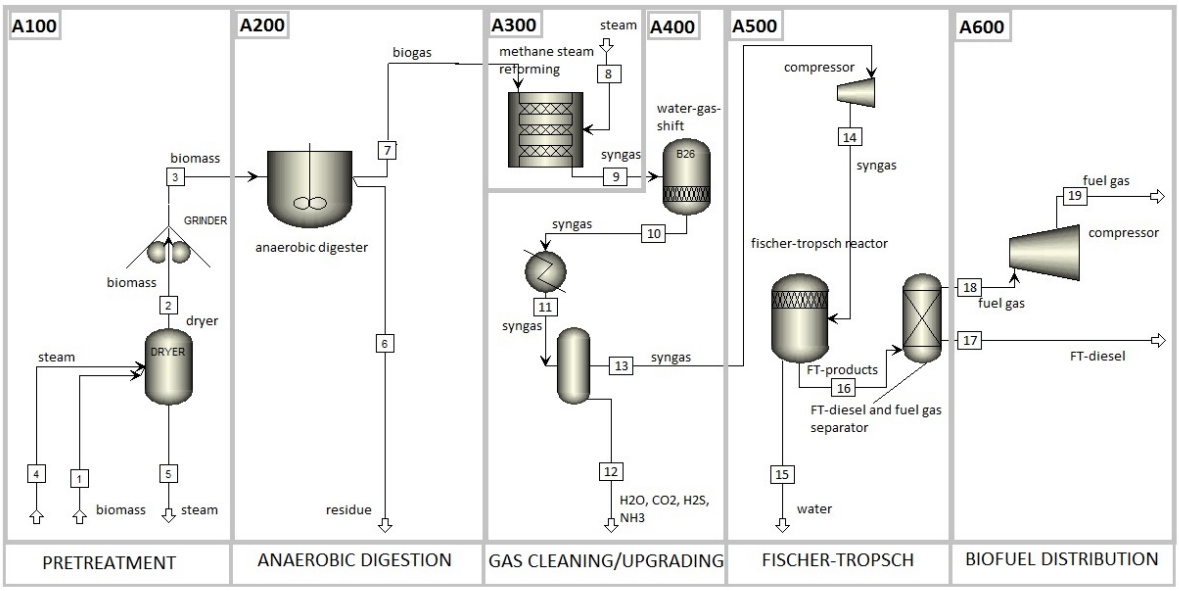

Figure 5-1: Plant overview, Biochemical Biomass-to-biofuel Conversion Plant.

Flow	1	2	3	4	5	6	7	8	9	10
Mass flow (ton/day)	873.34	727.76	727.76	1310.00	1310.00	279.10	493.54	332.64	826.22	826.22
Flow	11	12	13	14	15	16	17	18	19	
Mass flow (ton/day)	826.22	524.26	644.39	644.39	183.42	461.03	137.67	323.30	323.30	

Table 5-1: Plant flow values, Biochemical Biomass-to-biofuel Conversion Plant.

Biomass pretreatment (A100) represents the drying and grinding of the raw biomass feedstock to 50 mm size and 10% moisture content (chapter 4). Anaerobic digestion (A200) represents a dry batch anaerobic digestion process. Area A300 represents methane reforming of the raw biogas, which upgrades it into a raw syngas. Area A400 represents a second gas upgrading by water gas shift and the removal of gas impurities by membrane separation. Fuel synthesis (A500) represents Fischer-Tropsch synthesis, and area A600 represents the separation of liquid and gaseous biofuel. In

the following sections, processes A100 and A400-A600 will be given brief introductions for the purpose of basic understanding. Process A200 and A300 are developed in this work and will be described in chapter 5.1.3 and 5.1.4.

5.1.1.Process Description

Area A100: Biomass Steam Pretreatment

The biomass pretreatment area includes all operations required for preparing the raw biomass to be used as a feedstock for anaerobic digestion. 873 ton/day biomass enters the pretreatment area (flow 1 Figure **5-1**) (wet basis) at 22% moisture. Recall that the birch lower heating value equals 14.83 MJ/kg and 150 MW input thus correspond to 873 ton input. The moisture content is 6% larger than the biomass moisture content given in the proximate analysis of the birch (table 2.2, chapter 2) to compensate for extrinsic moisture content. Recall from chapter 2 that extrinsic moisture content is moisture absorbed by the material as a result of surrounding humid weather conditions. The biomass enters a direct-contact steam dryer, where the biomass is heated and decomposed with steam (flow 4, 5 Figure **5-1**). 1310 ton/day steam is utilized in the process, which is a value obtained from similar simulations performed by R.S. Kempegowda (R.S Kempegowda, 2013). 145 ton/day moisture evaporates from the biomass, which leaves the dryer with a moisture content of 10% (not shown in Figure **5-1**). The biomass is next grinded (flow 2, Figure **5-1**) in a biomass crusher designed to grind the biomass into particles of 50 mm size (flow 3, Figure **5-1**). The grinding into 50 mm sizes may seem arbitrary. It is a result of the same pretreatment being used for the gasification, where biomass particulate size is a dimensioning factor. The grinding makes the hemicellulose more available for the anaerobic microorganisms in the next process step. The steam dryer is assumed to be constructed as an open cycle, enabling the mixing of steam and biomass before drying. The steam dryer thus serve as a mild steam pretreatment process that further improves hemicellulose availability for the anaerobic microorganisms in the next process step in accordance with chapter 4.

Process A200: Dry Batch Anaerobic Digestion

The biomass-to-biogas conversion process consists of an anaerobic dry batch digester converting 728 ton/day dry biomass (flow 3, Figure **5-1**) to 494 ton/day raw biogas (flow 7, Figure **5-1**) and 279 ton/day digester residue (flow 6, Figure **5-1**). The anaerobic digestion process is modeled by using Aspen Plus and FORTRAN and will be presented in detail in chapter 5.1.3.

Process A300: Methane Reforming

494 ton/day raw biogas enters the first step of gas conditioning (flow 7, Figure **5-1**). Biogas is a gas rich in methane, and therefore the first step of gas conditioning is a methane reforming process, converting methane to carbon monoxide and hydrogen by the addition of 332 ton/day steam (flow

8, Figure **5-1**). Recall from chapter 4.2.4 the steam-methane reforming reaction, which converts methane to carbon monoxide and hydrogen by the addition of steam, and the amount of steam is estimated based on this equation. The biogas leaving the methane reforming makes up 826 ton/day (flow 9, Figure **5-1**). The gas now consists of mostly hydrogen and carbon monoxide, and it has thus been converted from raw biogas to a raw syngas. The methane reforming is modeled by using Aspen Plus and FORTRAN and will be presented in detail in chapter 5.1.4.

Process A400: Water Gas Shift and Membrane Separation

The biogas leaving the first syngas cleaning process (flow 9, Figure **5-1**) makes 826 ton/day and must be cleaned to only contain H_2 and CO before the gas can be applied to the Fischer-Tropsch synthesis. Also, recall from chapter 4.3 that the H_2/CO-ratio should be increased to 2.1 before Fischer-Tropsch synthesis can be applied. The second gas cleaning step preferably removes H_2S, NH_3 and increase the H_2/CO-ratio. The raw syngas undergoes a water gas shift where the gas is mixed with 342 ton/day steam (not shown, Figure **5-1**) to enhance the water gas shift-reaction. Recall from chapter 4.2.4 that the water gas shift reaction transforms carbon monoxide to hydrogen and carbon dioxide by the addition of steam. Thus steam requirement is based on the water-gas-shift reaction rate (flow 10, 11, Figure **5-1**). Water is rejected from the syngas after the WGS reactor (not shown, Figure **5-1**) and gas impurities removal is performed by membrane separation. 524 ton/day of gas impurities are extracted from the syngas (flow 12, Figure **5-1**) and the syngas, now makes up 644 ton/day (flow 13, Figure **5-1**).

Process A500: Fischer-Tropsch Synthesis

The Fischer-Tropsch synthesis converts 644 ton/day syngas to 461 ton/day liquid biofuel and fuel gas (flow 16, Figure **5-1**). The main operations in this process are the FT-synthesis reaction and FT-product separation processes. The syngas is compressed before entering the synthesis (flow 14, Figure **5-1**). The FT-synthesis takes place in a reactor where the syngas is converted to a 138 ton/day liquid biofuel (flow 17, Figure **5-1**). Remaining gas results in 323 ton/day of fuel gas that can be compressed and used as a transportation fuel or injected to the gas grid (flow 18, 19, Figure **5-1**). The separation of the fuel gas from the liquid FT-diesel is performed by a separator. A part of the fuel gas are compressed and re-injected into the FT-reactor. The separation of 183 ton/day water (flow 15, Figure **5-1**) from the FT-diesel and fuel gas is performed in a flash tank before the fuels are ready for commercial use.

Area A600: FT-diesel and Fuel-gas Separation and Distribution

The products from the Fischer-Tropsch synthesis are 138 ton/day Fischer-Tropsch diesel, 323 ton/day fuel gas and 138 ton/day water. In Figure **5-1**, area 6 describes the separation of gaseous and liquid biofuel. In the following chapters area 6 is merged with area 5 (the Fischer-Tropsch synthesis) for simplicity and will not be considered any further in this work.

5.1.2.Detailed Model Descriptions, Biochemical Plant

The biochemical plant has now been introduced, and it is time to delve into the modeling details of the plant. The part of the plant that has been modeled in this work constitutes the dry batch anaerobic digester (area A200) and the methane reforming (area A300). Hence, these processes are described in detail in the following. The other processes are developed by R.Kempegowda and is described in appendix I. The model is developed by using Aspen Plus and FORTRAN declarations, as outlined in the chapter 5 introductions. To understand the models it is essential to understand the nomenclature used when building up the model as well as how Aspen and FORTRAN works. Aspen Plus, FORTRAN and the specific nomenclature used when developing the model will be presented in the following, followed by introductions to the biochemical pathway model, the dry batch anaerobic digestion and the methane reforming models in chapter 5.1.3 and 5.1.4. The dry batch anaerobic digestion and the methane reforming models are described by evaluating each process block separately and by expressing the process conditions numerically.

Aspen Plus and FORTRAN

Aspen Plus is a tool that link process components together with mass flows to simulate a process. The tool allows for values on mass composition and mass flow rates and operational conditions like temperature and pressure. The process components can also be specified in order to perform chemical reactions, where details considering heats of reaction among others can be specified. It is a step-by-step simulator, calculating the mass flows of the process by numerical iterations. In general it manipulates predefined mass flows by splitting and mixing mechanisms. Sometimes, we want to perform operations that Aspen Plus cannot do by itself. Consider a process component in Aspen Plus that works as a combustion unit, combusting biomass by the addition of oxygen (and energy, but it is excluded from this simple example). The biomass flow is defined in Aspen Plus, and we want to estimate the amount of oxygen (which is also considered a mass flow) that is required for the combustion. The required amount of oxygen follows constant oxygen to biomass ratio and will vary with varying biomass input flow. This cannot be modeled in Aspen Plus alone. Instead, we use an external mathematical commando to perform the operation. This mathematical commando is performed by the FORTRAN calculator.

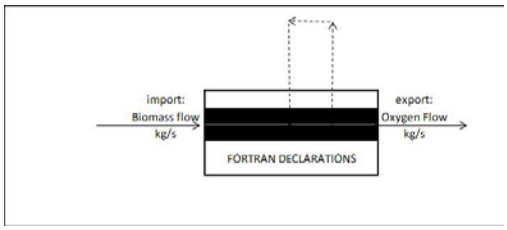

Figure 5-2: FORTRAN execution in Aspen Plus, example.

To understand the models it is essential to understand the usefulness of adding external calculators in Aspen Plus. External calculators can be seen as manipulators that force Aspen to take specific conditions into consideration. illustrate how the FORTRAN calculator works. The figure represents a FOTRAN calculator, represented by a square block. The block calculates the oxygen demand for a combustion reaction based on the amount of fuel input to the combustion. The fuel is biomass, and is indicated by the biomass input flow on the left side of the calculator block. This

flow is an *import* flow. Import flows can be a flow or a parameter defined in Aspen Plus. The desired output is a specific amount of oxygen. If it is known that oxygen demand is 10 % of the biomass input, the FORTRAN block manipulates the flow by stating that:

$$\text{Oxygenflow} = \text{Biomassflow}*0{,}10 \qquad (5\text{-}1)$$

This is the FORTRAN declaration. FORTRAN is integrated into Aspen Plus, and by establishing a new calculator in Aspen Plus and write the statement in equation (5-1) in addition to define import and export variables the declaration is understood by Aspen Plus and performed in simulations. Calculators used in the model are described in appendix II. Now, the oxygen output flow will be following this declaration, and the oxygen flow is an *export flow.* The export flow is not a constant flow as it will vary with varying biomass input flow. This is illustrated by the dotted arrows in .

Stream/Block Nomenclature

In this work, all the blocks and flows modeled in Aspen Plus follow a specific notation in order to present the model with consistency and clarity through the processes. The notation methodology is taken from a NREL-report made by R.M. Swanson et.al (R.M. Swanson, 2010). Each area in the model (area A200 anaerobic digestion for example) has a two-letter abbreviation (AD for anaerobic digestion area) that is used for naming both flows and blocks. The abbreviation is chosen to be descriptive (like BMAS for describing biomass flows). In Aspen Plus software flow and block names can consist of 8 blocks in maximum. The notation for flows, blocks, heat flows and work flows are given as follows in Table 5-2, Table 5-3, Table 5-4 and Table 5-5. Table 5-2 shows the notation for model flows, exemplified by biomass flow number six in the anaerobic digestion area.

Area		Number		Name			
A	D	0	6	B	M	A	S

Table 5-2: Flow nomenclature used in model.

Table 5-3 shows the notation for model blocks, exemplified by reactor block number one in the anaerobic digestion area.

Area		Name				Number	
A	D	R	E	A	C	0	1

Table 5-3: Block nomenclature used in model.

Table 5-4 shows the notation for model heat flows, exemplified by heat flow from reactor one in the anaerobic digestion area.

Q or W		Area		Name			Nr
Q	-	A	D	R	E	A	1

Table 5-4: Heat flow nomenclature used in model.

Table 5-5 shows the notation for model work flows, exemplified by work flow from reactor one in the anaerobic digestion area

Q or W		Area		Name			Nr
W	-	A	D	R	E	A	1

Table 5-5: Work flow nomenclature used in model.

Table 5-6 contains a detailed description of the abbreviations for areas, blocks and flows used in the model. Area enumeration is given in column one, followed by a short area description in column two. Area name is given in column three. The blocks used in the model are described in column four, and their model name is given in column 5. The flows used in the model are described in column six, followed by the flow name in column seven.

Area	Description	Name	Block	Name	Flow	Name
Plant	All Areas	PL	Heater	HEAT	Biomass	BMAS
A100	Pretreatment	PR	Dryer	DRY	Steam	STM
A100DRY	Drying	DR	Grinder	GRIN	Water	WAT
A100GRIN	Grinding	GR	Separator	SEPR	Oxygen	OXYG
A200	Anaerobic Digestion	AD	Mixer	MIXR	Char	CHAR
HV101	HHV/LHV	HV	Decomposer	DCOM	Raw Biogas /Syngas	SYNG
A200ELEM	Biomass Decomposition	EL	Reactor	REAC	Gas Impurities	IMPU
A300	Methane Reforming	MR	Cyclone	CYCL	Heat	Q-HEA
A400	Water Gas Shift, Membrane Sep	CL	Compressor	COMP	Acid Gas	AGAS
A400WGS	Water Gas Shift	WG	Duplicator	DUPL	Compressor Work	W-CMP
A500	Fuel Synthesis	FS	Gas Cleaning Filter	FILT	Fischer-Tropsch fuel	FTRO
HHVF	HHV/LHV	HV	Membrane Separator	AGAS	Syngas Separated from FT-fuel	SGA
					Fuel Gas	FGAS

Table 5-6: Description of abbreviations for areas, blocks and flows used in Aspen Plus model.

The Aspen Plus Model

An overall process flow diagram for the biochemical pathway was introduced in the beginning of chapter 3 to describe the main features of it. The pathway as it appears in Aspen Plus is illustrated in Figure 5-3. It is divided into five hierarchies, each represented by an area block. The hierarchies represent the different steps in the biomass-to-biofuel production plant. Block A100 represents the biomass steam pretreatment, block A200 represents the anaerobic digestion process, block A300 represent methane reforming, block A400 represents water gas shift and membrane separation

and block A500 represents the Fischer-Tropsch synthesis. Together these five blocks represent the biochemical biomass-to-biofuel conversion pathway.

The mass input and output flows for each block is indicated by arrows in Figure 5-3. The pretreatment process A100 represents the steam drying and milling of biomass. The raw biomass input to block A100 is indicated by flow PL00BMAS. The process requires steam for heating and decomposition of the raw biomass which is indicated by the input flow PL81STM. The steam output flow from block A100 is PL84STM. The excess moisture extracted from the dried biomass is indicated by the output flow PL92WAT, and the pretreated biomass ready for anaerobic digestion is the flow PL06BMAS from block A100 to anaerobic digestion in block A200. The modeling details are described in appendix I, figure I-1 to I-3.

The mass balance for the anaerobic digestion process represented by block A200 in Figure 5-3 includes one input -and two output flows. The pretreated biomass flow PL06BMAS from block A100 is the input flow. The anaerobic digestion products include a raw biogas output flow indicated by PL21BGAS from block A200 and a residue output flow indicated by PL22RESD from block A200. The modeling details are described in chapter 5.1.3.

The raw biogas enters the methane reforming block A300 as flow PL21BGAS. The products of the methane reforming are a raw syngas output flow PL32SYNG. The output flow PL33IMPU represents eventual excess steam or gas impurities related to the methane reforming. The modeling details are described in chapter 5.1.4.

Block A400 represents gas upgrading by water-gas-shift and gas cleaning by membrane separation. The syngas flow PL32SYNG and steam flow PL85STM are input flows to block A400. The output flows are a clean syngas PL41SYNG and impurities rinsed out of the syngas PL42AGAS. The modeling details can be viewed in appendix I, figure I-5 and I-6.

Block A500 represents the Fischer-Tropsch synthesis which converts the syngas to a liquid fuel. The syngas input flow PL41SYNG is converted to a Fischer-Tropsch diesel PL53FTRO and a fuel gas PL52FGAS. The detailed process description can be viewed in appendix I, figure I-7.

In the next chapters 5.1.3 to 5.1.4, the anaerobic digestion block A200 and the methane reforming block A300 is described in detail.

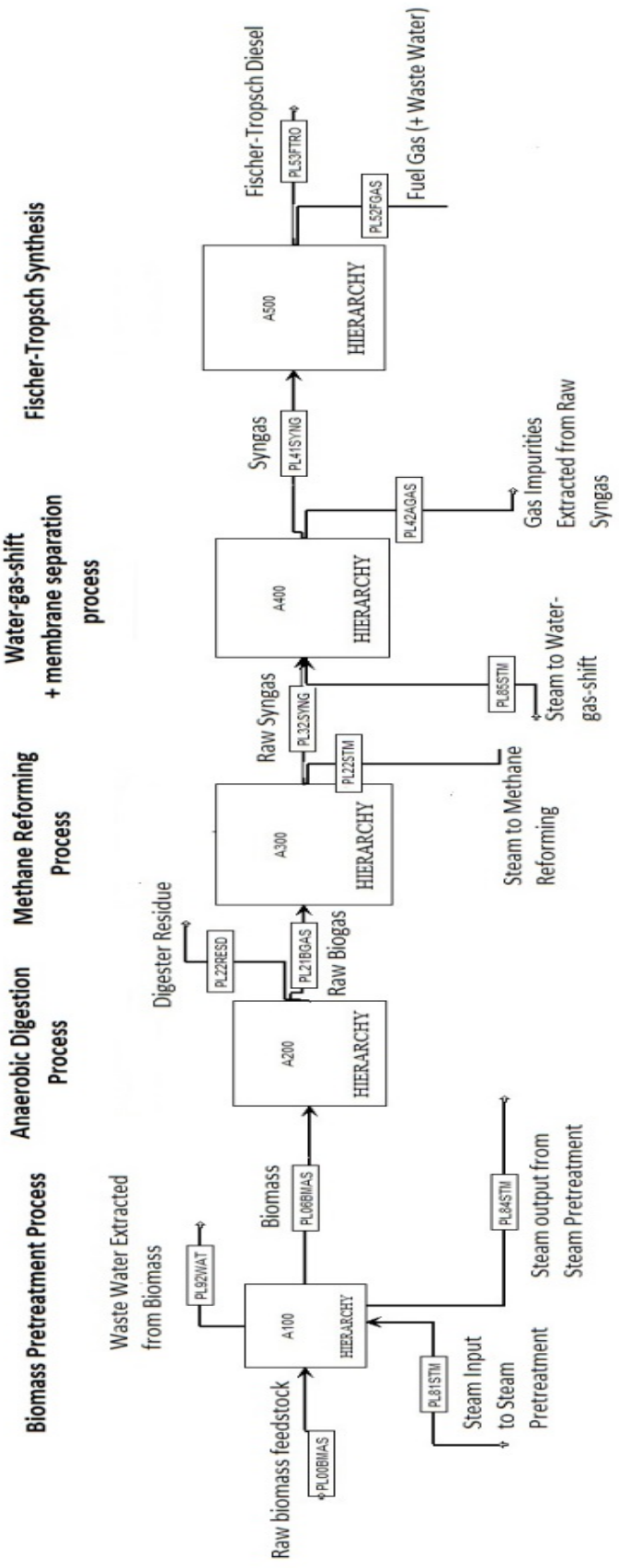

Figure 5-3: The Biochemical Plant in Aspen Plus.

5.1.3.Area A200: Aspen Plus Dry Batch Anaerobic Digestion

The Aspen Plus dry batch anaerobic digestion model is illustrated in Figure 5-4. By clicking on the hierarchy block A200 in Figure 5-3 the model appears. It consists of a heating value calculator HV101 and an anaerobic digester reactor ADREAC01.

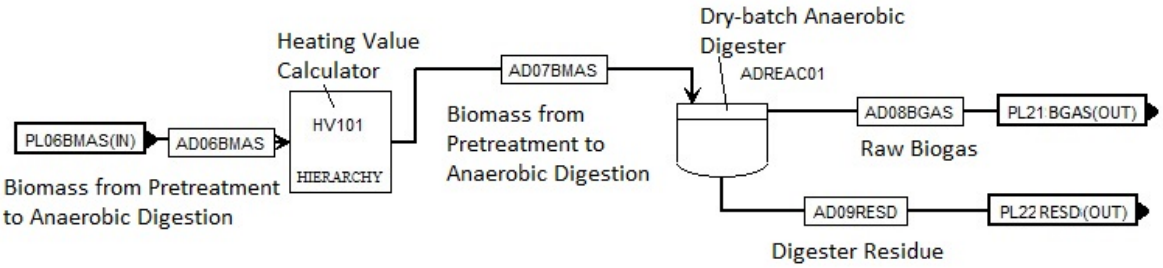

Figure 5-4: Area A200: Dry Batch Anaerobic Digestion modeled in Aspen Plus.

The heating value calculator calculates the higher and lower heating values of the biomass input flow AD06BMAS. This flow is an input flow from the overall process plant (Figure 5-3) as indicated by PL06BMAS(IN). The calculator is made in FORTRAN and the declaration is described in appendix II. It does not affect the biomass flow, and AD07BMAS is equal to AD06BMAS in composition and magnitude.

The block ADREAC01 represents the dry batch anaerobic digestion process. It is modeled by using a batch reactor in Aspen Plus. The *batch reactor* allows for setting a constant reactor temperature and biomass residence time. Anaerobic digestion operation is complex and involves several reaction steps including the decomposition of fats, carbohydrates and protein of which form gas and acids as explained in chapter 3.1. The task to identify and model all these reactions is not the scope of this thesis. The reactor also needs to operate anaerobically, which means in excess of oxygen. The batch reactor provides no such mode of operation. The batch reactor has been manipulated to act as an anaerobic digester by integrating a FORTRAN calculator to it. The calculator sets a specific biogas concentration based on theoretical values on biogas yield. Typical biogas yields from biomass anaerobic digestion were obtained from reports on biogas generation made by A. Petersson and M.C. Bjune (A. Petersson, 2008), (Bjune, 2009), and where introduced in chapter 3.2. The FORTRAN declarations are described in appendix II. The numerical values determined in Aspen Plus are specified in Table 5-7.

The resulting output flows are the raw biogas product AD08BGAS and the digester residue AD09RESD. The flows leave block A200 as indicated by PL21BGAS(OUT) and PL22RESD(OUT) in Figure 5-4.

Specifications		Operation times	
Pressure	1.01 bar	total cycle time	30 days
Temperature	303 K	maximum calculation time	30 days

Table 5-7: Numerical values, Anaerobic Reactor.

5.1.4.Area A300: Methane Reforming

The Aspen Plus Methane Reforming converts the raw biogas into a raw syngas by applying methane reforming as described in chapter 4.2.4. The Aspen Plus model is illustrated in Figure 5-5. This model occurs when clicking on hierarchy block A300 in Figure 5-3.

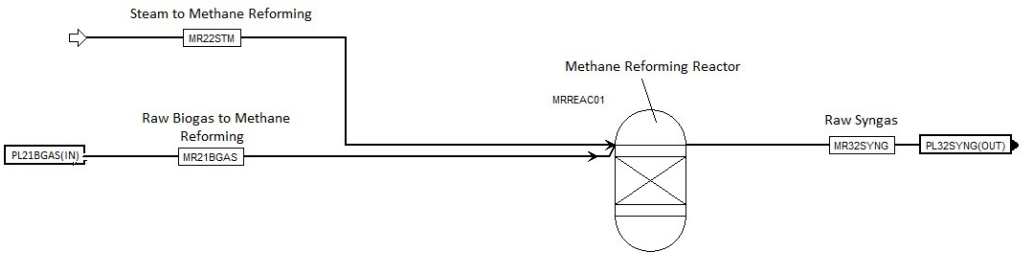

Figure 5-5: Aspen Plus Steam Reforming Process.

Raw biogas MR21BGAS is entering the methane reforming reactor MRREAC01. The flow PL21BGAS(IN) illustrates that it is an input flow from the plant (Figure 5-3). Steam MR22STM is required for the reforming reaction. The raw syngas MR32SYNG is transported out to the plant via the PL32SYNG flow. The reactor chosen for the reforming reaction is a Gibbs reactor.

The *Gibbs Reactor* follows the Gibbs equilibrium, which is the equilibrium where chemical potential is minimized for constant temperature and pressure. The reactions that are taking place needs to be specified, and consist of the methane reforming reaction (reaction 4-1, chapter 4.2.2). Then, operation temperature, pressure and restricted conditions are set. Temperature and pressure is obtained from R. Kempegowda (Kempegowda). The methane reforming conditions are summarized in Table 5-8.

Specifications		Products	Restricted Equilibrium
Temperature	498.15 K	H2	Individual Reaction:
Pressure	2.8 bar	CO	CH4+H2O→CO+3H2
Restrict Chemical Equilibrium - specify T approach		H2S	
Include vapor phase		NH3	

Table 5-8: Numerical Values, Methane Reforming Reactor

The calculation is done in Aspen Plus automatically by restricted chemical equilibrium for a specified temperature. The allowed products are specified to include hydrogen, carbon monoxide, hydrogen sulfide and ammonia only. The Gibbs reactor thus makes it possible to force which products are allowed to being made in the reforming.

5.2. Model Description of Thermochemical Plant

The thermochemical biomass-to-biofuel conversion pathway is based on bubbling fluidized bed gasification and is developed from the same Aspen Plus model basis as the one presented for the biochemical model. Figure 5-6 gives a simplified plant overview. The thermochemical scenario is a 873 ton/day 150 MW dry birch-fed bubbling fluidized bed gasification biorefinery that produces liquid fuel and fuel gas to be used as a biofuel feedstock, similar to the biochemical plant in chapter 5.1. The only changes made are done to area A200 and A300, where the anaerobic digestion process is replaced with a bubbling fluidized bed gasification process in area A200, and the methane reforming is replaced with a gas filtration device. The gas conditioning requirement is also changed, by replacing the steam reforming from the biochemical plant with a baghouse cloth filter in area A300. These changed can be observed in Figure 5-6. The mass flow values are presented in Table 5-9.

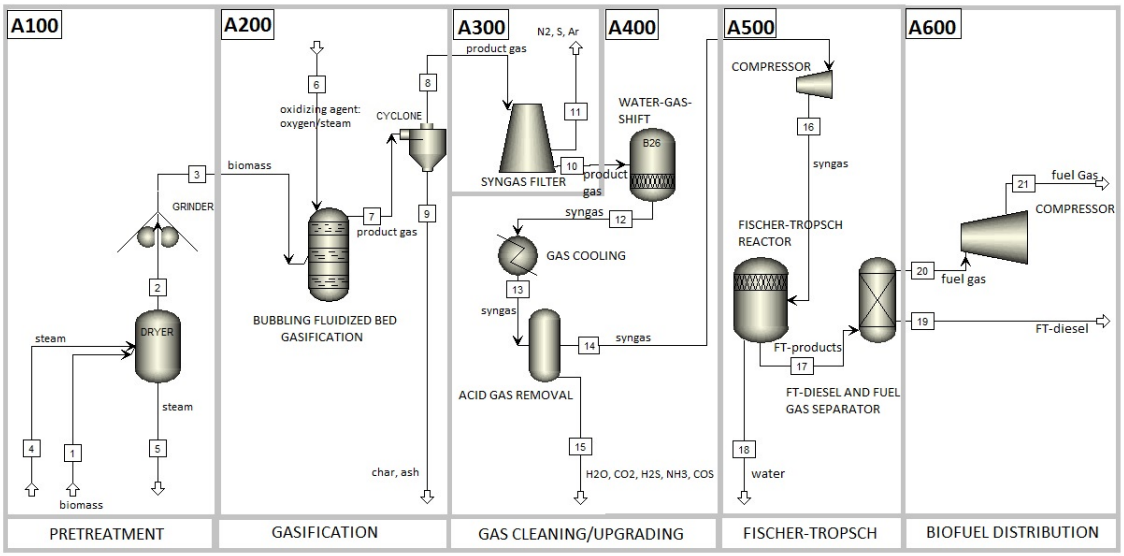

Figure 5-6: Plant overview, Thermochemical Biomass-to-biofuel Conversion Plant.

Flow	1	2	3	4	5	6	7	8	9	10	11
Mass flow (ton/day)	873.34	727.78	727.78	1310.00	1210.00	300.00	1028.16	1027.97	0.19	922.69	105.28
Flow	12	13	14	15	16	17	18	19	20	21	
Mass flow (ton/day)	922.69	922.69	296.10	673.92	296.10	222.79	73.31	53.12	169.67	169.67	

Table 5-9: Plant flow values, Thermochemical Biomass-to-biofuel Conversion Plant.

Biomass pretreatment (A100) represents the drying and grinding of the raw biomass feedstock to 50 mm size and 10% moisture content to meet the required biomass particulate size for bubbling fluidized bed gasifiers as discussed in chapter 3.2. Gasification (A200) represents a bubbling

fluidized bed gasification biomass-to-biogas conversion process. Area A300 represents gas filtering with a baghouse cloth filter. Area A400 represents gas upgrading by water gas shift and the removal of gas impurities by membrane separation. Fuel synthesis (A500) represents Fischer-Tropsch synthesis and area A600 represents the separation of liquid and gaseous biofuel. In the following subchapters, processes A100 and A300-A600 will be given brief introductions for the purpose of basic understanding. Process A200 is developed in this work and will be described in chapter 5.2.2. Process A300, together with the other processes obtained from R.S. Kempegowda are described in appendix I.

5.2.1.Process Description

Area A100: Biomass Drying and Grinding Pretreatment

The biomass pretreatment area includes all operations required for preparing the raw biomass to be used as a feedstock for gasification. The process is equal to the biochemical pretreatment process and is described in detail in chapter 5.1.1.

Process A200: Bubbling Fluidized Bed Gasification

The biomass-to-biogas conversion process consists of a bubbling fluidized bed gasifier converting 728 ton/day dry biomass (flow 3, Figure 5-6) to 1028 ton/day raw product gas (flow 7, Figure 5-6). The gasification furnace is supplied with 300 ton/day oxidation agent (flow 6, Figure 5-6). The oxidation agent consist of oxygen and steam mixed at a 40/60 ratio based on a report made by NREL (R.M. Swanson, 2010) as discussed in chapter 3.2. The amount of oxidation agent supplied to the process is obtained by calculations as will be explained in chapter 5.3.3. The raw product gas flows through a cyclone (flow 7, Figure 5-6) where 0.19 ton/day ash is separated from the product gas (flow 9, Figure 5-6). The gasification process is modeled by using Aspen Plus and FORTRAN and will be presented in detail in chapter 5.2.2.

Process A300: Baghouse Cloth Filtering

1028 ton/day raw product gas enters the baghouse cloth filter (flow 8, Figure 5-6). The gas must be conditioned to syngas quality before Fischer-Tropsch synthesis can be applied. Recall from chapter 4.3 that the maximal amount of contaminants allowed in the gas is small, and the baghouse cloth filter absorbs carbon, tar and ash from the gas. The syngas leaving the A300 process makes 923 ton/day (flow 10, Figure 5-6). Carbon, tar and ash are completely removed and makes 105 ton/day (flow 11, Figure 5-6).

Process A400: Gas Cleaning Part 2

The product gas leaving the baghouse cloth filter (flow 9, Figure 5-6) makes 923 ton/day. The process is similar to area A400 of the biochemical plant as described in chapter 5.1.1. The water-gas-shift reactions require a steam input of 47 ton/day (not shown, Figure 5-6). 674 ton/day of gas

impurities are extracted from the syngas (flow 15, Figure 5-6) and the syngas now makes up 296 ton/day (flow 14, Figure 5-6).

Process A500: Fischer-Tropsch Synthesis

The Fischer-Tropsch synthesis is similar to the one described for the biochemical plant in chapter 5.1 but the mass flows are different. Here, it converts 296 ton/day syngas to 223 ton/day liquid biofuel and fuel gas (flow 17, Figure 5-6). The syngas is converted to a 53 ton/day liquid biofuel (flow 19, Figure 5-6) and 170 ton/day of fuel gas (flow 20, 21, Figure 5-6). The separation of 73 ton/day water (flow 18, Figure 5-6) from the FT-diesel and fuel gas is performed before the fuels are ready for commercial use.

Area A600: FT-diesel and Fuel-gas Separation and Distribution

The products from the Fischer-Tropsch process are a FT-diesel, a fuel gas and water. In the following chapters area 6 is merged with area 5 (the Fischer-Tropsch synthesis) for simplicity and will not be considered any further.

5.2.2.Detailed Model Descriptions, Thermochemical Plant

The plant has now been briefly described, and it is time to delve into the modeling details of it. The model is developed by using Aspen Plus and FORTRAN declarations, and follows the same procedure as outlined for the biochemical plant. The steam and block nomenclature is the same and can be reviewed in chapter 5.1.2.

The abbreviations have been changed to some extent and Table 5-10 contains a detailed description of the abbreviations for areas, blocks and flows used in the thermochemical model. Area enumeration is given in column one, followed by a short description in column two. The area name is given in column three. The blocks used in the model are described in column four, and their model name is given in column 5. The flows used in the model are described in column six, followed by the flow name in column seven.

Area	Description	Name	Block	Name	Flow	Name
Plant	All Areas	PL	Heater	HEAT	Biomass	BMAS
A100	Pretreatment	PR	Dryer	DRY	Steam	STM
A100DRY	Drying	DR	Grinder	GRIN	Water	WAT
A100GRIN	Grinding	GR	Separator	SEPR	Oxygen	OXYG
A200	Gasification	GS	Mixer	MIXR	Char	CHAR
HV101	HHV/LHV	HV	Decomposer	DCOM	Product gas /Syngas	SYNG
A200ELEM	Biomass Decomposition	EL	Reactor	REAC	Gas Impurities	IMPU
A300	Product Gas Cleaning 1	GC	Cyclone	CYCL	Heat	Q-HEA
A400	Product Gas Cleaning 2	CL	Compressor	COMP	Acid Gas	AGAS
A400WGS	Water Gas Shift	WG	Duplicator	DUPL	Compressor Work	W-CMP
A500	Fuel Synthesis	FS	Gas Cleaning Filter	FILT	Fischer-Tropsch fuel	FTRO
HHVF	HHV/LHV	HV	Acid Gas Removal	AGAS	Syngas Separated from FT-fuel	SGA
					Fuel Gas	FGAS

Table 5-10: Detailed description of area, block and flow nomenclature.

The Aspen Plus Model

An overall process flow diagram was introduced in the beginning of chapter 5.2 to illustrate the main features of the thermochemical biomass-to-biofuel plant. The plant as it appears in Aspen Plus is illustrated in Figure 5-7. It is divided into five hierarchies, each represented by a block. The hierarchy blocks represent the different steps in the biomass-to-biofuel conversion pathway. The setup is similar to the biochemical plant model presented in chapter 5.1. Block A100 represents the biomass drying and grinding pretreatment, block A200 represents the gasification process, block A300 represents the baghouse cloth filter, block A400 represents water gas shift and membrane separation and block A500 represents the Fischer-Tropsch synthesis. Linked together by mass flow arrows, these five blocks represent the thermochemical biomass-to-biofuel conversion pathway.

The arrows in Figure 5-7 represent mass flows. Block A100 represents the drying and milling of raw biomass. The raw biomass enters the plant by flow PL00BMAS to block A100. Steam is required for pretreatment and is indicated by the input flow PL81STM. The steam flows out of block A100 as PL84STM. The excess moisture extracted from the dried biomass is indicated by the output flow PL92WAT. The pretreated biomass is ready for gasification and is transported as flow PL06BMAS to the gasification area represented by block A200. The process is described in detail in appendix I, figure I-1 to I-3.

Block A200 in Figure 5-7 represents the biomass gasification and includes three input -and two output flows. Flow PL06BMAS represents the input of pretreated biomass to the gasification furnace. The gasification furnace requires an oxidation agent which is represented by flows PL90OXYG and PL90STM, representing oxygen and steam respectively. The gasification products consist of a raw product gas PL21SYNG and an ash residue PL22IMPU. The process is described in detail in chapter 5.2.3.The raw product gas enters block A300 as flow PL21SYNG. Block A300 represents the baghouse cloth filter that separates gas impurities from the raw product gas. The products of block A300 is a cleaned product gas flow PL32SYNG and a gas impurity residue flow PL33IMPU containing ash and char. The process is described in detail in appendix I, figure I-4.

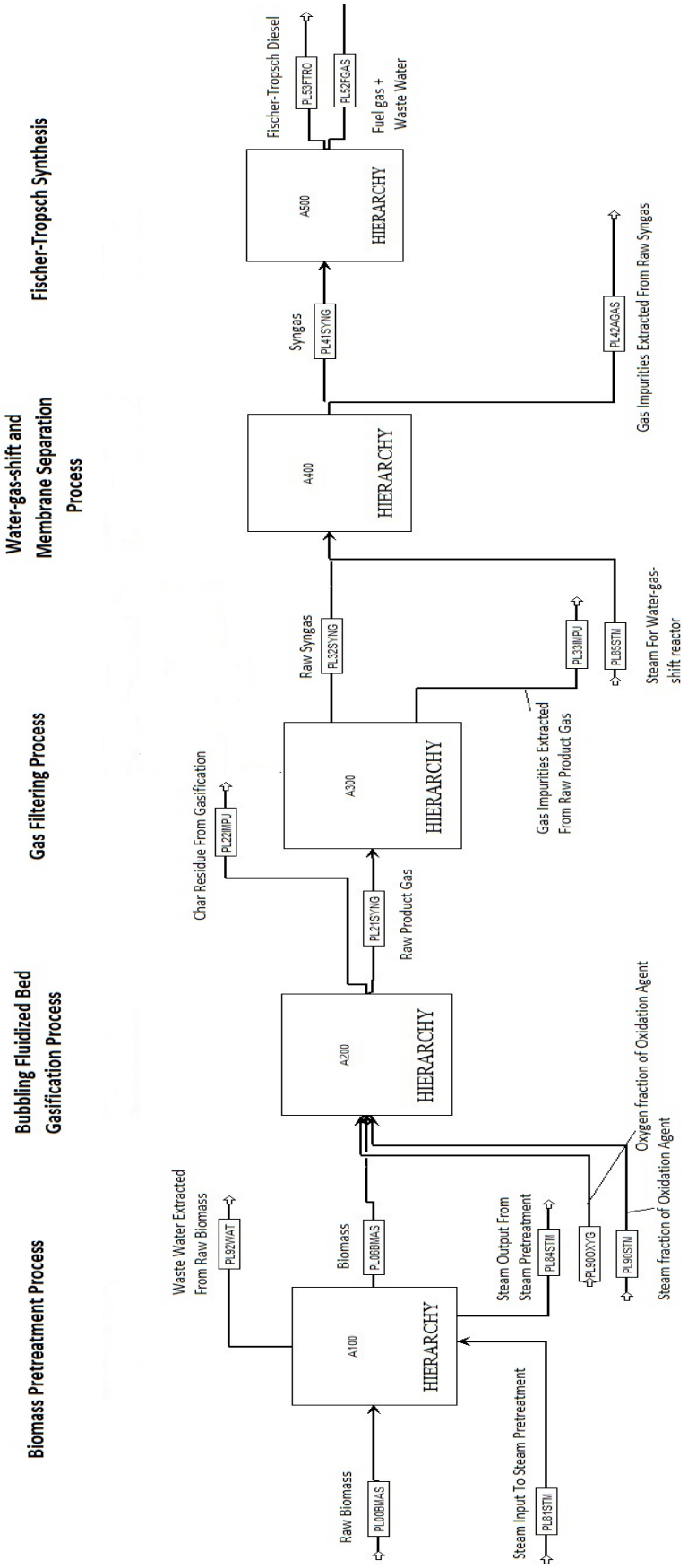

Figure 5-7: Thermochemical biomass-to-biofuel plant model, Aspen Plus.

Block A400 represents gas upgrading by water-gas-shift and gas cleaning by membrane separation. The product gas flow PL32SYNG and steam flow PL85STM are input flows to block A400. The output flows are a clean syngas PL41SYNG and impurities rinsed out of the syngas PL42AGAS. The detailed process description can be viewed in appendix I, figure I-5 and I-6.

Block A500 represents the Fischer-Tropsch synthesis which converts the syngas to a liquid biofuel. The syngas input flow PL41SYNG is converted to a Fischer-Tropsch diesel PL53FTRO and a fuel gas PL52FGAS. The detailed process description can be viewed in appendix I, figure I-7. For the thermochemical plant the only block developed in this work is block A200. Thus, only block A200 will be described in detail here. The other hierarchy blocks are described in appendix I.

5.3.3.Area A200: Bubbling Fluidized Bed Gasification

Block A200 in Figure 5-7 represents the thermochemical gasification process. The gasification process consists of a bubbling fluidized bed for biomass-to-biogas conversion and a cyclone for ash removal. Recall from chapter 3.2 that the bubbling fluidized bed (BFB) is a gasification process where controlled combustion of fuel particles is performed by injecting a solid, non-reactive bed material with high heat transmitting capacity into the gasification furnace together with a controlled supply of oxidation agent. To be able to simulate the thermochemical gasification process a bubbling fluidized bed has been modeled by using Aspen Plus. By clicking on block A200 in Figure 5-7 the model appears as illustrated in Figure 5-10. The model contains several blocks that together represent the gasification furnace of the BFB. Figure 5-9 contains a BFB-gasification furnace together with the Aspen Plus model to illustrate the different phases of a BFB process and the corresponding components in the Aspen Plus model of which they represent.

Aspen Plus contains standard ideal reactors that are executed in sequences from the beginning to the end of the designed process. The BFB is not a standard ideal reactor. It consists of both gas and solid particles that co-exist under specific dynamic physical and chemical conditions. The physical conditions are the bed hydrodynamics, including bed properties and emulsion phases. Typical hydrodynamic parameters can be gas bubble or biomass particle diameter and velocity. The chemical conditions are the chemical changes occurring in each of the BFB phases, including drying, pyrolysis, reduction and gasification. These conditions coexist in the BFB and represent a challenge in Aspen Plus modeling. Many solutions have been provided for the modeling of similar systems. M.B. Nikoo et.al developed a model that considers the hydrodynamic and reaction rate kinetics simultaneously by combining three reactors – one for the gas phase and two for the solid - with kinetic calculations made in FORTRAN (M.B. Nikoo, 2008). R. Jafari et.al developed a stepwise model with reactors in pairs – one to model the gas phase and one to model the solid phase for each step (R. Jafari, 2004).

In this thesis, the BFB is modeled by separating the gas and solid phases into separate reactors. The gas phase reactor handles the volatile matter fraction of the biomass. The solid phase reactors handle the fixed matter fraction of the biomass including fixed carbon and ash. The solid phase reactors thus handle char combustion reactions by applying chemical kinetics. Hydrodynamics are not considered in the model for simplicity reasons.

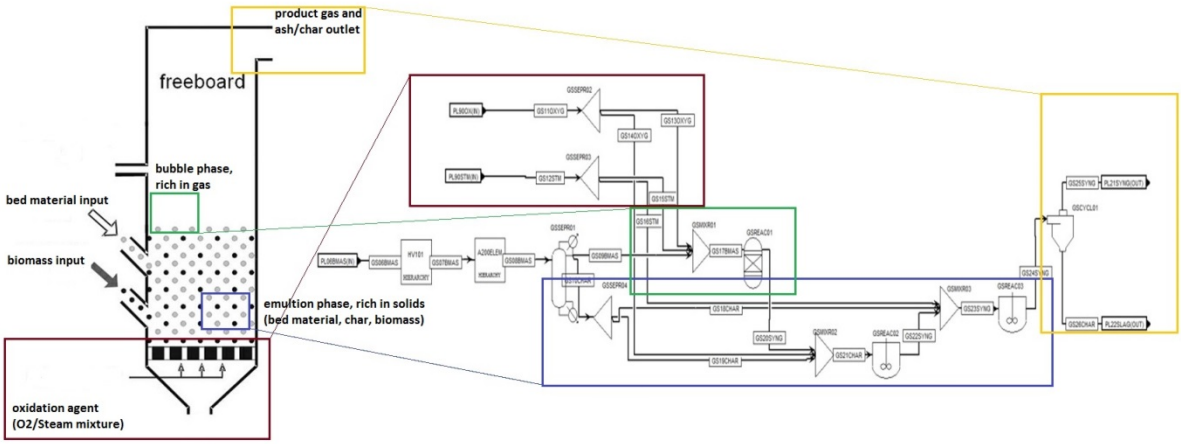

Figure 5-8: BFB furnace and Aspen Plus Model.

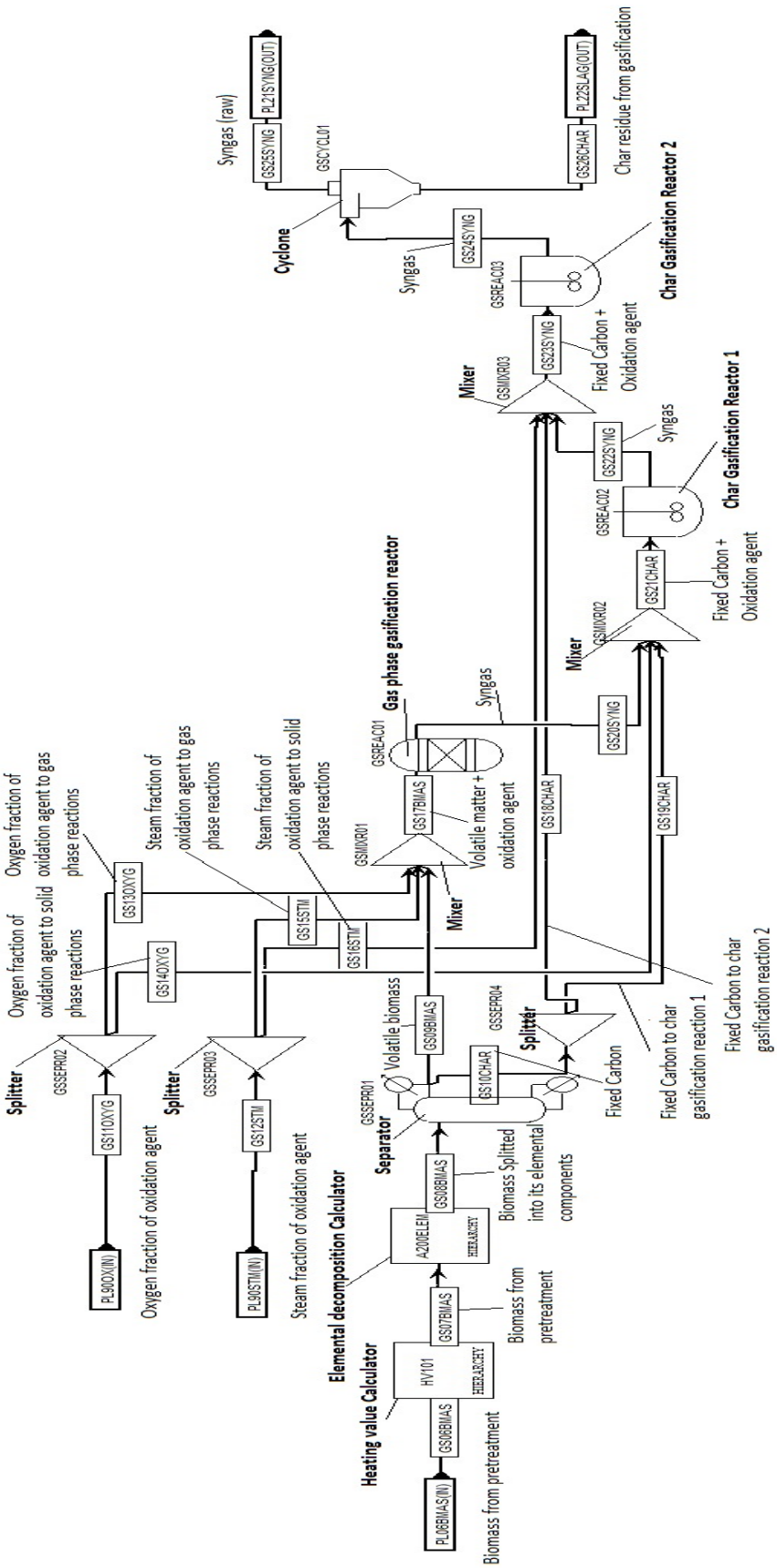

Figure 5-9: The Gasification process modelled in Aspen Plus.

In the following, the BFB will be explained step by step. Dried and grinded biomass enters the gasification process via flow PL06BMAS in Figure 5-10. The flow is renamed to GS06BMAS to emphasize that it is a plant flow (PL) that has entered the gasification area (GS). The first process it reaches is the HV101 block, illustrated in Figure 5-11. It contains a calculator that measures the higher and lower heating values of the biomass flow GS06BMAS. The calculator is described in appendix I, figure I-8. Notify in Figure 5-9 that the block does not represent a specific area of the BFB gasifier. Thus, it does not represent any real physical process in the gasifier and the output flow GS07BMAS is not affected by the block. GS06BMAS and GS07BMAS are equal in composition and numerical value.

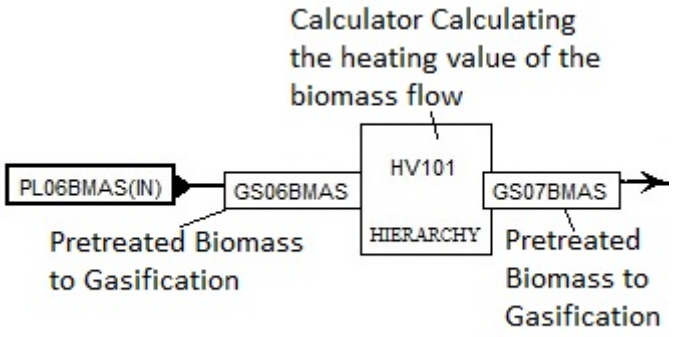

Figure 5-10: HV101 Block

GS07BMAS enters the elemental composition block, A200ELEM as shown in the block framed in a rectangular box at the upper left in Figure 5-12. By clicking on the block, the main process in Figure 5-12 appears. The flow is renamed EL07BMAS to emphasize that it flows from the gasification area (GS) to the elemental decomposition area (EL). This block splits the biomass flow into its basic elements obtained from the biomass ultimate analysis. It is emphasized that this is a virtual block and not a physical process taking place. The block ELDCOM01 is a decomposer that splits biomass into moisture, fixed carbon, volatile matter, ash, carbon, hydrogen, nitrogen, chlorine, sulfur and oxygen. The block spesifications are atmospheric temperature and pressure conditions, and the proximate and ultimate analysis for birch. The decomposition is executed in Aspen Plus by using a FORTRAN calculator. The calculations are shown in appendix II. The output flow EL08BMAS consist of biomass flow split into mass fractions corresponding to the ultimate analysis.

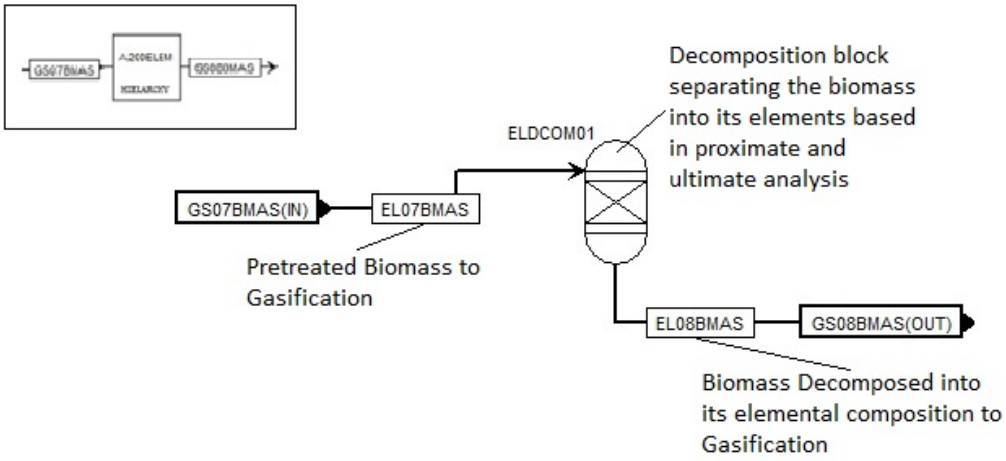

Figure 5-11: The A200ELEM block in Aspen Plus.

This block does not represent any real physical process in the BFB gasifier, but it is the key to model the fluidized bed with both gaseous and solid phase occurrence at the same time. It splits the biomass into fractions of volatile matter (VM) and fixed carbon to enable modeling of the fluidized bed with parallel gaseous and solid phases.

The biomass flow GS08BMAS enter block GSSEPR01, illustrated in Figure 5-13. This block separates the volatile matter and water vapor from the fixed carbon and ash. From now on, gaseous phases and solid phases in the gasifier are separated into two parallel model sequences. The block is a separator block in Aspen Plus that splits the biomass into the desired output by applying split fractions. The volatile matter and water vapor leaves the separator as GS09BMAS. The fixed carbon and ash leaves the separator as GS10CHAR.

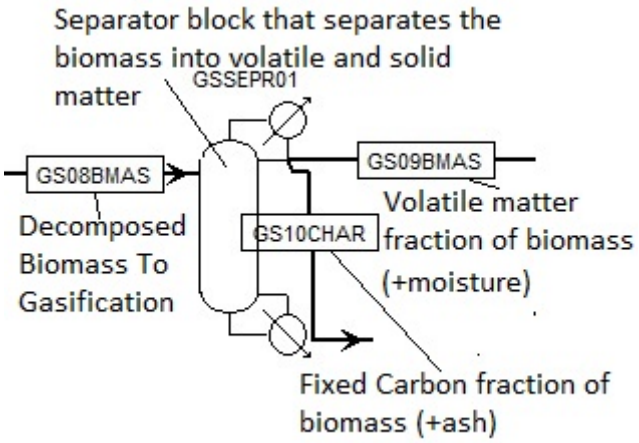

Figure 5-12: The GSSEP01 block in Aspen Plus.

The oxidation agent supply is marked with a red rectangular box in Figure 5-9 and consists of oxygen and steam. These two agents are added to the process by two separate flows, GS11OXYG

represents the oxygen flow and GS12STM represents the steam flow. Recall that in this model, the gasification reactions follow two parallel sequences: one for the gaseous phase and one for the soild phase inside the gasifier. In practice, these two phases are mixed inside the gasifier, meaning that the oxidation agent will mix uniformly into both phases. To model this in Aspen Plus, the oxidation agent flows must be split into two flows. One flow for the gaseous model sequence and one flow for the solid model sequence.

Figure 5-15 illustrates the oxygen supply, represented by GS11OXYG. PL90OXYG emphasizes that the oxygen supply is flowing in from the external thermochemical plant. The flow enters a separation block GSSEPR02 that separates the oxygen supply into two flows GS13OXYG and GS14OXYG. GS13OXYG supplies the gas reaction phase with a very small amount of oxygen whereas GS14OXYG supplies the solid reaction phase with oxygen as illustrated in Figure 5-10.

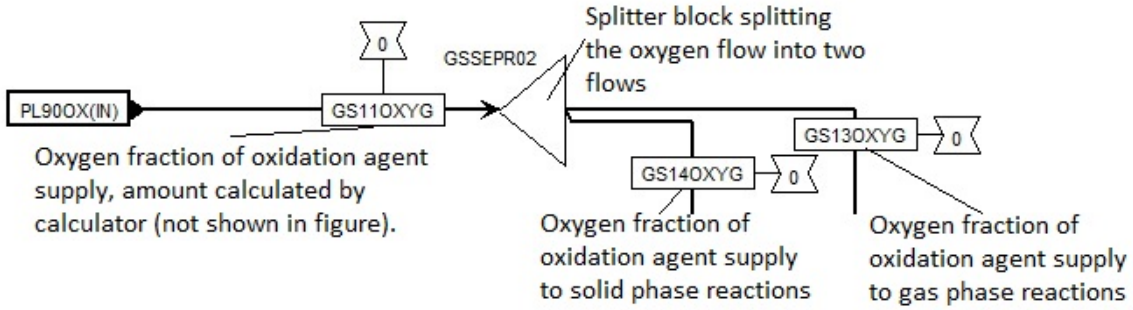

Figure 5-13: The Oxygen fraction of oxidation agent in Aspen Plus.

Figure 5-16 illustrates the steam supply, represented by GS12STM. The steam and enters a separation block GSSEPR03. This block separates the steam supply into two flows GS15STM and GS16STM. GS15STM supplies the gas reaction phase steam whereas GS16STM supplies the solid reaction phase steam (Figure 5-10). The steam-to-oxygen ratio should be 40/60. To obtain this, external FORTRAN calculators are developed. The calculators are presented in appendix II.

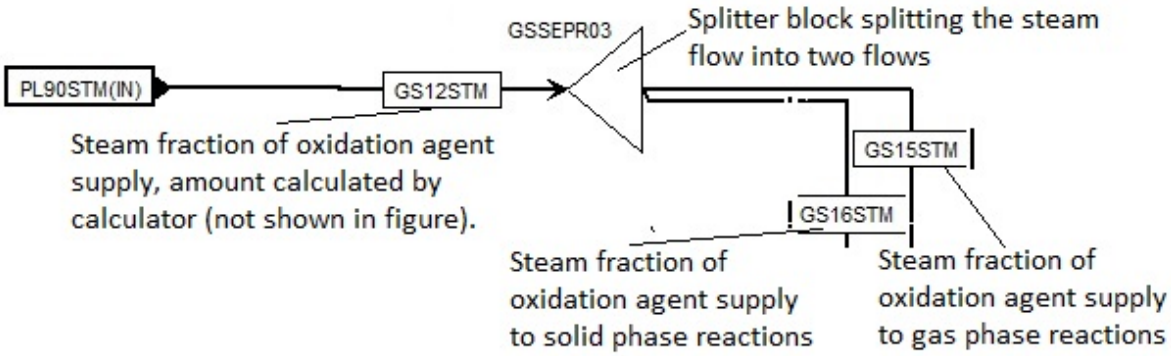

Figure 5-15: The steam supply, Area A200 in Aspen Plus.

The gaseous phase in the gasifier consist of a mixer block GSMIXR01 and a GIBBS reactor GSREAC01. This block section represents the chemical reactions occurring in the gas bubbles of the BFB as illustrated with a green rectangular box in Figure 5-17. The mixer GSMIXR01 mixes the oxygen (GS13OXYG), steam (GS15STM) and volatile matter plus water vapor (GS09BMAS). The mixed flow GS17BMAS enters GSREAC01 where the biomass is gasified under the assumption that combustion reactions follow Gibbs Equilibrium. Reactor data are given in Table 5-11. The flow GS20SYNG represents the resulting product gas.

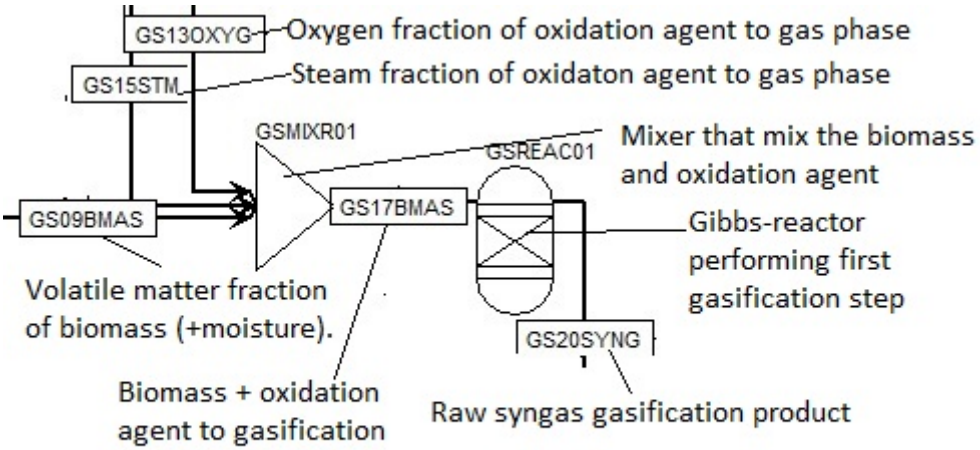

Figure 5-16: The Aspen Plus BFB gas phase reactor.

The solid phase reactions consist of two sets of char gasification reactions and are divided into two parts. The gasification reactions consist of reactions 3-1 and 3-2 from chapter 3, converting carbon into carbon dioxide and carbon monoxide by the addition of oxygen and into hydrogen and carbon monoxide by the addition of steam. For this reason, part one only mixes the oxygen flow of the oxidation agent with the fixed carbon flow, whereas the steam flow and fixed carbon is mixed in part two. In total, parts one and two represent char combustion with an oxidation agent consisting of an oxygen/steam mixture. In practice, gas bubbles with product gas will flow through the gasifier and mix with char. The product gas from the gas phase described in the previous section is therefore added to the solid combustion phase. Since the solid combustion is divided into two parts, the fixed carbon flow GS10CHAR in Figure 5-10 is split into two flows GS18CHAR and GS19CHAR. GS19CHAR. GS19CHAR represents the fixed carbon flow into part one. GS18CHAR represents the fixed carbon flow into part two.

Reactions	
CO + 3 H2 --> CH4 + H2O	
2 CARBON + 1.5 O2 --> CO2	
CARBON + H2O --> H2 + CO	
SULFUR + H2 --> H2S	
.5 N2 + 1.5 H2 --> NH3	
CO + H2S --> COS + H2	
CARBON + CO2 --> 2 CO	
CO + H2O --> CO2 + H2	
Pressure	Temperature
28 bar	1134.15 K

Table 5-11: Numerical flow values, process conditions and chemical reactions.

The first char gasification reaction is illustrated in Figure 5-18. Block GSMIXR02 represent the mixing of oxidation agent GS14OXYG, of the fixed carbon

fraction of the biomass GS19CHAR and product gas output from the gas phase reactions GS20SYNG. The mixed input GS21CHAR now represents the fluidized bed in the gasification furnace and enters the reactor block GSREAC02. This block performs char combustion with the data given in Table 5-13.

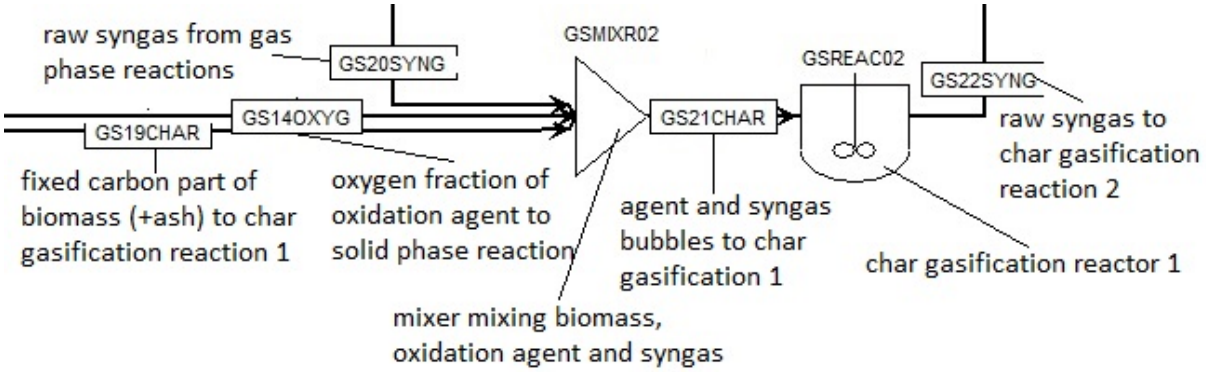

Figure 5-17: The Aspen Plus solid phase reactor 1.

The block is a CSTR reactor in Aspen Plus. The reaction kinetics for the GSREAC02 block follows the Arrhenius expression (5-2). The rate of which a chemical reaction occurs depends on temperature. The higher the temperature is, the faster the chemical reaction will proceed. This relationship is quantitatively given by the Arrhenius expression:

$$k = k_o T^n e^{-\frac{E}{RT}}, \qquad \textbf{(5-2)}$$

where k_0 is the pre-exponential factor, E is the activation energy (the energy required to ensure that the reaction happens), T is the reaction temperature (the gasification temperature in this case) and R is the ideal gas constant. Values for k_0 and E are obtained from literature. A char gasification table performed by I.I. Ahmed et.al for temperature from 800-900 ^{o}C was used (I.I. Ahmed, 2010). Since the temperature of this work is lower, the correct activation energy and pre-exponential factor will vary from the values used here. This may result in unrealistic product gas results and constitutes a model weakness. The values are given in Table 5-13.

Reaction	
2 CARBON + 1.5 O2 --> CO2 + CO	
Pre exponential factor k0	0,002
Activation energy E	123000 J/kmol

Table 5-12: Numerical data, flow values and reactor for solid phase reaction 1.

The second char gasification reaction is represented in Figure 5-19. Block GSMIXR03 represent the mixing oxidation agent GS16STM, fixed carbon of the biomass GS18CHAR and the product gas output from the first char combustion reactions GS22SYNG. The mixed input GS23SYNG enters the reactor block GSREAC03. The block is a CSTR reactor and is modeled similar to GSREAC02. The only

change is the char combustion reaction, which now is reaction 2. The block performs char combustion as illustrated in Table 5-14. The product gas output GS24SYNG composition is given in Table 5-14.

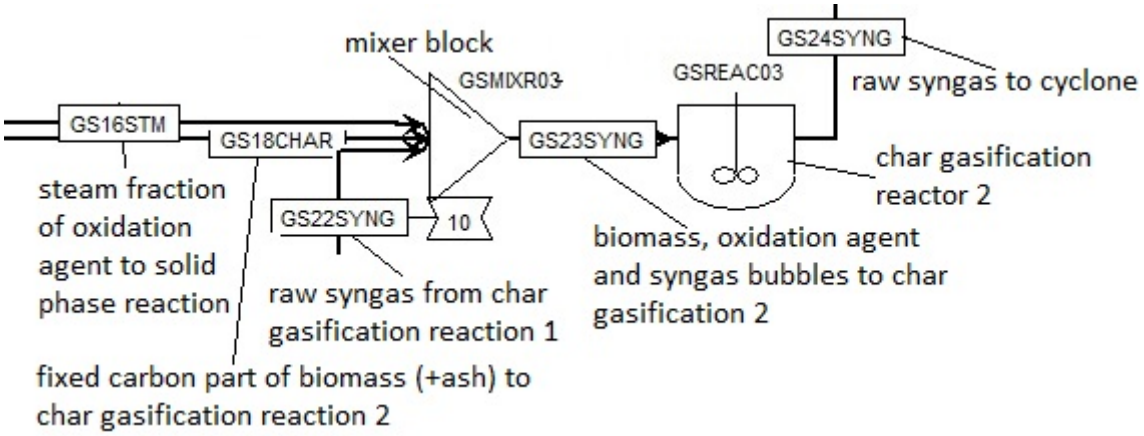

Figure 5-18: The Aspen Plus solid phase reactor 2.

Reaction	
CARBON + H2O --> H2 + CO	
Pre exponential factor k0	0,002
Activation energy E	123000 J/kmol

Table 5-13: Numerical flow and reactor data for the solid phase reactor 2.

The activation energy and pre-exponetial factors are assumed to be equal to the one for reaction x, obtained from I.I Ahmed et.al (I.I. Ahmed, 2010). Because the reaction is different this is not assumed to be a correct assumption, and it affect the reliability on the product gas output. This represents a weakness in the model. The product gas leaves the gasification furnace as GS24SYNG. It contains small amounts of tar, ash and carbon amongst other components that must be removed before the gas can be converted to a liquid. The carbon is for this case assumed to represent char particles released with the gas. The gas enters block GSCYCL01, the cyclone, in order to separate these compounds from the product gas (Figure 5-20). The cyclone functions as a separator by setting the ash and char fractions in GS26CHAR equal to 1. The rinsed gas leaves as GS25SYNG and the compounds captured by the cyclone leaves as GS26CHAR. The product gas leaves the gasification area A200 and is transported to the next process area by flow PL21SYNG. The ash leaves the gasification area by flow PL22SLAG and is deposited (Kempegowda).

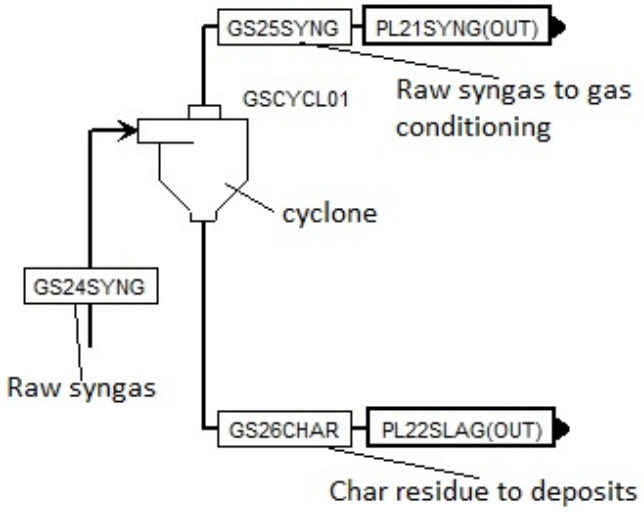

Figure 5-19: The cyclone modeled in Aspen Plus.

6. Results

The results obtained from simulations in Aspen Plus consist of mass flow rates and mass flow composition. What is to be investigated is the energy content of these flows. To estimate energy flows the composition of some key mass flows for each process are identified, and calorific value calculations are performed to estimate the energy content. This chapter first provides a presentation and analysis of the mass flow balance for the biochemical and the thermochemical pathway in chapter 6.1. Thereafter the mass flow compositions for biomass, biogas, product gas, syngas and Fischer-Tropsch diesel are identified and calorific value calculations are performed in chapter 6.2. Finally, chapter 6.3 provides a presentation and analysis of the energy flows for the biochemical and the thermochemical pathway, providing comparable data on feed-to-fuel ratios and the Fischer-Tropsch diesel quality as a liquid biofuel.

6.1. Mass Balance for Biochemical and Thermochemical Pathways

Figure 6-1 and Figure 6-2 presents ESankey diagrams illustrating the mass flows (in ton/day) for the biochemical and thermochemical pathway respectively. The diagrams are made by collecting mass-flow data from simulations in Aspen Plus. The underlying mass flow data will be presented and analyzed process by process below. Figure 6-1 illustrates the mass flows for the *biochemical* pathway. It consists of 5 colored rectangular boxes representing the 5 processes making up the biochemical pathway. The blue arrows represent mass flows, and their values are indicated in the figure. The orange box represents the biomass pretreatment converting raw biomass into dried and grinded biomass. The yellow box represents the anaerobic digestion converting the biomass into raw biogas and digester residue by-product. The green box represents methane reforming converting the raw biogas to a raw syngas. The blue box represents the water-gas-shift and membrane separation converting raw syngas to syngas and gas impurities by-product. The purple box represents the Fischer-Tropsch synthesis converting the syngas to a liquid biofuel and by-products. From the figure it is emphasized that all input flows other than the biomass feedstock is steam flows. The figure illustrates that 873 ton/day biomass is converted to 138 ton/day Fischer-Tropsch (FT)-diesel. Two steam inputs are identified, representing 332 ton/day to methane reforming and 342 ton/day to water-gas-shift respectively. Four mass flow outputs (other than the FT-diesel) are identified, represented by 146 ton/day of waste water from the biomass pretreatment process, 179 ton/day digester residue from the anaerobic digestion, 524 ton/day gas impurities removed from membrane separation and 507 ton/day fuel gases and waste waters from the Fischer-Tropsch synthesis.

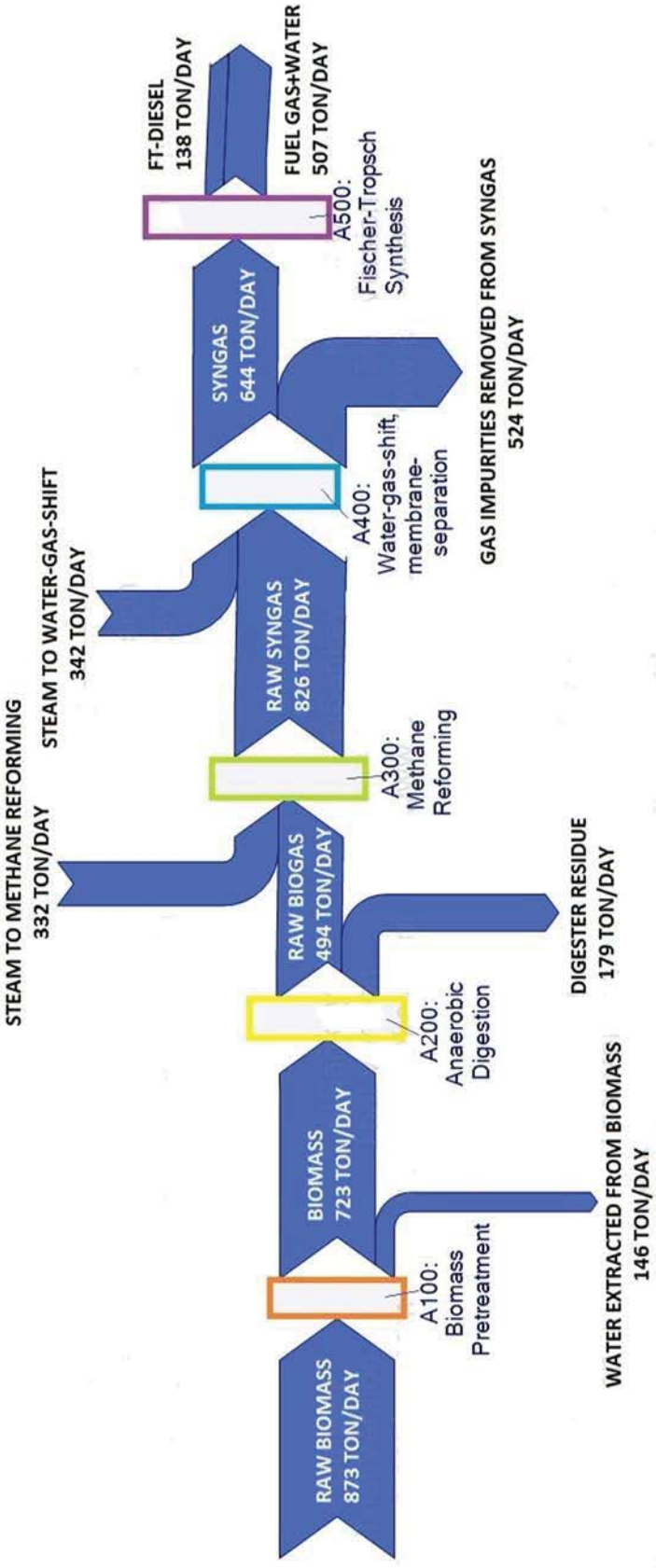

Figure 6-1: ESankey-diagram illustrating the mass flows (ton/day) for the biochemical pathway.

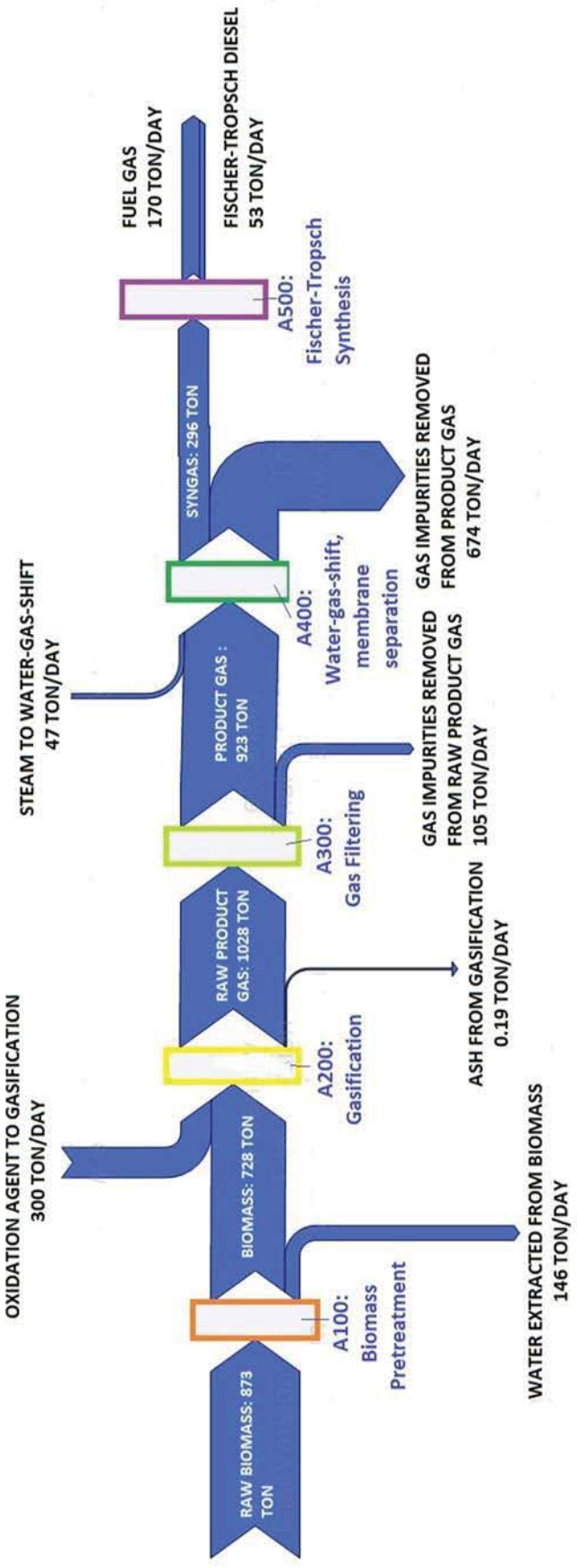

Figure 6-2: ESankey-diagram illustrating the mass flows (ton/day) for the thermochemical pathway.

Figure 6-2, follows the same structure as Figure 6-1, and consists of 5 colored rectangular boxes representing the 5 processes making up the thermochemical pathway. Only the yellow box and the green box differ from Figure 6-1. The yellow box represents the gasification converting the biomass into raw product gas and ash by-product. The green box represents gas filtering converting the raw product gas to a product gas and gas impurities by-product. Also in this case the mass flow inputs other than the biomass feedstock are steam. The figure illustrates that 873 ton/day biomass is converted to 53 ton/day Fischer-Tropsch-diesel. Two mass flow inputs are identified, representing 300 ton/day of oxidation agent to the gasifier and 47 ton/day of steam to water-gas-shift respectively. Five mass flow outputs (other than the Fischer-Tropsch diesel) are identified, represented by 146 ton/day of waste water from the biomass pretreatment process, 0.19 ton/day of ash by-product from the gasification, 105 ton/day of gas impurities removed from the raw product gas by gas filtering, 674 ton/day of gas impurities removed from the product gas by membrane separation and 170 ton/day fuel gases and waste waters from the Fischer-Tropsch synthesis.

Compared to the biochemical pathway the steam input and the Fischer-Trospch diesel output is lower for the thermocemical pathway. The mass flow losses are also varying between the two pathways. In the following sections the mass balance evaluations for the two pathways are given in detail. The data is evaluated by identifying the percentage of mass flow input that is converted to each of the output flows for the processes 1 to 5. The percentages are denoted by

$$M_{ijn}, \qquad \textbf{(6-1)}$$

where the subscript *"i"* represent each of the pathway processes 1 to 5 where 1 is biomass pretreatment, 2 is biomass-to-gas conversion process, 3 is gas conditioning step one, 4 is gas conditioning step two and 5 is the gas-to-liquid conversion process. The subscript *"j"* represents the pathway, 1 is the biochemical pathway and 2 is the thermochemical pathway. Subscript *"n"* represents the output flow that is evaluated. The calculations are performed by equations IV1-IV24 in appendix IV, and summarized in table IV-1. In tables 6-1 to 6-5 in the following, biochemical and thermochemical conversion pathways are given the abbrevations *scenario 1* and *scenario 2* respectively. Thus, the conversion pathways are referred to as scenario 1 and scenario 2 consistently in the forthcomming text.

Area A100 Biomass Pretreatment

Recall from chapters 4 and 5 that the biomass pretreatment process consist of a steam dryer and a grinder, and that it is similar for both scenarios. This is reflected in Table 6-1, where the mass flows are equal for both. The detailed results are rendered with two decimal places. As explained in chapter 5, the mass flows for the biomass pretreatment process consist of a raw biomass feedstock input (PL00BMAS) of 873.34 ton/day, and a pretreated

biomass output PL06BMAS equal to 727.78 ton/day. The process requires 1310.00 ton/day of steam (PL81STM), of which is leaving the process (PL84STM) at the same rate as the input (1310.00 ton/day). 145.56 ton/day of moisture is extracted from the raw biomass in the drying process (PL92WAT).

Area A100 SCENARIO 1	Input		Output		
Flow	PL00BMAS	PL81STM	PL06BMAS	PL84STM	PL92WAT
Mass flow (ton/day)	873.34	1310.00	727.78	1310.00	145.56
Area A100 SCENARIO 2	Input		Output		
Flow	PL00BMAS	PL81STM	PL06BMAS	PL84STM	PL92WAT
Mass flow (ton/day)	873.34	1310.00	727.78	1310.00	145.56

Table 6-1: Mass Flow Simulation Data, Area A100 Biomass Pretreatment.

Area A200 Biomass-to-gas Conversion

Recall from chapters 3 and 5 that the biomass-to-gas conversion processes are a dry batch anaerobic digestion process for scenario 1 and bubbling fluidized bed gasification for scenario 2. The mass flow data are presented in Table 6-2. Both scenarios receive the same biomass input (PL06BMAS) of 727.78 ton/day. In scenario 1, the anaerobic digester output consists of 493.54 ton/day biogas (PL21BGAS) and 279.10 ton/day digester residue (PL22RESD). In scenario 2, the biomass input to the gasifier consists of both biomass (PL06BMAS) and 300.00 ton/day oxidation agent (PL90OXYG and PL90STM). Recall that the oxidation agent consists of oxygen and steam. The mass flow data show that only steam is applied in the process. 0.00 ton/day of oxygen and 300.00 ton/day of steam is utilized in the gasifier. The gasification products consist of 1027.97 ton/day of product gas (PL21SYNG), and 0.19 ton/day ash (PL22CHAR).

Area A200 SCENARIO 1	Input		Output		
Flow	PL06BMAS	-	PL21BGAS	PL22RESD	PL22RESD
Mass flow (ton/day)	727.78	-	493.54	279.10	234.24
Area A200 SCENARIO 2	Input			Output	
Flow	PL06BMAS	PL90OXYG	PL90STM	PL21SYNG	PL22CHAR
Mass flow (ton/day)	727.78	0.00	300.00	1027.97	0.19

Table 6-2: Mass Flow Simulation Data, Area A200 Anaerobic Digestion.

Notice from Table 6-2 that the mass flow does not balance for scenario 1 because the total mass output is larger than the mass flow input. The percentage difference is calculated by equation (6-2).

$$M_{21TOT} = \frac{Total\ Output\ flow}{Total\ Input\ flow} = \frac{PL21BGAS + PL22RESD}{PL06BMAS} = \frac{(493.54 + 279.10)\frac{ton}{day}}{727.78\frac{ton}{day}} * 100 = 106.16\%. \quad \textbf{(6-2)}$$

Equation (6-2) indicate that the output mass flows is 6.16% larger than input mass flows. This is an error that must be accounted for in the analysis of both mass and energy flows. The error can be a result of a calculation error in the BIOGAS calculator (appendix II). To adjust for the error, the digester residue flow is adjusted down to 234.24 ton/day as indicated by the red shading in Table 6-2. The biogas output is assumed to be correct. Put this way, the error does not affect the processes downstream of the anaerobic digester, and there is no need to account for the error in downstream processes.

Recall from chapter 3.2 that the oxidation agent is a mixture of steam and oxygen. The oxygen to steam ratio should be 40/60. Based on the simulation data, the oxygen flow is so small that it is rounded to zero and steam alone serve as the oxidation agent. This is an error, and there are two possible answers to why this phenomenon occurs. There may be a possible error in the oxidation agent calculator that fails to take oxygen into account. There may also be a possible error in the reactor configurations in Aspen Plus. The error is considered further in discussions and conclusion in chapters 7 and 8.

Area A300 Gas Conditioning 1

The resulting gas after biomass-to-gas conversion consists of impurities that must be removed before the gas can be applied to the Fischer-Tropsch synthesis. In scenario 1, biogas is a methane-rich gas and a methane reforming process is applied to shift the methane gas into hydrogen and carbon monoxide as described in chapter 4.2.2. The mass flows for the methane reforming process are shown in Table 6-3. The mas flow inputs consist of the 493.64 ton/day of raw biogas (PL21BGAS) and 332.64 ton/day of steam (PL22STM). The steam is required for the methane reforming reaction (equation 4-1, chapter 4.2.2).

The product gas produced in scenario 2 consists of particles that must be removed prior to further gas conditioning. A filter is applied to clean the gas from these particulates in accordance with chapter 4.2.1. The mass flow input to the filter (PL21SYNG) consists of 1027.97 ton/day of hot raw product and the mass flow output consists of 922.69 ton/day product gas rinsed for large particulates (PL32SYNG), and 105.28 ton/day of particulate residue (PL33IMPU).

Area A300 SCENARIO 1	Input		Output		
Flow	PL21BGAS	PL22STM	PL32SYNG	PL33IMPU	-
Mass flow (ton/day)	493.54	332.64	826.22	0.00	-
Area A300 SCENARIO 2	Input		Output		
Flow	PL21SYNG	-	PL32SYNG	PL33IMPU	-
Mass flow (ton/day)	1027.97	-	922.69	105.28	-

Table 6-3: Mass Flow Simulation Data, area A300 Methane Reforming.

Area A400 Gas Conditioning 2

After the first step of gas conditioning, the gases produced in both scenarios have improved properties in terms of impurities concentration and hydrogen and carbon monoxide content. However, the gas composition is not optimal for none of the gases and a second gas conditioning step becomes necessary. Thus, impurities are removed by membrane separation and the H_2/CO-ratio is improved by water-gas-shift as described in chapter 4.2.2 and 4.2.3. The mass flows for the second gas conditioning process are shown in Table 6-4.

For scenario 1, 826.22 ton/day of raw syngas (PL32SYNG) enters the membrane separation and water-gas-shift reactor. The water-gas-shift reactor is supplied with 342.42 ton/day of steam (PL85STM). 644.39 ton/day of syngas product (PL41SYNG) leaves the process and 524.26 ton/day of gas impurities (PL42AGAS) are removed from the gas

For scenario 2, 922.69 ton/day of product gas (PL32SYNG) enters the membrane separation and water-gas-shift reactor. The water-gas-shift reactor is supplied with 47.33 ton/day of steam (PL85STM). 296.10 ton/day of syngas product (PL41SYNG) leaves the process, and 673.92 ton/day of gas impurities (PL42AGAS) are removed from the raw syngas in the process.

Area A400 SCENARIO 1	Input		Output		
Flow	PL32SYNG	PL85STM	PL41SYNG	PL42AGAS	-
Mass flow (ton/day)	826.22	342.42	644.39	524.26	-
Area A400 SCENARIO 2	Input		Output		
Flow	PL32SYNG	PL85STM	PL41SYNG	PL42AGAS	-
Mass flow (ton/day)	922.69	47.33	296.10	673.92	-

Table 6-4: Mass Flow Simulation Data, Area A400 Water-gas-shift and Membrane Separation.

Area A500 Fischer-Tropsch Synthesis

After two gas-conditioning steps the syngas consist mostly of hydrogen and carbon monoxide, and is ready for conversion to a liquid biofuel. The gas liquefaction is performed by a Fischer-Tropsch synthesis that is equal for both scenarios. The liquid biofuel produced is a Fischer-Tropsch diesel, and bi-products are fuel gases and water. The size of the syngas input to the process varies between the scenarios as shown in Table 6-5. In scenario 1, 644.39 ton/day of syngas (PL41SYNG) enters the Fischer-Tropsch synthesis. The Fischer-Tropsch synthesis products are 137.67 ton/day Fischer-Tropsch diesel (PL53FTRO), 323.30 ton/day fuel gases (PL52FGAS) and 183.42 ton/day of waste water (PL93WAT). For scenario 2, 296.10 ton/day of syngas (PL41SYNG) enters the Fischer-Tropsch synthesis. The products are 53.12 ton/day Fischer-Tropsch diesel (PL53FTRO), 169.67 ton/day fuel gas (PL52FGAS, and 73.31 ton/day of waste water product (PL93WAT).

Area A300 SCENARIO 1	Input		Output		
Flow	PL41SYNG	-	PL53FTRO	PL52FGAS	PL93WAT
Mass flow (ton/day)	644.39	-	137.67	323.30	183.42
Area A300 SCENARIO 2	Input		Output		
Flow	PL41SYNG	-	PL53FTRO	PL52FGAS	PL93WAT
Mass flow (ton/day)	296.10	-	53.12	169.67	73.31

Table 6-5: Mass Flow Simulation Data, Area A500 Fischer-Tropsch Synthesis.

The mass flows locate some of the sites in which energy losses will be found. However it is important to understand that the flows are mass flows, and that the energy content of them may vary regardless of the size of the flows. Figures 6-1 and 6-2 does indicate energy losses related to both pretreatment, biomass-to-gas conversion, gas conditioning processes and Fischer-Tropsch synthesis because mass flow losses are identified. However, to evaluate their significance they must be related to energy content. To obtain the energy flows, calculations in terms of heating value are performed in the next chapter.

6.2. Heating Value Calculations, Thermochemical Pathway

The *heating value* (or calorific value) is an indicator of the possible energy content in the fuel and can be measured at both solid (biomass), gaseous (biogas, product gas, syngas) and liquid (biofuel) states. To be able to estimate the energy flows, lower heating values for the fuel on different process stages in the pathway have been calculated. Recall from chapter 2 that the *lower heating value* represents the amount of energy released when the material is combusted in air, without taking into consideration the latent heat contained in eventual moisture content in the material. The lower heating value is chosen because latent heat

cannot be used efficiently and is thus the preferred approximation in this type of analysis where actual energy utility is of interest.

Gas	LHV [MJ/kg]
CH4	50.00
CO	10.16
H2	119.96
H2S	17.39
H2O	0.00
NH3	18.65
C	32.81
CO2	0.00
O2	0.00

Table 6-6: Theoretical Lower Heating Values (NIST Chemistry WebBook, 2013).

The heating values for the biomass and the final Fischer-Tropsch diesel are calculated in Aspen Plus and are being used directly. This heating value model is explained step-by-step in appendix I. The heating values for the biogas, product gas and syngas is not measured in simulations and they are thus calculated. Mass flow compositions obtained from simulations and theoretical heating values for different gases have been used for the calculations. The theoretical heating values are obtained from NIST Chemistry WebBook and are presented in Table 6-6. Water vapor, carbon dioxide and oxygen is not combustible and thus, they do not have a heating value, which is why they are equal to zero in Table 6-6. They are included in the table to give a better feeling for the composition of the mass flow that is evaluated.

Table 6-7 shows the heating value calculation data for scenario 1. Recall that the heating values for biomass and FT-diesel is found directly from simulations. Thus, the biomass pretreatment process (are A100) and the Fischer-Tropsch synthesis (area A500) is not presented in the table. The section marked with yellow color addresses the biogas produced in the anaerobic digestion process (area A200). The section marked with green color addresses the raw syngas product from methane reforming (area A300). The section marked with blue color addresses the syngas product from water-gas-shift and membrane separation (area A400). For each of the three sections, column one (raw biogas) lists the biogas composition for gas component *i*=1 to *i*=4. Column two (LHV) lists the theoretical heating values for the respective biogas components *i*=1 to *i*=4 in MJ/kg. Column three (mass fraction) lists the mass fractions of the respective gas components *i*=1 to *i*=4 relative to total biogas (measured in kg/s). The mass fraction is dimensionless. Column four measures the calculated heating value for the respective gas component *i*=1 to *i*=4. The calculations are performed by the following equations (6-3) to (6-4):

$$HV_{gas}[\frac{\mathrm{MJ}}{\mathrm{kg}}] = \sum_i HV_i\,[\frac{\mathrm{MJ}}{\mathrm{kg}}] \qquad \textbf{(6-3)}$$

where

$$HV_i\left[\frac{\mathrm{MJ}}{\mathrm{kg}}\right] = LHV_i\left[\frac{\mathrm{MJ}}{\mathrm{kg}}\right] * \text{mass fraction}_{\text{i.}} \qquad \textbf{(6-4)}$$

HV_{gas} is the heating value of the gas in MJ/kg. HV_i is the heating value contribution by gas *i* to the total gas measured in MJ/kg, LHV_i is the general theoretical lower heating value of gas *i* measured in MJ/kg and mass fraction *i* is the mass fraction of gas *i* relative to the total gas mass.

Scenario 1											
Area A200				Area A300				Area A400			
Raw Biogas	LHV [MJ/kg]	mass fraction	HVgas [MJ/kg]	Raw Syngas	LHV [MJ/kg]	mass fraction	HVgas [MJ/kg]	Syngas	LHV [MJ/kg]	mass fraction	HVgas [MJ/kg]
CO2	0.00	0.46	0.00	H2	119.96	0.11	13.31	H2	119.96	0.16	19.41
CH4	50.00	0.49	24.7	CO	10.16	0.86	8.73	H2O	0.00	0.00	0.00
H2S	17.39	0.03	0.44	H2S	17.39	0.01	0.26	CO2	0.00	0.00	0.00
NH3	18.65	0.03	0.47	NH3	18,646	0.01	0.28	CO	10.16	0.83	8.44
Raw Biogas Heating Value			25.6	Raw Syngas Heating Value			22.58	Syngas Heating Value			27.85

Table 6-7: Heating Value Calculations Data for area A200 Anaerobic Digestion, area A300 Methane Reforming and area A400 Water-gas-shift and Membrane Separation, Biochemical Pathway.

Table 6-8 shows the heating value calculation data for scenario 2. Also here, the heating values for biomass and FT-diesel is calculated in Aspen Plus. Thus, the biomass pretreatment process (are A100) and the Fischer-Tropsch synthesis (area A500) is not presented in the table. The section marked with yellow color addresses the raw product gas produced in the gasification process (area A200). The table area marked with green color addresses the product gas after gas filtering (area A300). The table area marked with blue color addresses the syngas product from water-gas-shift and membrane separation (area A400). The table follow the same structure as Table 6-7, and the calculations are performed by equations (6-3) to (6-4).

Scenario 2											
Area A200				Area A300				Area A400			
Raw Product Gas	HV [MJ/kg]	Gas mass fraction	HVgas [MJ/kg]	Product Gas	HV [MJ/kg]	Gas mass fraction	HVgas [MJ/kg]	Syngas	HV [MJ/kg]	Gas mass fraction	HVgas [MJ/kg]
CH4	50.00	0.04	2.13	CH4	50.00	0.05	2.37	H2	119.96	0.13	15.84
CO	10.16	0.27	2.70	CO	10.16	0.30	3.01	H2O	0.00	0.01	0.00
H2	119.96	0.03	4.00	H2	119.96	0.04	4.46	CO2	0.00	0.01	0.00
H2S	17.39	0.00	0.01	H2S	17.39	0.00	0.00	CO	10.16	0.70	7.08
H2O	0.00	0.33	0.00	H2O	0.00	0.37	0.00	CH4	50.00	0.15	7.39
NH3	18.65	0.00	0.01	NH3	18,646	0.00	0.01				
C	32.81	0.10	3.35	C	32,808	0.00	0.00				
CO2	0.00	0.23	0.00	CO2	0	0.25	0.00				
O2	0.00	0.00	0.00	O2	0	0.00	0.00				
Raw Product Gas Heating Value:			12.20	Product gas Heating Value:			9.86	Syngas Heating Value			30.31

Table 6-8: Heating Value Calculations Data for area A200 Gasification, area A300 Gas Filtering and area A400 Water-gas-shift and Membrane Separation, Thermochemical Pathway.

The heating values obtained from simulations and calculations for both scenarios are summarized in Table 6-9 and presented graphically in Figure 6-3.

Scenario 1 (Biochemical Plant)	Heating Value [MJ/kg]	Scenario 2 (Thermochemical Plant)	Heating Value [MJ/kg]
Biomass Feedstock	14.83	Biomass Feedstock	14.83
Biomass, pretreated	15.88	Biomass, Pretreated	15.88
Biogas	25.6	Raw Product Gas	12.20
Raw Syngas	22.58	Product Gas	9.86
Syngas	27.85	Syngas	30.31
FT-Diesel	47.89	FT-Diesel	66.34

Table 6-9: Heating Values obtained from both simulations and calculations, Biochemical and Thermochemical Pathways.

The first row in Table 6-9 renders the biomass lower heating value obtained from theory whereas the second row is the calculated value obtained from Aspen Plus. The third to fifth rows renders calculated values from tables 6-7 and 6-8 and the sixth and last row is the calculated Fischer-Tropsch diesel heating value obtained from Aspen Plus.

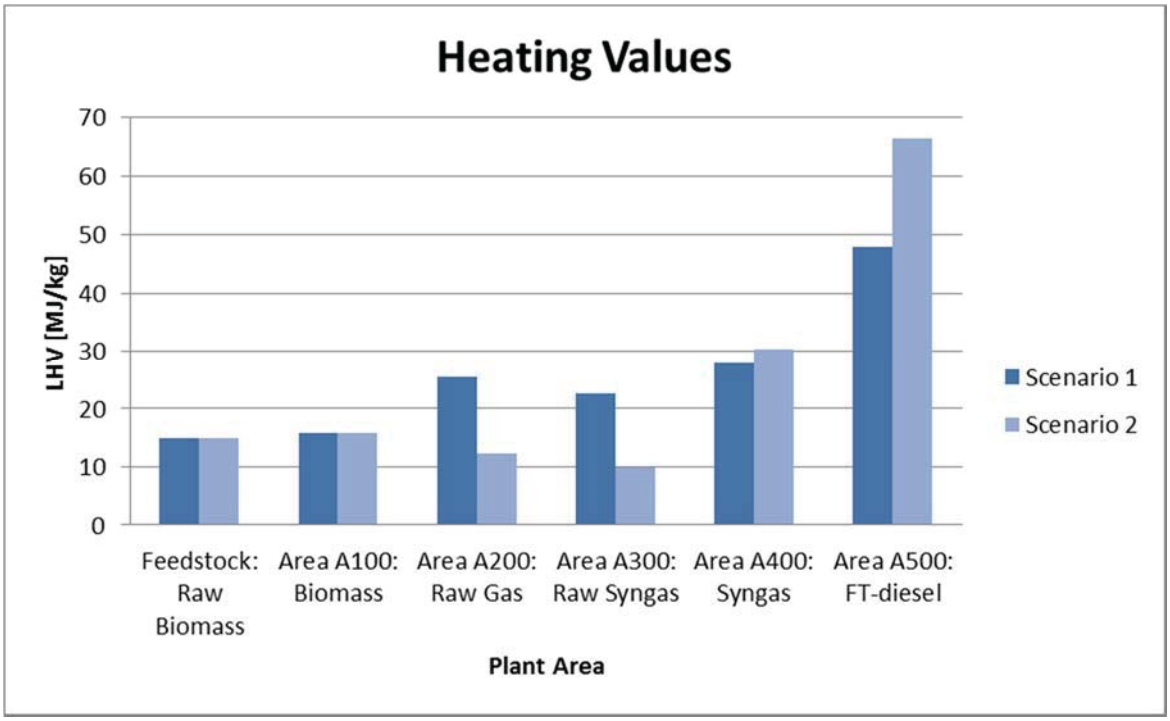

Figure 6-3: Heating values obtained from both simulations and calculations illustrated graphically, Scenario 1 and Scenario 2.

Figure 6-3 shows that the heating value for the raw biomass in column one and pretreated biomass in column two equals 14.83 MJ/kg and 15.88 MJ/kg and is similar for both scenarios. This is expected since the processes are equal with equal inputs for both scenarios. The difference between the measured value and the calculated value are not expected. Recall that the biomass pretreatment only extracts water from the raw biomass. Since calculations are performed in terms of lower heating value, the heating value should not be affected by the pretreatment. The calculated result might be higher due to a calculation error in Aspen Plus.

Regarding the biomass-to-raw gas conversion illustrated in column three and the first gas conditioning step in column four, the results indicates the better heating value results for scenario 1. For scenario 1 the figure indicates a raw gas heating value of 25.6 MJ/kg and a raw syngas heating value of 22.58 MJ/kg. For scenario 2 the heating value results indicate 12.20 MJ/kg raw gas heating value and 9.86 MJ/kg raw syngas heating value. The tendency changes when taking a look at the second gas cleaning step in column five and the Fischer-Tropsch synthesis in column six. Here, the heating value results have improved for scenario 2 and exceeds the heating value results for scenario 1. For scenario 1 the figure indicates a syngas heating value of 27.85 MJ/kg and a Fischer-Tropsch diesel heating value of 47.89 MJ/kg, whereas scenario 2 results in a syngas heating value of 30.31 MJ/kg and a Fischer-Tropsch diesel with a heating value of 66.34 MJ/kg is being obtained. The results indicate a good Fischer-Tropsch diesel heating value for scenario 1 and a heating value exceeding realistic values for scenario 2. The result will be discussed further in chapter 7.

6.3. Energy Balance for Biochemical and Thermochemical Pathways

To this point, both mass flow data and relevant heating value calculations have been collected. In this chapter, these flows are first combined to obtain the energy flows and thereafter feed-to-fuel and feed-to-loss ratios are obtained. Energy flow number *i* is determined by applying one of the following equations (6-5) to (6-6):

$$E_i = m_i HV_{i,} \qquad \textbf{(6-5)}$$

where E_i represents energy flow number *i* measured in MW, m_i represent mass flow number *i* measured in (kg/s) and HV_i represents the lower heating value of mass flow *i* measured in MJ/kg. The steam flows are not calculated by heating value. Instead, a *steam-to-energy coefficient* obtained from K. Panther et.al is being used (K. Panther, 2006). The energy flow for steam is thus calculated by equation (6-6):

$$E_{i,steam} = m_i e_{i,} \quad \textbf{(6-6)}$$

where $E_{i,steam}$ represent the energy content of steam mass flow *i*, measured in MW, m_i represent mass flow *i* measured in kg/s and e_i represent the steam-to-energy coefficient measured in MJ/kg. Note that not all mass flows investigated in chapters 1 and 6.2 have a heating value. This is the case for the waste water residue flow in the biomass pretreatment process, the char residue from biomass gasification and the fuel gas and waste water bi-product from the Fischer-Tropsch synthesis. For simplicity the energy content related to these flows are obtained from mass balance. The calculations are performed sequentially for each of the five pathway processes and are described in detail process by process in appendix IV, table IV-2 to IV-6.

The calculation results are presented in Figure 6-4 and Figure 6-5, of which presents ESankey-diagrams illustrating the energy flows (in MW) for the two scenarios. The diagrams are made from energy flow calculations as performed by equations (6-5) and (6-6). The underlying calculation details are described process by process in appendix IV. Both Figure 6-4 and Figure 6-5 are structured in the same way as the mass flows presented in chapter 6.1.

Figure 6-4 consists of five rectangular boxes that represent the pathway processes of the *biochemical* pathway, referred to as scenario 1 throughout this chapter. The orange box represents biomass pretreatment the yellow box represents anaerobic digestion, the green box represents methane reforming, the blue box represents water-gas-shift and membrane separation and the purple box represents Fischer-Tropsch synthesis. The arrows represent the energy flows, and their size reflects the size of the energy flow.

The figure shows that with a 150 MW biomass input, 76 MW Fischer-Tropsch diesel is produced. Additional energy inputs to the process comprises 59 MW heat supply to the anaerobic digester, 270 MW steam for methane reforming and 278 MW steam for water-gas-shift reactions. Total energy input (biomass plus additional) equals 757 MW. Energy losses are related to all five processes. 16 MW is lost through the waste water flow in the biomass pretreatment process. 47 MW is lost through digester residue from the anaerobic digestion. 200 MW is lost as excess heat from the methane reforming. 286 MW is lost from water-gas-shift and membrane separation, of which 5 MW is lost through gas impurities and 181 MW is lost as excess heat. 132 MW is lost through Fischer-Tropsch bi-products. Total energy losses related to the process equals 681 MW.

Figure 6-5 consists of five rectangular boxes that represent the processes of the *thermochemical* pathway, referred to as scenario 2 throughout this chapter. Figure 6-5 is structured in the same way as figure 6-4. The only exception is the yellow and green boxes. The yellow box represents gasification. The green box represents gas filtering.

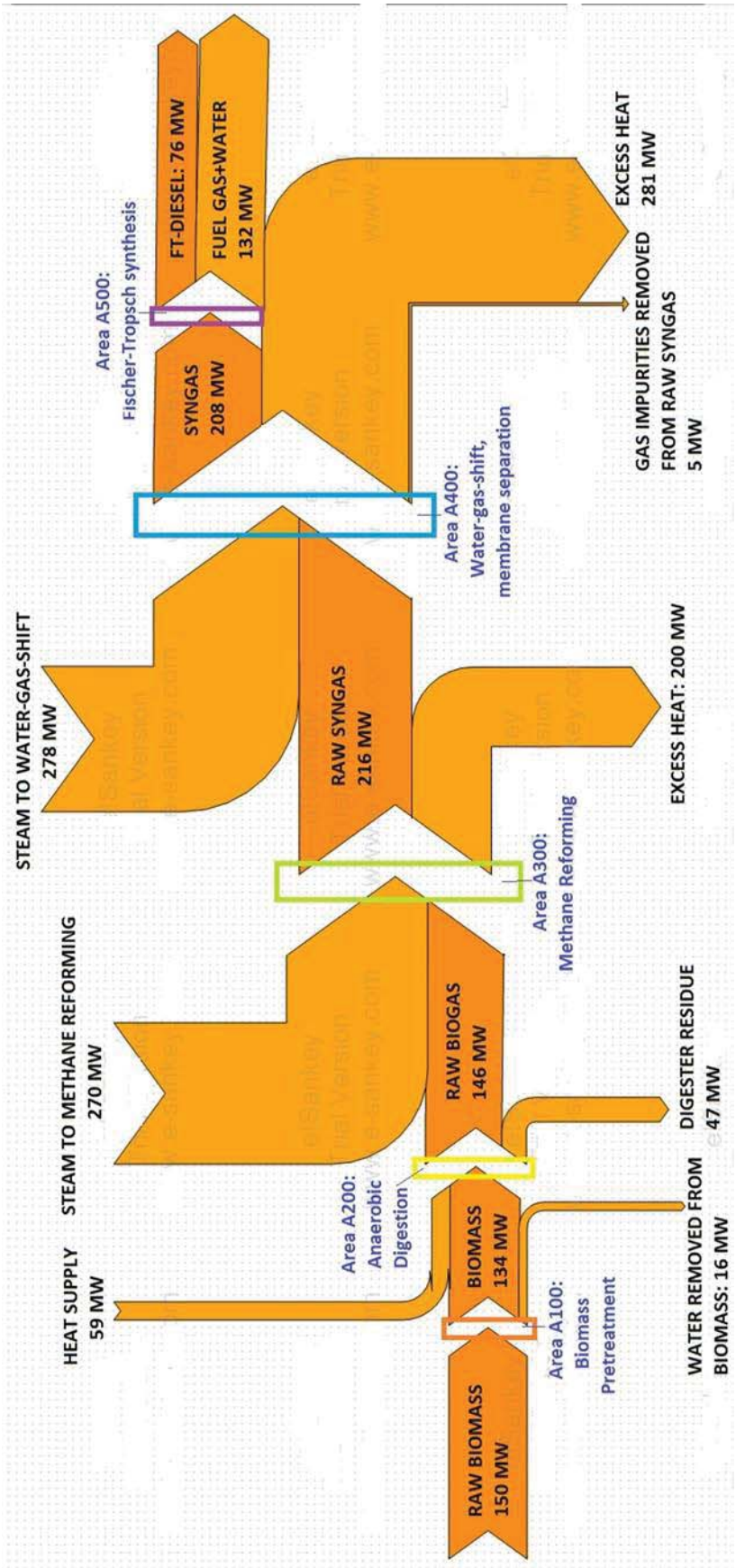

Figure 6-4: ESankey-diagram illustrating the energy flows (MW) for the biochemical pathway.

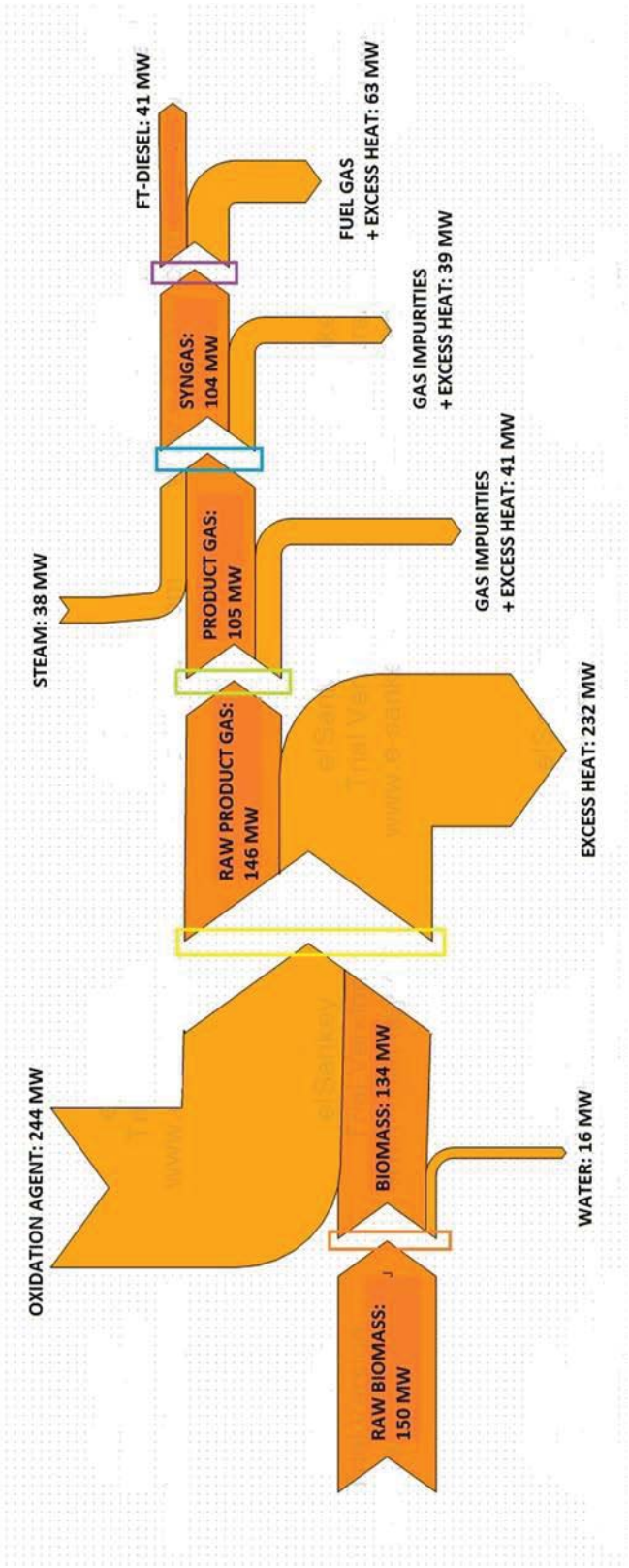

Figure 6-5: ESankey-diagram illustrating the energy flows (MW) for the thermochemical pathway.

The figure shows that with a 150 MW biomass input, 41 MW Fischer-Tropsch diesel is produced. Additional energy inputs to the process comprise 244 MW oxidation agent to the gasifier and 38 MW steam for water-gas-shift reactions. Total energy input (biomass plus additional) equals 432 MW. Energy losses are related to all five processes. 16 MW is lost through the waste water flow in the biomass pretreatment process. 232 MW is lost as excess heat in the gasification process. 41 MW is lost as gas impurities (1 MW) and excess heat (40 MW) through gas filtering. 39 MW is lost from water-gas-shift and membrane separation, of which 0.23 MW is lost through gas impurities and 38.77 MW is lost as excess heat. 63 MW is lost through Fischer-Tropsch bi-products. Total energy losses related to the process equals 391 MW.

In the following sections the energy flow data is evaluated by calculating the *feed-to-fuel and feed-to-loss ratio* process by process for both scenarios and are denoted by expression (6-7)

$$E_{ijn}, \qquad \textbf{(6-7)}$$

where the subscript *"i"* represent each of the pathway processes 1 to 5 where 1 is biomass pretreatment, 2 is biomass-to-gas conversion process, 3 is gas conditioning step one, 4 is gas conditioning step two and 5 is the gas-to-liquid conversion process. The subscript *"j"* represents the pathway, 1 is the biochemical pathway and 2 is the thermochemical pathway. Subscript *"n"* represents the output flow that is evaluated, expressed by flow name. The calculations are performed in appendix IV, equations IV-29 to IV-46 and table IV-7 and the results are presented in Table 6-10 below.

Table 6-10 lists the results of calculations performed in appendix IV. Each row represents the resulting feed-to-fuel or feed-to-loss ratio for a given process. The process areas are listed in column one. The calculated parameter is listed in column two. Column three lists the feed-to-fuel ratios for scenario 1 and scenario 2 respectively, whereas column four lists the feed-to-loss ratios. The equation numbers from appendix are listed in column five. The results will be presented process by process below, before this chapter is ended with a graphical illustration of the feed-to-fuel ratios from Table 6-10 above. The illustration will constitute a sound basis for discussion in the next chapter 7.

Process	E_{ijn}	Feed To Fuel [%] Scenario1	Feed To Fuel [%] Scenario 2	Feed To Loss [%] Scenario1	Feed To Loss [%] Scenario 2	Equation
A100 Biomass Pretreatm.	E_{11BMAS}	89.33				IV-29
	E_{12BMAS}		89.33			IV-29
	E_{11WAT}			10.67		IV-30
	E_{12WAT}				10.67	IV-30
A200: Biomass to Gas	E_{21BGAS}	108.96				IV-31
	E_{22PGAS}		38.62			IV-33
	E_{21RESD}			35.07		IV-32
	E_{22CHAR}				0.03	IV-34
A300: Gas Cond. Step 1	E_{31BGAS}	51.92				IV-35
	E_{32PGAS}		71.92			IV-37
	E_{31IMPU}			0.00		IV-36
	E_{32IMPU}				0.00	IV-36
Area A400: Gas Cond. Steap 2	E_{41SYNG}	42.11				IV-39
	E_{42SYNG}		72.73			IV-41
	E_{41IMPU}			1.01		IV-40
	E_{42IMPU}				0.16	IV-42
Area A500: Fischer-Tropsch Synthesis	E_{51FUEL}	36.54				IV-43
	E_{52FUEL}		39.42			IV-44
	E_{51EFF}	51				IV-45
	E_{52EFF}		27			IV-46

Table 6-10: Calculation Results, Feed-to-fuel and Feed-to-Loss ratios.

Area A100: Biomass Pretreatment

Recall from chapter 6.1 that the mass flows related to biomass pretreatment were equal for both scenarios. Likewise, the energy flows related to both scenarios are equal. The energy flow data are given in Table 6-11. The data is rendered with zero decimal places for consistency with the input energy basis of 150 MW defined for this work.The energy contained in the raw biomass input (PL00BMAS) equals 150 MW. Steam input (PL81STM) and output (PL84STM) related to the steam drying equals 1064 MW. The moisture extracted from the biomass (PL92WAT) corresponds to 16 MW energy flow.

Area A100 SCENARIO 1	Input		Output		
Flow	PL00BMAS	PL81STM	PL06BMAS	PL84STM	PL92WAT
Energy flow (MW)	150	1064	134	1064	16
Area A100 SCENARIO 2	Input		Output		
Flow	PL00BMAS	PL81STM	PL06BMAS	PL84STM	PL92WAT
Energy flow (MW)	150	1064	134	1064	16

Table 6-11: Energy Flow Data, area A100 Biomass Pretreatment.

Based on results presented in Table 6-11, the feed-to-fuel and feed-to-loss ratios can be calculated. In Table 6-12 it follows that 89% of the raw biomass feedstock is conserved in the pretreated biomass for both scenarios. The waste water discharge corresponds to 11% of the raw biomass feedstock.

Process	E_{ijn}	Feed To Fuel [%]		Feed To Loss [%]		Equation
		Scenario1	Scenario 2	Scenario1	Scenario 2	
A100 Biomass Pretreatm.	E_{11BMAS}	89				IV-29
	E_{12BMAS}		89			IV-29
	E_{11WAT}			11		IV-30
	E_{12WAT}				11	IV-30

Table 6-12: Feed-to-fuel and Feed-to-Loss ratios, Area A100 Biomass Pretreatment.

Area A200: Biomass-to-gas Conversion

The anaerobic digestion process in scenario 1 differs substantially from the gasification process in scenario 2. This is prominent in the energy flow data given in Table 6-13. The energy flow data in Table 6-13 show that for scenario 1, the energy flow related to the biomass input (PL06BMAS) equals 134 MW. The energy output equals 146 MW of biogas (PL21BGAS) and 47 MW digester residues (PL22RESD). For scenario 2, the gasification process is supplied with 244 MW oxidation agent (PL90OXYG+PL90STM). Recall from chapter 6.1 that mass flows gives a supply of steam only. Therefore, oxygen energy flow (PL90OXYG) is zero. The gasification products consist of 146 MW product gas (PL21SYNG) and 0.1 MW char residue (PL22CHAR)

.

Area A200 SCENARIO 1	Input	Output			
Flow	PL06BMAS	PL21BGAS	PL22RESD	-	-
Energy flow (MW)	134	146	47	-	-
Area A200 SCENARIO 2	Input			Output	
Flow	PL06BMAS	PL90OXYG	PL90STM	PL21SYNG	PL22CHAR
Energy flow (MW)	134	0	244	146	0.1

Table 6-13: Energy Flow Data, area A200 Anaerobic Digestion/Gasification.

Table 6-14 shows that for scenario 1, 109% of the energy in the pretreated biomass is conserved in the biogas. The 9% increase is a result of mass flow composition change; biogas has a higher heating value than biomass. The digester residue contains 35% of the incoming energy. For scenario 2, 39% of the energy content in the biomass is conserved in the product gas. The char residue contains 0% of the biomass energy. Both percentages are lower than for scenario 1.

Process	E_{ijn}	Feed To Fuel [%]		Feed To Loss [%]		Equation
		Scenario1	Scenario 2	Scenario1	Scenario 2	
A200: Biomass to Gas	E_{21BGAS}	109				IV-31
	E_{22PGAS}		39			IV-33
	E_{21RESD}			35		IV-32
	E_{22CHAR}				0	IV-34

Table 6-14: Feed-to-Fuel and Feed-to-loss ratios, Area A200 Biomass-to-gas Conversion.

Area A300: Gas Conditioning Part 1

Recall that the first step of gas conditioning is methane reforming for scenario 1 and gas filtration for scenario 2. The energy flow data are given in Table 6-15. During methane reforming, 146 MW of raw biogas from anaerobic digestion (PL21BGAS) enters the methane reformer. 270 MW steam is provided (PL22STM) to the reactor. The syngas product after steam reforming (PL32SYNG) has an energy content of 216 MW. During gas filtration, 146 MW product gas (PL21SYNG) enters the filtration device. The filter products consist of 105 MW rinsed product gas (PL32SYNG) and 40 MW of particles trapped in the filter (PL33IMPU).

Area A300 SCENARIO 1	Input		Output		
Flow	PL21BGAS	PL22STM	PL32SYNG	PL33IMPU	-
Energy flow (MW)	146	270	216	-	-
Area A300 SCENARIO 2	Input		Output		
Flow	PL21SYNG	-	PL32SYNG	PL33IMPU	-
Energy flow (MW)	146	-	105	40	-

Table 6-15: Energy Flow Data, area A300 Methane Reforming/Gas Filtering

Table 6-16 shows that 52% of the raw biogas is conserved in the biogas after methane reforming, whereas 72% of the raw product gas is conserved in the gas after gas filtration. There are no losses (in terms of combustible energy) for the processes. Based on conservation of energy, 48% and 28% of the energy in the scenarios are not accounted for. The energy is assumed to represent energy loss in terms of excess heat, as is apparent in the ESankey diagrams in figures 6-1 and 6-2.

Process	E_{ijn}	Feed To Fuel [%] Scenario1	Feed To Fuel [%] Scenario 2	Feed To Loss [%] Scenario1	Feed To Loss [%] Scenario 2	Equation
A300: Gas Cond. Step 1	E_{31BGAS}	52				IV-35
	E_{32PGAS}		72			IV-37
	E_{31IMPU}			0		IV-36
	E_{32IMPU}				0	IV-36

Table 6-16: Feed-to-Fuel and Feed-to-Loss ratios, Area A300 Gas Conditioning Part 1.

Area A400: Gas Conditioning Part 2

As discussed in chapter 4, another gas conditioning step is required before Fischer-Tropsch synthesis can be applied. The energy flow data is presented in Table 6-17. For the scenario 1, 216 MW raw syngas enters the gas conditioning process (PL32SYNG). 278 MW steam (PL85STM) is required for the water-gas-shift reactor. The gas conditioning generates 208 MW clean syngas (PL41SYNG) and 5MW gas impurities (PL42AGAS) removed from the gas. For scenario 2, 105 MW product gas enters the gas conditioning process (PL32SYNG). 38 MW steam (PL85STM) is required for the water-gas-shift reactor. The gas conditioning produces 104 MW clean syngas (PL41SYNG) and 0.23 MW gas impurities (PL42AGAS) is removed from the gas.

Area A400 SCENARIO 1	Input		Output		
Flow	PL32SYNG	PL85STM	PL41SYNG	PL42AGAS	-
Energy flow (MW)	216	278	208	5	-
Area A400 SCENARIO 2	Input		Output		
Flow	PL32SYNG	PL85STM	PL41SYNG	PL42AGAS	-
Energy flow (MW)	105	38	104	0.23	-

Table 6-17: Energy Flow Data, area A400 Water-gas-shift and Membrane Separation.

Table 6-18 verifies that in scenario 1, 42% of the raw syngas is conserved in the syngas after the second gas conditioning. 1% of the energy is lost with the gas impurities. In scenario 2, 73% of the energy in the product gas is conserved in the syngas. 0% of the total energy input to the gas conditioning is conserved in the gas impurities extracted from the syngas. Based on conservation of energy, an energy loss equal to 57% and 27% for the two scenarios are not accounted for in the analysis. The energy loss is assumed to consist of excess heat from the gas conditioning processes which are present in the ESankey diagrams in figures 6-1 and 6-2.

Process	E_{ijn}	Feed To Fuel [%] Scenario1	Feed To Fuel [%] Scenario 2	Feed To Loss [%] Scenario1	Feed To Loss [%] Scenario 2	Equation
Area A400: Gas Cond. Steap 2	E_{41SYNG}	42				IV-39
	E_{42SYNG}		73			IV-41
	E_{41IMPU}			1		IV-40
	E_{42IMPU}				0	IV-42

Table 6-18: Feed-to-Fuel and Feed-to-Loss ratios, Area A400 Gas Conditioning Step 2.

.

Area A500: Fischer-Tropsch Synthesis

The Fischer-Tropsch synthesis converts syngas to a liquid biofuel, namely the Fischer-Tropsch diesel (FT-diesel), fuel gases and waste water. The energy flows related to the scenarios are shown in Table 6-19 . In scenario 1, 208 MW syngas (PL41SYNG) is converted to 76 MW FT-diesel (PL53FTRO). In scenario 2, 104 MW syngas (PL41SYNG) is converted to 41 MW FT-diesel (PL53FTRO).

Area A500 SCENARIO 1	Input		Output		
Flow	PL41SYNG	-	PL53FTRO	PL52FGAS	-
Energy flow (MW)	208	-	76	-	-
Area A500 SCENARIO 2	Input		Output		
Flow	PL41SYNG	-	PL53FTRO	PL52FGAS	-
Energy flow (MW)	104	-	41	-	-

Table 6-19: Energy Flow Data, area A500 Fischer-Tropsch Synthesis.

Table 6-20 verifies that 37% of the syngas is conserved in the Fischer-Tropsch diesel in scenario 1 whereas 39% of the syngas is conserved in the Fischer-Tropsch diesel for scenario 2.The fuel efficiencies are calculated below.

Process	E_{ijn}	Feed To Fuel [%]		Feed To Loss [%]		Equation
		Scenario1	Scenario 2	Scenario1	Scenario 2	
Area A500: Fischer-Tropsch Synthesis	E_{51FUEL}	37				IV-43
	E_{52FUEL}		39			IV-44
	E_{51EFF}	51				IV-45
	E_{52EFF}		27			IV-46

Table 6-20: Feed-to-Fuel and Feed-to-Loss ratios, Area A500 Fischer-Tropsch Synthesis.

The fuel efficiency for scenario 1 is calculated by dividing the energy content of the Fischer-Tropsch diesel with the energy content of the biomass feedstock, expressed by equation (6-8).

$$E_{51EFF} = \frac{FT - diesel\ Output}{Biomass\ Input} = \frac{PL53FTRO}{PL00BMAS} = \frac{76MW}{150MW} = 0.51 \qquad \textbf{(6-8)}$$

Equation (6-8) verifies that the fuel efficiency for scenario 1, the biochemical pathway is 0.51 which means that 51% of the energy input into the pathway by biomass is converted to useful biofuel energy output. The fuel efficiency for the total pathway in scenario 2 is calculated by equation (6-9).

$$E_{52EFF} = \frac{FT - diesel\ Output}{Biomass\ Input} = \frac{PL53FTRO}{PL00BMAS} = \frac{41MW}{150MW} = 0.27 \qquad \textbf{(6-9)}$$

Equation (6-8) verifies that the fuel efficiency for scenario 2, the thermochemical pathway is 0.27, which means that 27% of the energy input into the pathway by biomass is converted to useful biofuel energy output. The fuel efficiency for the biochemical pathway is 0.51, which is 53% higher than the efficiency obtained for the thermochemical pathway. This result will be investigated in chapter 7. The result is presented in Table 6-20 above.

Finally, the resulting feed-to-fuel ratios are illustrated graphically in Table 6-6 below.

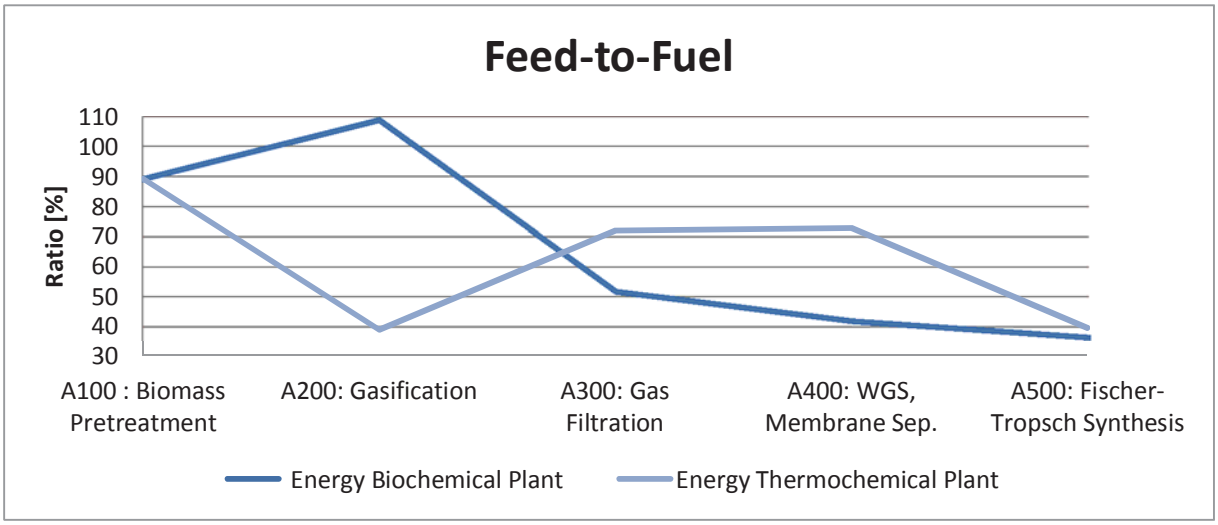

Figure 6-6: Feed-to-fuel ratios

Figure 6-6 represents both *biochemical* and *thermochemical* pathways. The energy feed-to-fuel ratio is given in percentage (y-axis) for each of the five conversion pathway processes (x-axis). The feed-to-fuel ratio is measured in terms of fuel output divided on total energy input to each process. The figure reflects what was observed in the above sections. For the biochemical pathway, the anaerobic digestion is performing a high ratio of 109% while the gas conditioning is performing a low ratio with a minimum for the Fischer-Tropsch synthesis of 37%. The thermochemical feed-to-fuel ratio is the opposite, with a minimum of 39% for the gasification. The ratio increases during gas conditioning and reaches a maximum for water-gas-shift and membrane separation where it equals 73%.'The Fischer-Tropsch synthesis feed-to-fuel ratio is equal to 39% which is slightly higher than for the biochemical pathway. The results will be discussed in the next chapter 7.

7. Discussion

The results obtained to this point provide the basis for a comparative study of the energy flows through the conversion pathways. The key finding is the considerable deviation between the biomass to gas conversion and gas conditioning processes. A discrepancy in feed-to-fuel conversion between the two pathways is also prominent. The results obtained will be presented graphically to highlight the topics put up to discussion. Topics from the theory in chapter 2, 3 and 4 are included when considered appropriate. Results from previous work are included to discuss the reliability of the results obtained.

It is emphasized that the energy flows are obtained by a simplified approach. The heating value approach applied only consider the potential energy released by combustion, and does not take into account thermal and mechanical losses related to the pathways. Pathways involving mass flow will consist of pumps, pipelines, stirring devices, heaters and coolers that are related to mechanical losses like friction losses and thermal energy losses in terms of heat transfers and radiation to mention a few. Work are provided for the equipment to operate and the pathways both require and release heat due to both thermal energy transfers and chemical energy changes (H.N. Shapiro, 2006). The energy analysis performed does still give a good indication of which challenges that can be expected by the two conversion pathways investigated, and the models that are developed creates a solid fundamental in which further an more detailed energy analysis can be performed upon. The first topic to be discussed are the energy flow results. An energy flow analysis is performed in chapter 7.1.

7.1. Energy Flow Analysis

The energy flow analysis include considerations regarding energy inputs and energy losses in the two coming sections.

Considerations regarding Energy Input

The energy input is presented in Figure 7-1 below.

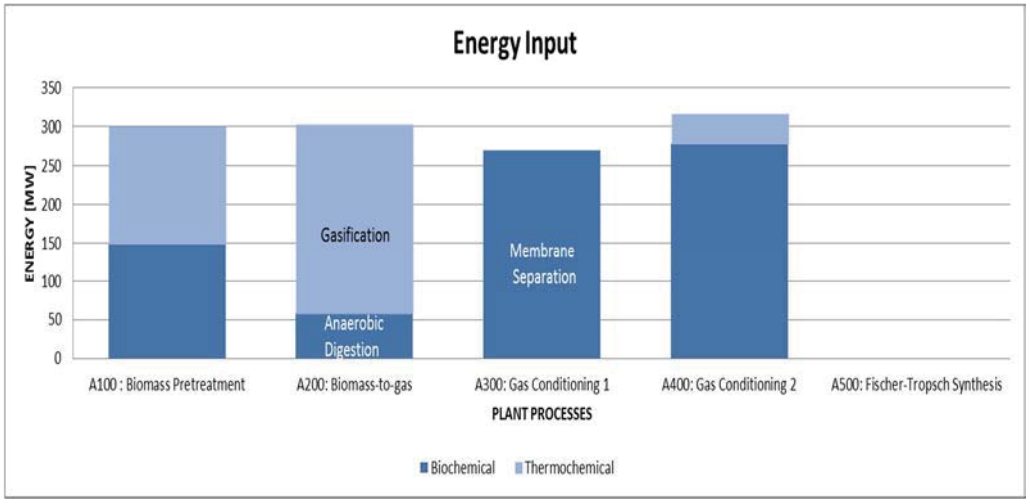

Figure 7-1: Energy Input Results for Biochemical Plant and Thermochemical Plant.

Figure 7-1 presents energy input flow (y-axis) for the five conversion pathway processes (x-axis). The biochemical and thermochemical energy flows are denoted by dark blue and light blue color respectively. Column one consist of a 150 MW biomass input whereas columns 2-4 consist of steam and heat. There is no energy input related to the Fischer-Tropsch synthesis. As highlighted in chapter 6, the energy input basis is 150 MW for both plants, which is also apparent in column one the figure.

The figure can be divided into two parts with distinctive results-one is represented by column two and the other is represented by columns 3 and four. The results illustrated in column two indicate that the gasification process is more energy demanding than the anaerobic digestion. From chapter 6 it is known that the energy flow contribution to the gasification process is the 244 MW oxidation agents supply, whereas 59 MW heat is required for the anaerobic digester, derived from conservation of energy principle. Thermal energy considerations are not included in this work, and the difference is expected to be even higher if thermal energy where included for the gasification process since the gasification is operational at a temperature of 861 ^{o}C compared to the mesophilic (30 ^{o}C) operational environment for the anaerobic digester.

The results illustrated in columns three and four indicate that both gas conditioning processes are characterized by high energy input for the biochemical pathway and correspondingly low energy input for the thermochemical pathway. This result may indicate that the process of upgrading biogas to a syngas quality require more energy than upgrading product gas to the same syngas quality. From chapter 6 it is known that the energy demand is represented by steam for both pathways, and that the steam demanding processes are represented by methane reforming and the water-gas-shift reaction. The result illustrated in column three can be explained by recalling that the methane rich biogas obtained in the biochemical pathway induces high methane reforming activity and does therefore require more steam than the thermochemical pathway with a low-methane product gas.

In column four the gas upgrading process is equal for both pathways. However, a deviation regarding energy input between the two processes is prominent, as expressed numerically equals 278 MW of energy requirement in terms of steam for the biochemical pathway compared to 38 MW for the thermochemical pathway. By recalling the gas compositions for the respective gases as presented in chapter 6.2 there are reason to believe that the water content of the syngas is causing this deviation. The thermochemical product gas contains 37% water whereas the biogas contains none. Recall from chapter 4.2 that product gas usually contain 38-61% water, so the water content might be assumed reasonable. This water content may reduce the steam demand for the thermochemical plant since the water-gas-shift reactor can shift the gas by using the water vapor already present in the gas. The biogas contains zero water vapor both before and after methane reforming and all water must be supplied by steam for water-gas-shift reaction to occur. Recall from chapter 4.2 that biogas usually contain 10-20% water. This information was not accounted for when designing the anaerobic digestion calculator in Aspen Plus. Water should have been accounted for as it might reduce the amount of steam necessary for water-gas-shift reactions, reducing both energy input and losses related to biochemical gas conditioning. This issue is considered a model weakness in this work and should be accounted for in further work.

Considerations regarding energy losses

The energy loss is presented in figure Figure 7-2 below.

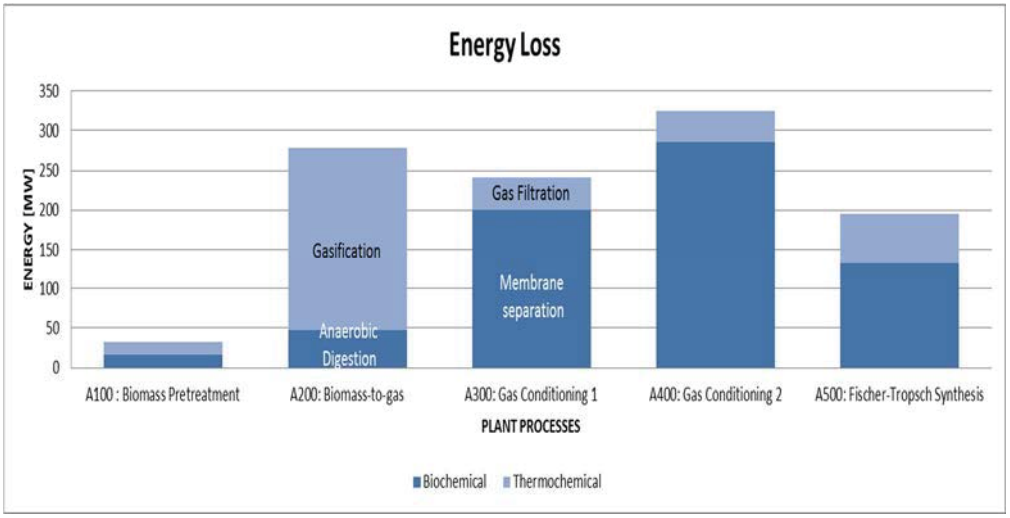

Figure 7-2: Energy Loss Results for Biochemical Plant and Thermochemical Plant.

Figure 7-2 presents energy loss flows (y-axis) for the five conversion pathway processes (x-axis) and is structured in the same way as Figure 7-1 above. Also here, the results obtained in the figure can be divided into two distinctive parts-one part is the biomass-to-gas conversion represented by column two and another represented by columns three, four and five. The energy losses associated

with biomass pretreatment in column one are related to the waste water extracted from the raw biomass. They are the smallest energy losses obtained and are equal for both conversion pathways.

Equivalent to the high energy input presented for the gasification process in Figure 7-1, the energy loss associated with the gasification is higher than for the anaerobic digester. The energy loss related to the anaerobic digestion is a 47 MW digester residue whereas the energy loss related to the gasification consists of excess heat and equals 232 MW. There is also a char residue related to the gasification process, but it is so small that it is neglected. The result supports the suggestion of higher thermal heat requirement for the gasification process than what is suggested in figure 7-1, and is related to the high gasification temperature.

In contrast, both column three, four and five presents high energy losses for the biochemical pathway. In column three the energy loss equals 200 MW and consists of excess heat from methane reformation. The high energy loss might be related to the high steam input. Correspondingly, for the thermochemical plant the energy loss equals 41 MW and consists of gas impurities and excess heat from gas filtration. A low energy loss where expected since gas filtration provides no external energy input. However, the excess heat obtained for gas filtration is unexpected and could be a result of consecutively gas cooling throughout the pathway. The gasification temperature of 861^{o}C would result in hot product gas leaving the gasification furnace. The pipelines transporting it to the gas filtration device are assumed to be placed in ambient temperature surroundings which would lead to radiation losses throughout the system if not merely insulated. However, since this energy flow is obtained from conservation of energy only the value is uncertain. If a thermal energy analysis were performed this loss might be even higher.

Column four present energy losses related to water-gas-shift and membrane separation, and are equal to 286 MW for the biochemical pathway and 39 MW for the thermochemical pathway. Both losses consist of excess heat and gas impurities, and the difference is remarkable. It might be a result of the very high energy input related to steam addition for water-gas-shift to the biochemical pathway as outlined above, which in general might indicate that high steam requirements are related to high energy loss in terms of heat.

The energy losses related to the Fischer-Tropsch synthesis in column five consist of fuel gases and waste water that are considered bi-products from the process. The figure shows that the energy loss of 132 MW is higher for the biochemical plant. The thermochemical plant energy loss equals 63 MW. From chapter 6.3 the difference may be explained by the larger energy input to the Fischer-Tropsch synthesis for the biochemical pathway. Taking this into account, the energy losses related to the Fischer-Tropsch synthesis might increase linearly with increasing syngas input. The energy loss is related to waste water and fuel gases.

The considerations given above indicate that the gasification process is more energy demanding than the anaerobic digestion, but that a considerably larger amount of energy is required for upgrading of the biogas to a syngas quality. The resulting energy losses reflect these results in high energy losses for gasification compared to anaerobic digestion, but there again larger energy losses

for the biogas conditioning compared to product gas conditioning. To be able to weight these results against the quality of the Fischer-Tropsch diesel output, the energy utility, feed-to-fuel ratio and heating values are presented in the next section.

7.2.Liquid Biofuel Quality

Before discussing the liquid biofuel quality obtained for the two conversion pathways, considerations concerning the feed-to-fuel ratio for selected energy flows and the composition of selected mass flows are evaluated.

Feed-to-fuel

The feed-to-fuel ratios for each of the five processes are illustrated in Figure 7-3 below.

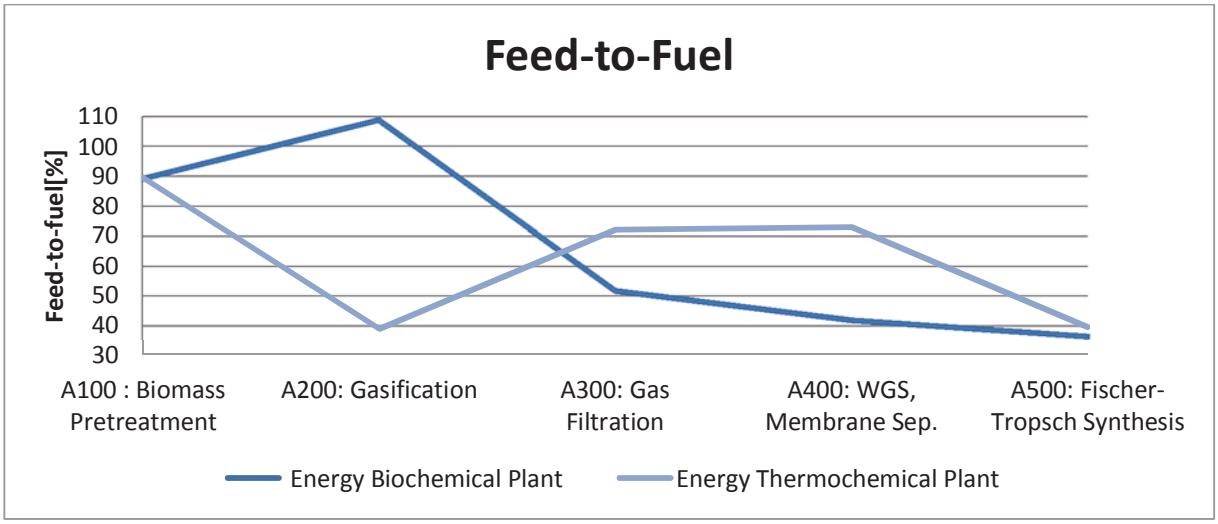

Figure 7-3: Energy Utility for Biochemical Plant and Thermochemical Plant.

Figure 7-3 represents both biochemical and thermochemical pathways. The feed-to-fuel ratio is given in percentage (y-axis) for each of the five conversion pathway processes (x-axis). The ratio is measured in terms of fuel output divided on total energy input to each process, as calculated in chapter 6, and the figure is reproduced from chapter 6.3.

Figure 7-3 illustrates that for the biochemical pathway, the feed-to-fuel ratio is high for biomass pretreatment, increase slightly for biomass-to-gas conversion, and then decrease when performing gas conditioning and Fischer-Tropsch synthesis. For the thermochemical pathway the tendency is the opposite. The feed-to-fuel ratio is high for biomass pretreatment but decrease for the gasification process. It increases when gas conditioning is performed, before a decrease again is observed for the Fischer-Tropsch synthesis process. By comparing these results with the results obtained for energy inputs and energy losses in the above sections there might be a correlation

between high energy inputs, resulting high energy losses and poor energy utility for the processes. The results obtained to this point may indicate that the biogas upgrading to syngas quality is more energy consuming than more conventional thermochemical product gas upgrading for the application to Fischer-Tropsch processes. Next, to understand the basis for Fischer-Tropsch synthesis output the syngas composition is given some extra attention.

The Composition of Selected Mass Flows

Two interesting observations made regarding the syngas composition for the two pathways is discussed in the following. Review the biogas, product gas and syngas composition in Table 7-2 as was presented in chapter 6.2.

Biochemical				Thermochemical			
Area A300:Biogas	mass fraction	Area A400: Syngas	mass fraction	Area A300: Product Gas	Gas mass fraction	Area A400: Syngas	Gas mass fraction
H2	0.11	H2	0.16	H2	0.04	H2	0.13
CO	0.86	CO	0.83	CO	0.30	CO	0.70
H2S	0.01	-	-	CH4	0.05	CH4	0.15
NH3	0.01	-	-	H2O	0.37	H2O	0.01
-	-	-	-	CO2	0.25	CO2	0.01

Table 7-1: Syngas Composition

As stated in the introduction above, two observations are made regarding the syngas composition. The thermochemical syngas contain 15% methane when entering the Fischer-Tropsch synthesis process. The methane may cause abnormal Fischer-Tropsch synthesis operation and lead to decreasing Fischer-Tropsch diesel yield. The methane content on this stage in the conversion pathway might be caused by a lack in removal of methane on gas conditioning steps prior to the Fischer-Tropsch synthesis. Recall from chapter 4.2 that the gas filtration only remove particulates and hence no methane. Also recall that the membrane separation process lacks to remove methane. The water gas shift reaction does not affect methane, and thus the gas conditioning sequence chosen for the thermochemical plant lacks a process to remove or reduce methane content in the product gas. This is a model weakness and the choice of gas conditioning processes should be re-evaluated to improve Fischer-Tropsch synthesis for thermochemical conversion pathway.

The other observation made from gas composition table is the hydrogen to carbon monoxide ratio. In this work it is equal to 0.19 for both conversion pathways. Recall from chapter 6.3 that optimal ratio is between 0.7 and 2.1. Reports investigating the Fischer-Tropsch diesel production via

biomass gasification generally get ratios between 0.45 and 2.1 (O.P.R. van Vliet, 2009). Thus, the ratios obtained in this work are low and may be a source of decreased Fischer-Tropsch Diesel yield. Both these issues underpins that the results obtained in terms of energy efficiency and Fischer-Tropsch diesel heating value must be evaluated with a critical mind as they are presented in the next section.

Feed to fuel Energy Conversion and Liquid Biofuel Heating Value

The feed-to-fuel ratio obtained for the entire plant in terms of calorific value calculations are presented in Table 7-2 below.

Pathway	Feed to Fuel [%]	Biofuel Heating Value [MJ/kg]
Biochemical	51	47.89
Thermochemical	27	66.34

Table 7-2: Energy Efficiency and Liquid Biofuel Heating Value for total Conversion Pathways.

Table 7-2 shows that the feed to fuel energy conversion obtained for the biochemical plant equals 51% and is higher than the 27% obtained for the thermochemical plant. An investigation of 14 different Fischer-Tropsch fuel production plants performed by O.P.R. van Vliet et.al concluded that the feed-to-fuel conversion for eucalyptus wood gasification performed with bubbling fluidized bed was 52%. In the same study, the range of feed to fuel conversion ratios for all the processes investigated was in the range of 49-52% (O.P.R. van Vliet, 2009). This might indicate that the feed to fuel conversion ratio for the biochemical plant can be compared to the ones obtained for thermochemical gasification production chains. The thermochemical feed-to-fuel conversion is lower than what is expected when compared to the same theoretical values.

Table 7-2 also present the Fischer-Tropsch diesel heating values obtained for the two conversion pathways. A study on the production of synthetic diesel from biomass performed by K. Laohalidanond et.al compares a Fischer-Tropsch diesel lower heating value equal to 44 MJ/kg to conventional diesel equal to 42.7 MJ/kg to state that the Fischer-Tropsch diesel has slightly improved combustible properties as a liquid transportation fuel (K. Laohalidanond, 2006). In this work the fuel properties in terms of heating value can be said to be even better compared to conventional diesel. The Lower heating value of the biochemical Fischer-Tropsch diesel equals 47.89 MJ/kg whereas the lower heating value obtained for the thermochemical Fischer-Tropsch diesel is higher and equals 66.34 MJ/kg. The value exceeds lower heating values found in literature and might seem unrealistically high. The reason for this matter can be an error in the Aspen Plus heating value calculator integrated in the model. If this is the case both heating value results obtained are doubted, and the calculator that performed the Fischer-Tropsch diesel heating value calculations should be revised. It would be of interest to know the composition of the Fischer-Trospch diesel obtained in this work. This issue in addition to model improvements is summarized in further work presented in the next chapter.

8. Conclusion and Further Work

8.1. Conclusion

In this work, one biochemical and one thermochemical biomass-to-liquid biofuel conversion pathway have been investigated. The focus has been on comparing the two conversion pathways in terms of identifying the energy flows and feed to fuel ratio. The work is bounded to consider lignocellulosic biomass as feedstock and Fischer-Tropsch diesel as liquid biofuel output. The pathways investigated comprise two-stage biomass to liquid biofuel conversion. The first stage is a biomass to gas stage considering anaerobic digestion and gasification for the respective conversion pathways. The second stage is a gas to liquid biofuel conversion performed by Fischer-Tropsch synthesis. The biomass feedstock is 873 ton/day birch, representing 150 MW basis for both conversion pathways.

Available technology applicable is investigated, and models are developed for the two conversion pathways by using Aspen Plus and FORTRAN. An energy analysis is performed by model simulations and heating value calculations to identify the energy flows through the two pathways.

Results obtained indicate that the biochemical conversion pathway is less energy effective in terms of gas-to-liquid conversion. This result is observed both in terms of energy demand, energy losses and energy utility for the pathway, and is a result of the steam required for methane reformation and water-gas-shift reaction. At the contrary, the thermochemical conversion pathway is less energy effective in terms of biomass to gas conversion, mainly because of the high temperature required for gasification.

The feed to fuel ratio obtained on the biochemical pathway of 51% correspond to previous work results obtained on thermochemical pathways and might indicate that obtaining competitive biofuel product by lignocellulose based biochemical pathway are feasible. The corresponding feed to fuel ratio obtained on the thermochemical pathway of 27% is lower than previous work performed on similar systems. The low ratio may be the result of model weaknesses in Aspen Plus model.

The syngas obtained in both conversion pathways has low H_2/CO ratios, indicating that the model developed is not optimal. The biogas obtained in the biochemical pathway lacks some substantial gas components like water vapor, which is the result of a simplified model approach in Aspen Plus. The syngas obtained in the thermochemical pathway contain methane that might prevent Fischer-Tropsch process from optimal operation.

8.2. Further Work

The conclusion given in chapter 8.1 indicates that the biochemical pathway is subject to challenges regarding the development of energy efficient gas-to liquid conversion technologies, but that the liquid Fischer-Tropsch diesel produced is competitive with more commercial Fischer-Tropsch diesel derived via thermochemical pathways. The methane rich biogas obtained in anaerobic digestion has a high heating value, and it could be interesting to develop and compare two new scenarios comparing the direct combustion of biochemically derived biogas to biochemically derived Fischer-Tropsch diesel.

The models developed in this work are subject to model weaknesses that are believed to reduce the credibility of the results, especially for the thermochemical pathway. It would be of interest to improve the models and reevaluate the results. Suggestions to improvement for the biochemical and thermochemical pathways separately are listed below.

Biochemical model:

- The pretreatment process technology chosen consist of a drier and a grinder, and is applied to enable the use of the same technology for both conversion pathways. The technology options should be re-evaluated and preferably a steam pretreatment method should be applied to improve cellulose availability before anaerobic digestion.
- The anaerobic digester is modeled as a simple calculator considering only methane, carbon dioxide, ammonia and hydrogen sulfide based on results obtained from theory. The model could be improved by integrating a more advanced calculator taking the cellulose content of the biomass and lignin into account. A more extensive range of gas components should be included in the gas.

Thermochemical model:

- The oxidation agent supply to the gasification process should be reinvestigated as it fails to supply the gasification reactions with oxygen. A sensitivity analysis could preferably be performed on the gasification process in the existing model to identify the optimal oxygen-to-steam ratio to be integrated in the model.
- The gas conditioning sequence should be reinvestigated as it lacks to remove methane from the product gas. A methane reforming reactor would probably be required.

References

A. Petersson, A. W. (2008). *Biogas upgrading technologies - development and innovations.* Malmö: IEA Bioenergy.

A. Steinhauser, D. D. (2011). *Biogas from Waste and Renewable Resources* (2.. utg.). Wiley VCH.

aspentech. (u.d.). *aspentech*. Hentet mai 02, 2013 fra http://www.aspentech.com/products/aspen-plus.aspx

A. vanderDrift, H. B. (2004). Entrained Flow Gasification of Biomass: ash behaviour, feeding issues, and system analyses. *ECN Biomass*, 1-58.

A.T.W.M. Hendriks, G. Z. (2008). Pretreatments to enhance the digestibility of lignocellulosic biomass. *Bioresource Technology*, 10-18.

Bjune, M. (2009). *Biogass fra blandinger av storfegjødsel og og industribasert matavfall . Mikrobiologiske , metodiske og prosessmessige aspekter ved metanproduksjon.* Oslo: Universitetet for Miljø-og biovitenskap.

C.N. Hamenlinck, A. F. (2004). Production of FT transportation fuels from biomass; technical options, process analysis and optimisation, and development potential. *Energy*, ss. 1743-1771.

Crofcheck, M. M. (2010). Chapter 2: Energy Crops for the Production of Biofuels. I M. Crocker, *Thermochemical conversion of biomass to liquid fuels and chemicals* (ss. 26-45).

D.Brown, J. S. (2012). Comparison of solid-state to liquid anaerobic digestion of lignocellulosic feedstocks for biogas production. *Bioresource Technology*, ss. 379-386.

Gerardi, M. H. (2003). *The microbiology of anaerobic digesters.* John Wiley and Sons.

G. Jacobs, B. D. (2010). Chapter 5: Conversion of Biomass to Liquid Fuels and Chemicals via the Fischer-Tropsch Synthesis Route. I M. Crocker, *Thermochemical Conversion of Biomass to Liquid Fuels and Chemicals* (ss. 95-123). Lexington: RSC Energy and Environment.

H.N. Shapiro, M.J (2006) Fundamentals of Engineering Thermodynamics. John Wiley and Sons

I.I. Ahmed, A. G. (2010, September 13). Pyrolysis and gasification of food waste: syngas characteristics and char gasification kinetics. *Applied energy*, ss. 101-108.

Kempegowda, R. (2013, February-May). Post Doctoral Fellow. (H. Ø. Berg, Intervjuer)

Johansson, N. (2008). *Production of liquid biogas, LBG, with cryogenic and conventional upgrading technology.* Department of Technology and Society. Lund: Lunds Tekniska Högskola.

K.Kim. (2013). Long-term operation of biomass-to-liquid systems coupled to gasification and Fischer-Tropsch processes for biofuel production. *Bioresource Technology*, 391-399.

K. Laohalidanond, J. H. (2006). *The Production of Synthetic Diesel from Biomass.* Aachen: RWTH Aachen University, Germany.

K. Panther, O. S. (2006). Maximising biogas in anaerobic digestion by using engine waste heat for thermal hydrolysis pre-treatment of sludge. *Water Science and Technology*, 101-108.

K. Zhang, J. C. (2012, February 6). Lignocellulosic biomass gasification technology in China. *Renewable Energy*, 175-184.

L. Devi, K. P. (2002, July 15). A review of the primary measures for tar elimination in biomass gasification processes. *Biomass and Bioenergy*, 125-40.

Lånke, A. F. (2013, February). Advisor, Rambøll Energi. (H. Ø. Berg, Intervjuer)

M.B. Nikoo, N. M. (2008, February 20). Simulation of biomass gasification in fluidized bed reactor using ASPEN PLUS. *Biomass and Bioenergy*, ss. 1245-1254.

M. Crocker, R. (2012). Chapter 1: The Rationale for Biofuels. I M. Crocker, *Thermochemical Conversion of Biomass to Liquid Fuels and Chemicals* (ss. 1-25). London: The Royal Society of Chemistry.

M.J. Prins, K. P. (2006). More efficient biomass gasification via torrefaction. *Energy 31*, 3458-3470.

M.J. Taherzadeh, K. K. (2008). Pretreatment of Lignocellulosic Wastes to Improve Ethanol and Biogas Production: A Review. *International Journal of Molecular Sciences*, 1621-1651.

M.J.A. Tijmensen, A. F. (2002, March 13). Exploration of the possibilities for production of Fischer Tropsch liquids and power via biomass gasification. *Biomass and Bioenergy*, ss. 129-152.

McKendry, P. (2001). Energy Production From Biomass (part 1): overview of biomass . *Bioresource Technology*, 37-46.

McKendry, P. (2002). Energy production from biomass (part 3): gasification technologies. *Bioresource Technology*, 55-63.

Neathery, J. (2010). Chapter 4 Biomass Gasification. I M. Crocker, & P. L. Peter (Red.), *Thermochemical Conversion of Biomass to Liquid Fuels and Chemicals* (ss. 67-93). Cambridge: The Royal Society of Chemistry.

NIST Chemistry WebBook. (u.d.). Hentet May 09, 2013 fra http://webbook.nist.gov/chemistry/

O.P.R. van Vliet, A. F. (2009). Fischer-Tropsch Diesel production in a well-to-wheel perspective: A carbon, energy flow and cost analysis. *Energy Conversion and Management*, 855-876

R. Gonzalez, J. D. (2011). Economics of cellulosic ethanol production in a thermochemical pathway softwood, hardwood, corn stover and switchgrass. *Fuel Processing Technology*, 113-122.

R. Jafari, R. S.-G. (2004, February 27). Modular Simulation of Fluidized Bed Reactors. *Chemical Engineering Technology*, ss. 123-129.

R.M. Swanson, J. S. (2010). *Techno-Economic Analysis of Biofuels Production Based on Gasification.* Golden, Colorado: National Renewable Energy Laboratory NREL.

R.S. Kempegowda, Q. T. (2013). Influence of wet and dry torrefaction process on biomass to liquid fuel production trough fischer-tropsch under norwegian conditions. *International Conference on Applied Energy, Paper ID: ICAE2013-249* (s. 10). Pretoria, South Africa: Department of Energy & Process Engineering, NTNU, Trondheim, Norway.

S. van Loo, J. K. (2008). *The Handbook of Biomass Combustion & Co-firing.* London: Earthscan.

T.A. Milne, R. E. (1998). *Biomass Gasifier "Tars": Their Nature, Formation and Conversion.* Golden, Colorado: National Renewable Energy Laboratory.

T. Patterson, S. E. (2011). An evaluation of the policy and thermo-economic factors affecting the potential for biogas upgrading for transport fuel use in the UK. *Energy Policy*, 1806-1816.

T.D.Foust, A. A. (2009). An economic and environmental comparison of a biochemical and a thermochemical lignocellulosic ethanol conversion processes. *Cellulose*, 547-565.

Tran, Q. (2012, October 01). Gasification and Pyrolysis. *Gasification and Pyroysis*. Trondheim, Sør Trøndelag, Norway: NTNU.

Tran, Q. (2012, Oktober). Soild Biomass As Fuel for Heat and Power Generation - Part 1. Trondheim, Trøndelag, Norway.

valhalla. (2001, February 27). *What Is Fortran?* Hentet May 02, 2013 fra http://valhalla.fcaglp.unlp.edu.ar/~computacion/Manuales/Online/prof77/node2.html

Waste Water System. (2013, May 17). *Industrial Waste Water Treatment System*. Hentet May 19, 2013 fra http://www.wastewatersystem.net/2011/04/anaerobic-reactor-suspended-growth.html

Weiland, P. (2009, September 24). Biogas Production: current state and perspectives. *Appl Microbiol Biotechnol*, ss. 849-860.

W. Torres, S. P. (2007). Hot Gas Removal of Tars, Ammonia, and Hydrogen Sulfide from Biomass Gasification Gas. *Catalysis Rewievs: Science and Engineering*, 407-454.

W. Yan, T. A. (2009, August 5). Thermal Pretreatment of Lignocellulosic Biomass. *Environmental Progress and Sustainable Energy, 28*(3), 435-440.

I. Process Models Developed in Aspen Plus

Area A100: Biomass Pretreatment Process

The biomass pretreatment consist of a drier and a grinder as illustrated in figures I-1 to I-3 on the next 3 pages. The entire process is illustrated in figure I-1. Raw biomass enters the biomass pretreatment area as flow PR00BMAS. The drying hierarchy A100DRY contains drying process as illustrated in figure I-2. The drier require steam input PL81STM and output PL84STM. Excess moisture from drying leaves as PR92WAT. Dried biomass enters grinding hierarchy A100GRIN via PR05BMAS. The grinder hierarchy is illustrated in figure I-3. Pretreated biomass leaves the grinder via flow PL06BMAS.

Figure I-2 illustrates the drying process of the pretreatment area A100. The raw biomass enters the drying process by DR01BMAS. Steam input DR1STM is mixed with biomass in the mixer DRHEAT01. Biomass and steam DR02BMAS enters the dryer DRDRY01 and is separated into dried biomass DR03BMAs and water and steam mixture DR01WAT. Water and steam enters a separator with steam output DR84STM and extracted water output DR92WAT. Water is re-injected to biomass via the mixer DRMIX01 by flow DR02WAT if dried biomass contains less than 10% water. Biomass DR04BMAS enters e heat exchanger DRHEAT02 and leaves the dryer via DR05BMAS.

Figure I-3 represent the biomass grinding process of the pretreatment process in area A100. The dried biomass enters the grinding process via GR05BMAS. It enters a mixer GRMIX01 that adds biomass particles recycled from grinding GR09BMAS. The mixture GR06BMAS enters the grinder GRGRIN01 and the grinded biomass GR02BMAS enters e separator GRSEP01 that sorts out the particulate sizes larger than 50 mm. To large particles are re-injected to grinder via GR09BMAS and biomass of satisfactory size leaves the grinder via GR07BMAS.

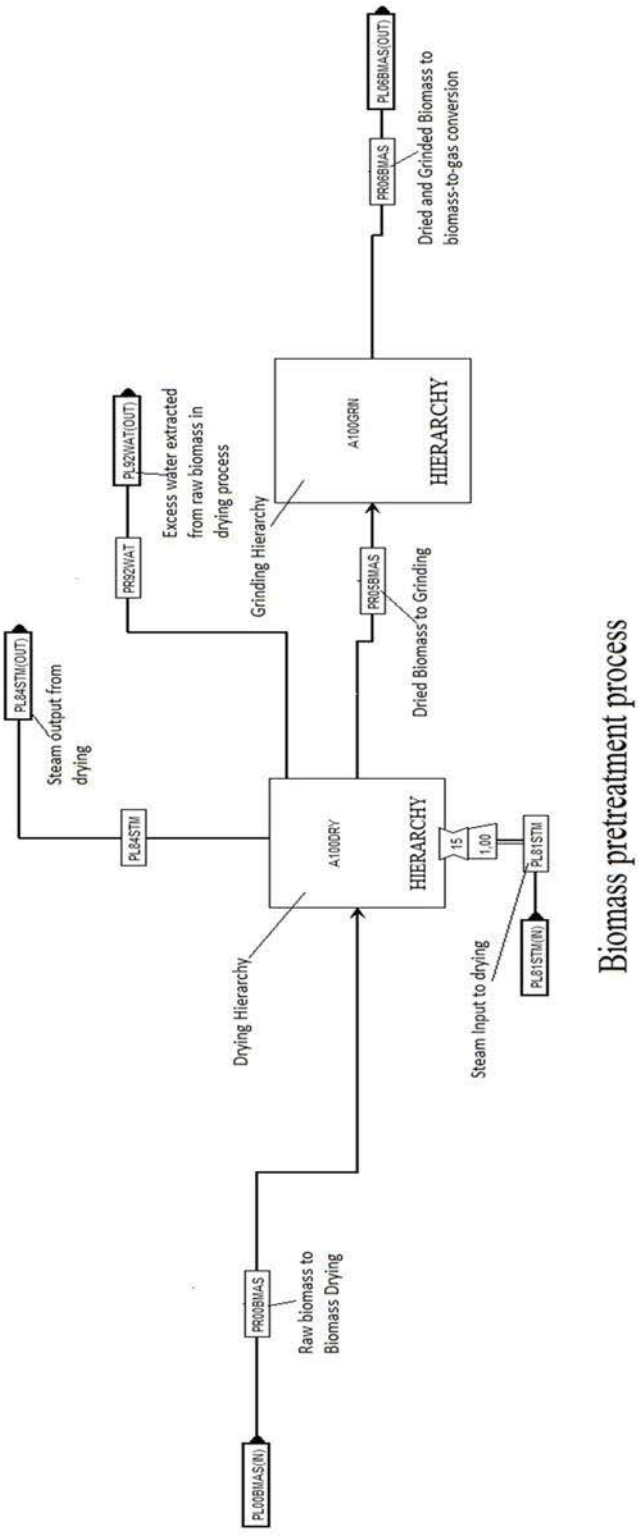

Figure I-1: Area A100: Biomass Pretreatment

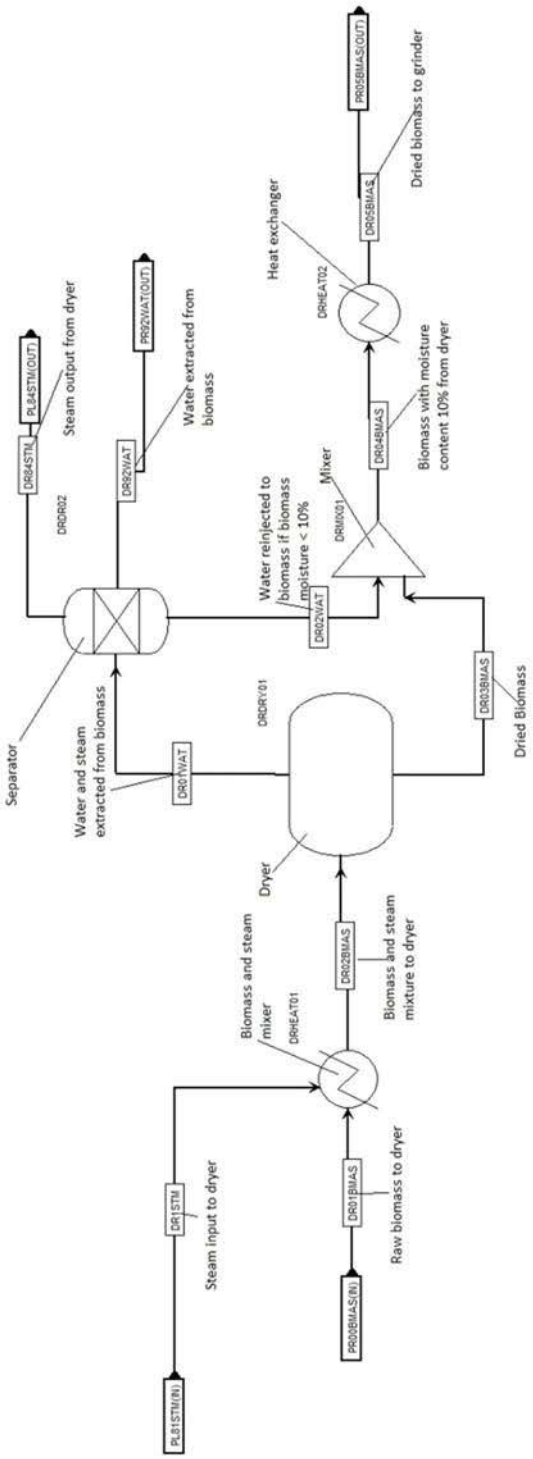

Figure I-2: Area A100: Biomass Drying

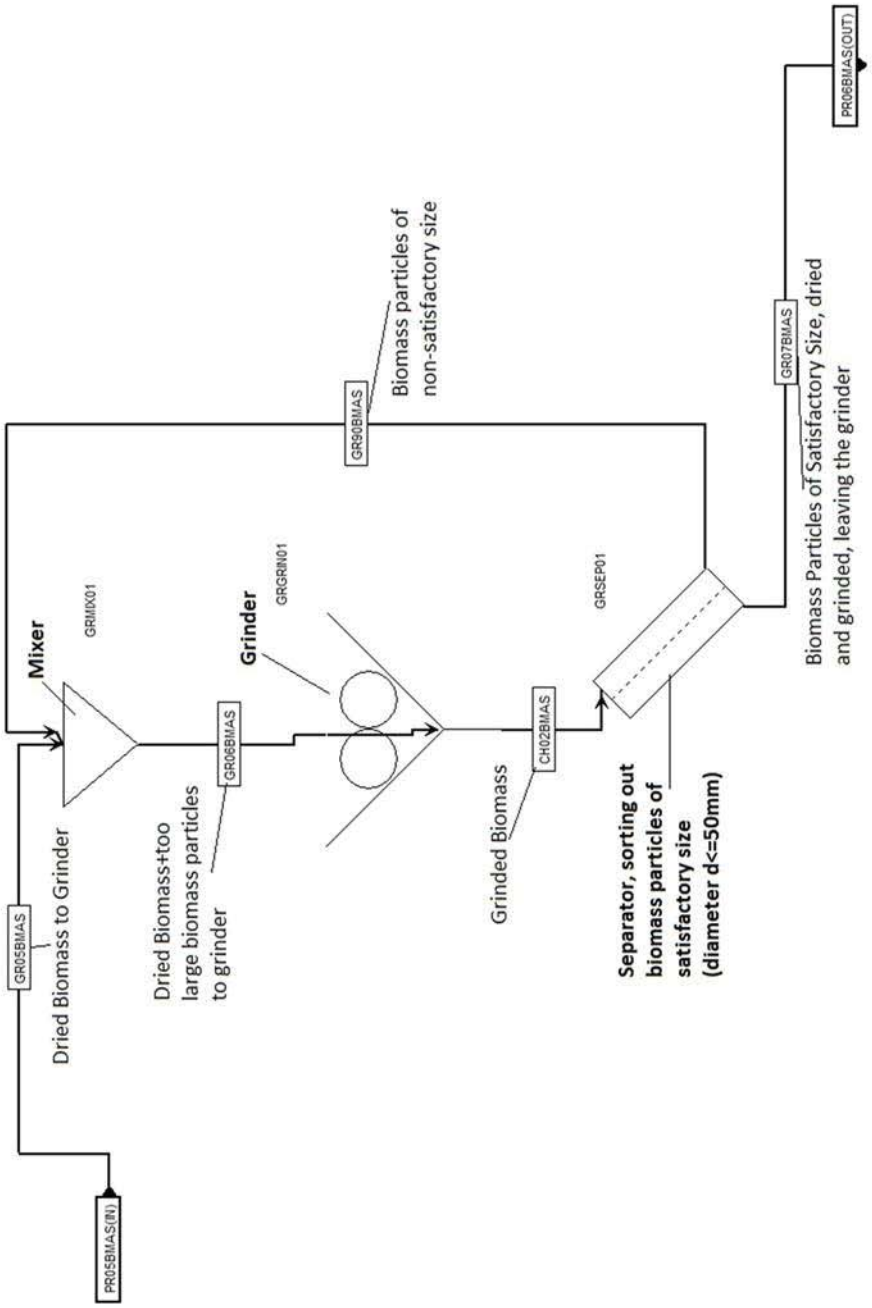

Figure I-3: Area A100: Biomass Grinding

Area A300: Gas Filtration, Thermochemical Plant

Gas filtration is illustrated in figure I-4. The product gas enters the gas filtration area A300 via PL21SYNG. It enters a heat exchanger and is entering the gas filtration unit PLSEP01. It filtrate the product gas, which leaves the process as PL31SYNG. The gas impurities filtrated out from the gas is extracted via PL33IMPU.

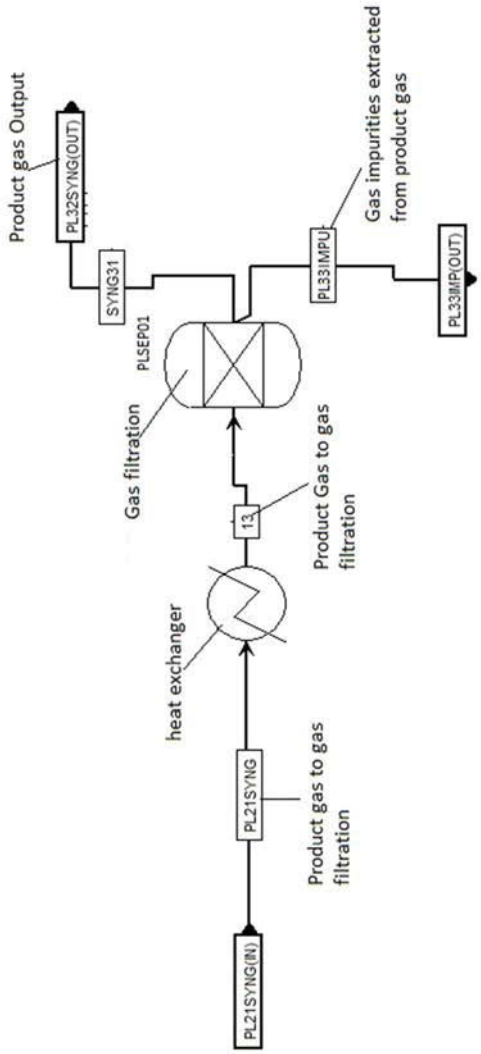

Figure I-4: Area A300: Gas Filtration

Area A400: Water-Gas-Shift (WGS) and Membrane Separation

The process is illustrated in figure I-5. The gas enters area A400 via CL32SYNG. It passes through a heat exchanger and a separator via CL33SYNG. The separator splits the flow into one product gas fraction CL22SYNG going to WGS and one fraction CL23SYNg going directly to membrane separator. Steam CL85STM and gas enters hierarchy A300SGS representing the WGS process as described in figure I-6. Shifted gas CL26AGAS is mixed with product gas CL23SYNG and enters the membrane separator AGASREM via CL24SYNG. Syngas leaves the process via CL25SYNG and gas impurities are extracted as CL42AGAS.

The WGS reactor represented by hierarchy A300SGS is illustrated in figure I-6. The product gas enters the reactor SGREAC01 via WG25SGAS. The reactor require steam, which is supplied via WG90STN and compressed by WGCOMP01 before it is injected in the reactor as WG91STM. The reactor products are a waste water WGWAT01 and a shifted syngas WG26SGAS leaving the WGS reactor.

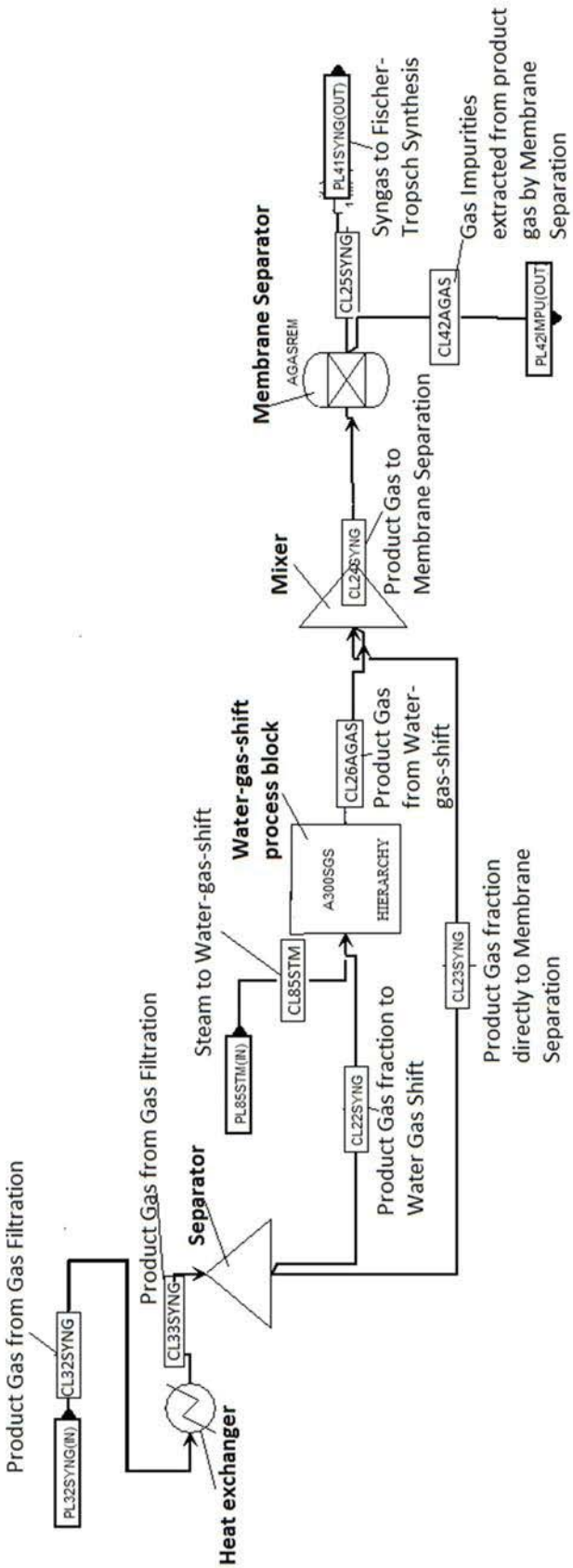

Figure I-5: Area A400: Water Gas Shift and Membrane Separation

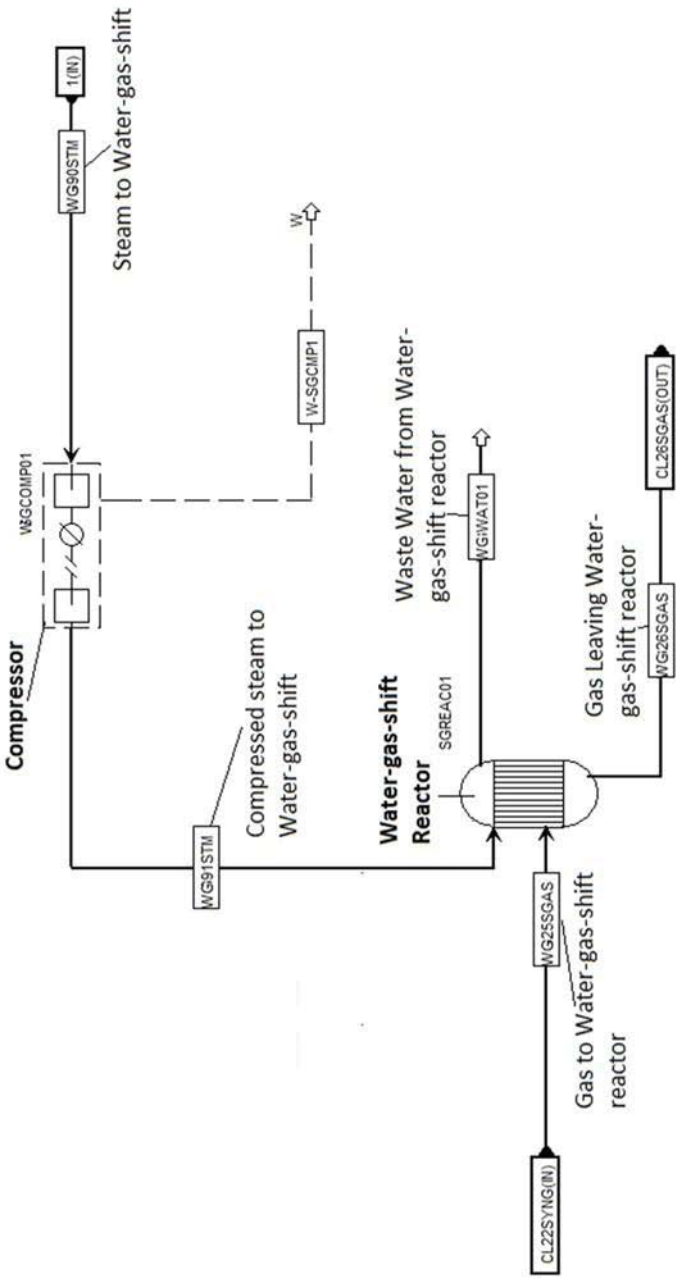

Figure I-6: Area A400 Water Gas Shift

Area A500: Fischer-Tropsch Synthesis

Figure I-7 represents the Fischer-Tropsch Synthesis. Syngas enters the process via PL41SYNG and is compressed to compressed gas FS51SYNG. It enters a heater and is mixed with recycled fuel gas via FS52SYNG. The fuel gas and syngas mixture FS53SYNG enters the Fischer-Tropsch reactor FSREAC01, and its products leaves as FS54FT. The products are heated and enter the liquid-gas separator as FS55FT. The separator separates liquid phases from gas phases, and fuel gas FS57GAS is separated into a combustible gas that is extracted and a fuel gas that is compressed and re-injected to the Fischer-Tropsch reactor as FS58SGAS. The Liquid Fischer-Tropsch Products FS56FT enters a second separator that separates waste water from the Fischer-Tropsch diesel FTPROD. The Fischer-Tropsch diesel enters a heating value calculator as illustrated in figure I-8 an leaves the Fischer-Tropsch synthesis process.

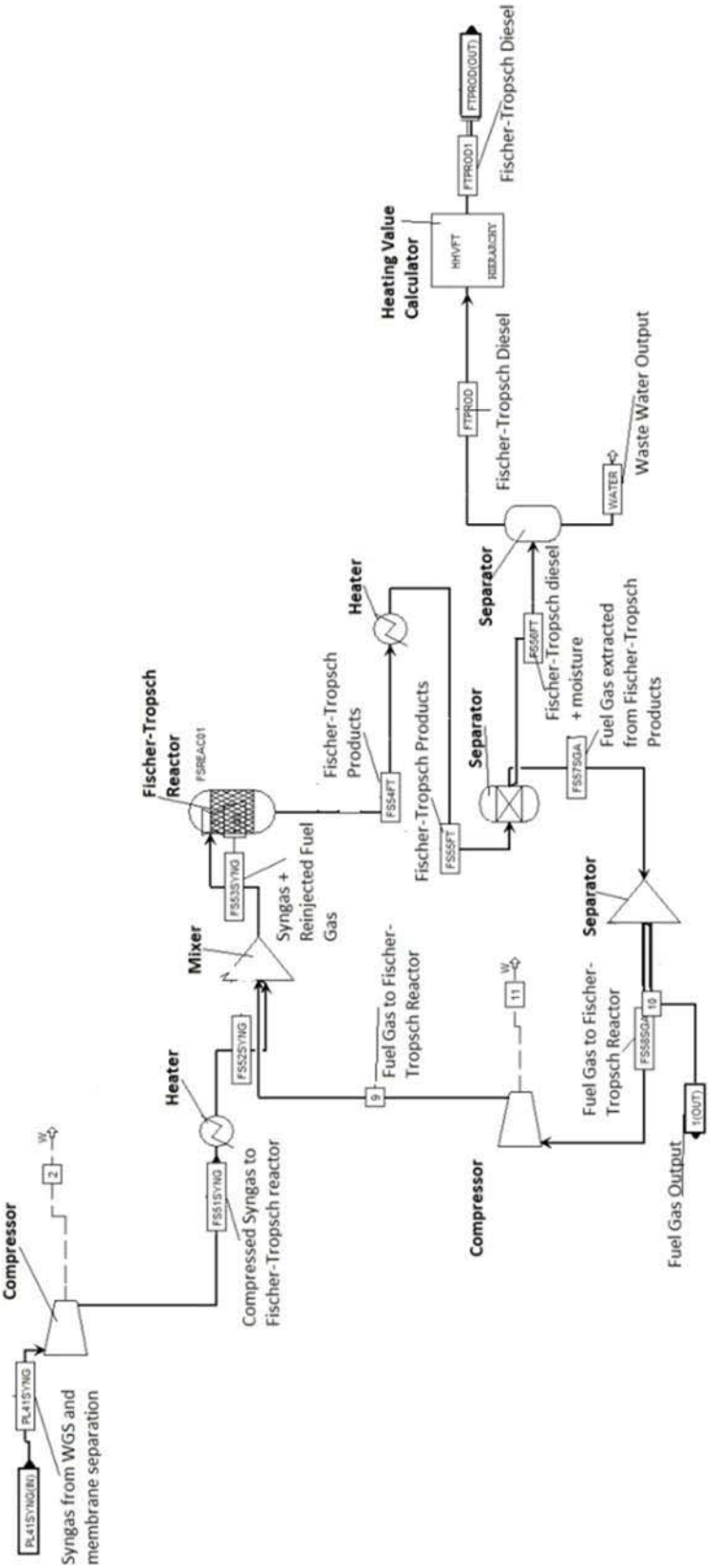

Figure I-7: Area A500: Fischer-Tropsch synthesis

Heating Value Calculator

The heating value calculator is illustrated in Figure I-8 below. It is used for both heating value calculations of biomass and the Fischer-Tropsch diesel. Here, only the biomass calculator is presented. The Fischer-Tropsch diesel calculator is similar; the only difference is the name and composition of the incoming and outgoing flows to and from the duplicator. The figure includes a brief description of how the calculator works, and a step-wise explanation will be given in this section. Each sequence explained in this text is enumerated. The number is also given in the figure with a purpose to enlightened understanding.

1: The biomass enters the heating value calculator block where it is duplicated into a separate flow RAW that the calculation is performed on. The biomass input and output to the calculator is thus not affected.

2: The duplicated biomass flow RAW enters a separator that splits the biomass into combustible and non-combustible fractions. The non-combustible fraction consists of ash, char and impurities and is rejected as flow REJECTX. The combustible biomass leaves the separator via the flow named BASIS.

3: The combustible biomass enters a combustion reactor as the flow BASIS. The combustion reactor is supplied with oxygen to perform complete combustion of the fuel. The heat of combustion QCOMB leaves the combustor and is the first contributor to the heating value that we seek.

4: A second combustion reactor is applied to enable the combustion of nitrogen oxides that is generated in stage 3. It releases heat through flow “4” and is the second contributor to the heating value that we seek.

5: Recall from theory presented in chapter 2 that in the lower heating value, the latent heat contained in the biomass is not considered, which is the heat released when phase changes of the biomass occur Thus, a separator is applied to separate evaporated and liquid fractions COMVAP of biomass from solid fractions COMBLIQ in combusted material.

6: The solid fraction COMBLIQ is cooled down to ambient temperature and gives of heat “10” which is the third and last contributor to lower heating value.

7: The heat released from combustion and cooling of dry biomass residue is summarized in block QNET and is the lower heating value for the biomass flow input.

8: To calculate the higher heating value, a separator separates the dry biomass RESIDUE from the water fraction WATERV of the biomass. The water fraction WATERV is cooled to ambient temperature (9) and release heat QVAP.

10: QVAP is added to the lower heating value to provide the higher heating value for the biomass in block B8.

.

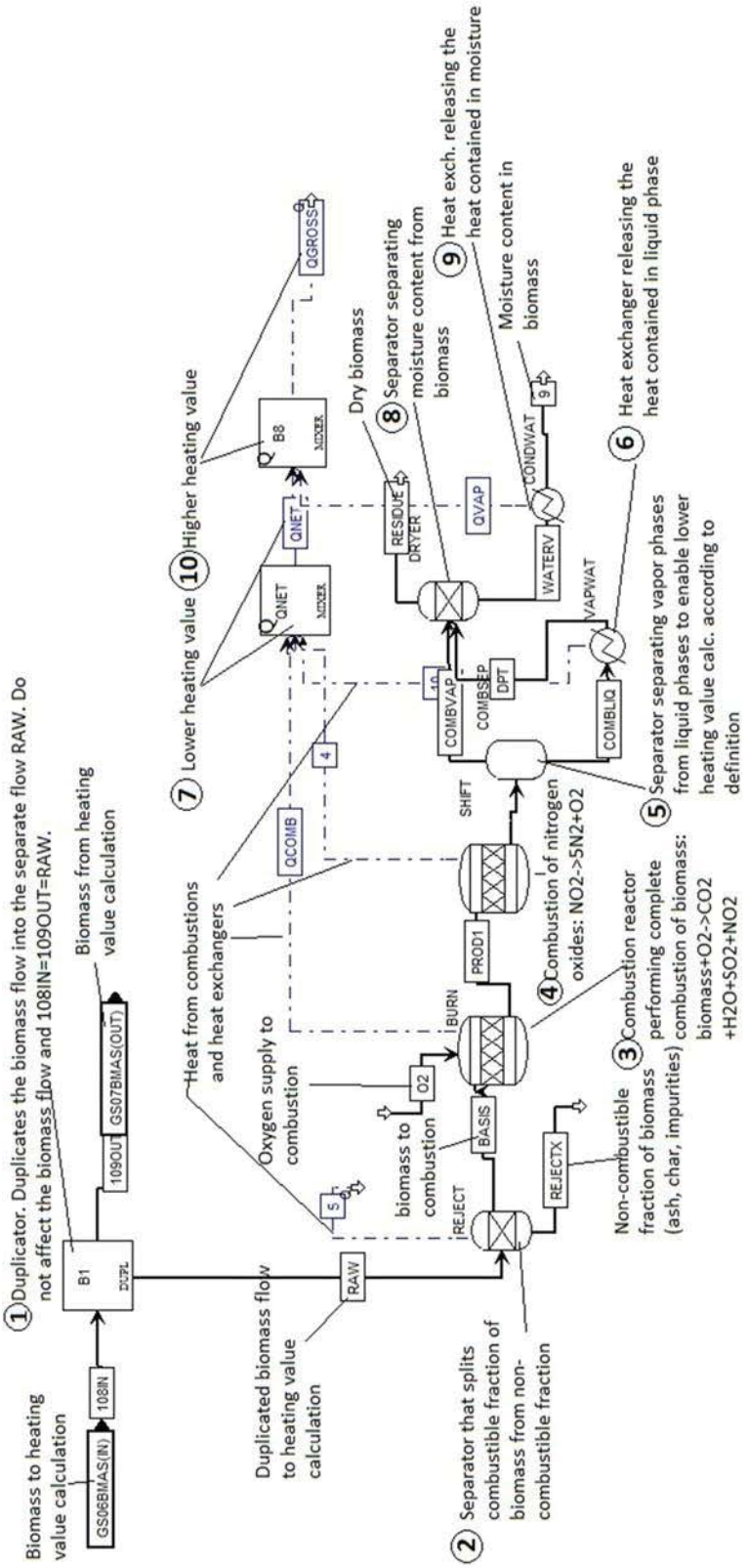

Figure I-8: Heating Value Calculator

II. Aspen Plus Calculator Block Descriptions

Four external calculators have been modeled in order to simulate the gasification process. The calculators are written in Aspen Plus with FORTRAN declarations methodology.

BIOELEM

The BIOELEM calculator splits the biomass input into carbon, hydrogen, oxygen, nitrogen, sulfur, and ash based on the biomass ultimate analysis. This is done in order to split the biomass flow into flows representing the amount of carbon, hydrogen, oxygen, nitrogen, sulfur and ash contained in the biomass. This is required in order to run combustion reactions when the biomass enters the gasification zone. All variables used in the calculator are described in table II-1.

Variable Name	Description	Variable Name	Description	Variable Name	Description
BIOMAS	The biomass input flow	HIN	Per cent hydrogen in the biomass input flow, calculated	HYDRO	Amount of hydrogen in the biomass output flow, calculated
CFEED	Amount of carbon in the biomass input flow, based on ultimate analysis	OXIN	Per cent oxygen in the biomass input flow, calculated	OXYGEN	Amount of oxygen in the biomass output flow, calculated
HFEED	Amount of hydrogen in the biomass input flow, based on ultimate analysis	SULIN	Per cent sulfur in the biomass input flow, calculated	SULFUR	Amount of sulfur in the biomass output flow, calculated
OFEED	Amount of oxygen in the biomass input flow, based on ultimate analysis	XNITIN	Per cent nitrogen in the biomass input flow, calculated	XNITRO	Amount of nitrogen in the biomass output flow, calculated
SFEED	Amount of sulfur in the biomass input flow, based on ultimate analysis	H2OOUT	Amount of water in the biomass input flow, calculated	H2OOUT	Amount of water in the biomass output flow, calculated
NFEED	Amount of nitrogen in the biomass input flow, based on ultimate analysis	ASHIN	Per cent ash in the biomass input flow, calculated	ASHOUT	Amount of ash in the biomass output flow, calculated
AFEED	Amount of ash in the biomass input flow, based on ultimate analysis	CARBON	Amount of carbon in the biomass output flow, calculated	BIOOUT	Amount of biomass in the output flow, set to zero to sustain mass balance
CIN	Per cent carbon in the biomass input flow, calculated				

Table II-1: BIOELEM Calculator Variable Name and Descriptions

The calculator input is shown in table II-2. The variable name is given in column one and five and is set in Aspen Plus. It is defined as either an import or export variable, as shown in column two and six. The import variable is always a fixed variable taken from one of the input flows – in this case the biomass input flow GS07BMAS as is described in column three and seven. The export variables are output variables that the FORTRAN calculator is estimating – in this case they are all contained in the output flow GS08BMAS as described in column three and seven. The calculator is shown in column four and eight. A row-by-row review of the table is given below.

FORTRAN DECLARATIONS, BIOELEM							
Variable Name	Variable type	Flow Name	Calculator	Variable Name	Variable type	Flow Name	Calculator
CFEED	Import	GS07BMAS	CIN = CFEED/100	HYDRO	Export	GS08BMAS	HYDRO = HIN*BIOMAS
HFEED	Import	GS07BMAS	HIN = HFEED/100	OXYGEN	Export	GS08BMAS	OXYGEN = OXIN*BIOMAS
OFEED	Import	GS07BMAS	SULIN = SFEED/100	SULFUR	Export	GS08BMAS	XNITRO = XNITIN*BIOMAS
SFEED	Import	GS07BMAS	XNITIN = NFEED/100	XNITRO	Export	GS08BMAS	SULFUR = SULIN*BIOMAS
NFEED	Import	GS07BMAS	OXIN = OFEED/100	H2OOUT	Export	GS08BMAS	H2OOUT = H2OIN
AFEED	Import	GS07BMAS	ASHIN = AFEED/100	ASHOUT	Export	GS08BMAS	ASHOUT = ASHIN*BIOMAS
BIOMAS	Import	GS07BMAS	CARBON = CIN*BIOMAS	BIOOUT	Export	GS08BMAS	BIOOUT = 0.0
CARBON	Export	GS08BMAS					

Table II-2: BIOELEM Calculator FORTRAN declarations.

Row two calculates the carbon fraction of the biomass. The carbon fraction is denoted CIN, and use the carbon content from the import variable CFEED. CFEED is given in Aspen Plus for the flow GS07BMAS. Then, in row 8 the amount of carbon in the biomass denoted by CARBON is calculated by multiplying the carbon fraction CIN by the entire biomass flow input BIOMASS. Row 9 show that CARBON is an export variable, meaning that its calculated value are transported in flow GS08BMAS: The same procedure is adopted for the rest of the rows in table II-2. The result is incoming biomass flow GS07BMAS carrying information about the ultimate and proximate biomass analysis converted by the calculator to an exported output flow consisting of the respective constituents given by the proximate and ultimate analysis.

OXYSET

This calculator sets the oxidization agent demand required in the gasification zone (which represents the bubbling fluidized bed furnace). It is divided into three independent calculators according to the Aspen Plus model. The calculators are named OXYSET1, OXYSET2 and OXYSET3. Each calculator represents a reactor in the gasification zone. OXYSET1 is connected to the gas phase reactor GSREAC01. OXYSET2 is connected to the char phase reactor GSREAC02. OXYSET3 is connected to the char phase reactor GSREAC03. They are presented individually below in two tables. One table explains the variables used and the other shows how oxygen and steam flows are calculated.. Oxygen to biomass ratios and steam to oxygen ratios are adopted from a NREL report on gasification (R.M. Swanson, 2010).

OXYSET1

Variable Name	Description
BMFLOW	The biomass input flow
O2FLOW	The oxygen demand when given a oxygen-to-biomass ratio of 26 %
ARFLOW	The amount of argon in the oxygen flow, set to 5 % of total flow
STFLOW	The steam demand when given a oxygen-to-steam ratio of 40/60

Table II-3: OXYSET1 Calculator Variables description

FORTRAN DECLARATIONS, OXYSET1			
Variable Name	Variable Type	Flow Name	Calculator
BMFLOW	Import	GS09BMAS	
O2FLOW	Export	GS13OXYG	O2FLOW = 26/100.0 * BMFLOW
ARFLOW	Export	GS13OXYG	ARFLOW = 0.05*O2FLO
STFLOW	Export	GS15STM	STFLOW = (2/3)*O2FLOW

Table II-4: OXYSET1 Calculator FORTRAN declarations

OXYSET2

Variable Name	Description
BMFLOW	The biomass input flow
O2FLOW	The oxygen demand when given a oxygen-to-biomass ratio of 26 %
ARFLOW	The amount of argon in the oxygen flow, set to 5 % of total flow

Table II-5: OXYSET2 Calculator Variables description

FORTRAN DECLARATIONS, OXYSET2			
Variable Name	Variable Type	Flow Name	Calculator
BMFLOW	Import	GS19CHAR	
O2FLOW	Export	GS14OXYG	O2FLOW = 26/100.0 * BMFLOW
ARFLOW	Export	GS14OXYG	ARFLOW = 0.05*O2FLOW

Table II-6: OXYSET2 Calculator FORTRAN declarations

OXYSET3

Variable Name	Description
BMFLOW	The biomass input flow
STFLOW	The steam demand when given a oxygen-to-stem ratio of 40/60

Table II-7: OXYSET3 calculator Variables description

FORTRAN DECLARATIONS, OXYSET3			
Variable Name	Variable Type	Flow Name	Calculator
BMFLOW	Import	GS18CHAR	
STFLOW	Export	GS16STM	STFLOW = (2/3)*(26/100*BMFLOW)

Table II-8: OXYSET3 calculator FORTRAN declarations

BIOGAS

The biogas calculator calculates the biogas output from the anaerobic digester. It is based on theoretical values obtained by R.S. Kempegowda and M.C. Bjune. The calculations procedure is shown in tables II-9 and II-10 below. Theoretical biogas composition is obtained from theory as listed in table II-9. Here, the biogas is assumed to consist of methane, carbon dioxide, ammonia and hydrogen sulfide. Only the volatile proportion of the incoming biomass can in practice become biogas, and thus also the volatile matter fraction is defined, based on procimate and ultimate analysis presented in chapter 2. The incoming biomass is separated into fractions of each of the gases in addition to residue. The “variable name” column lists the theoretical values used.

The calculations performed are presented in table II-10. Row 1 is an import variable and represent the incoming biomass to anaerobic digestion. Row 2 calculates the methane fraction of biogas by multiplying the incoming biomass with volatile matter fraction and methane fraction. The same procedure is performed on the three other gas constituents. The digester residue generally consists of solid and liquid material and the volatile matter fraction is thus not taken into account. The residue fraction is obtained by multiplying the incoming biomass with the residual fraction obtained from theory.

Variable Name	Description	Variable Name	Desription	Source
BIOMAS	The biomass Input Flow to Anaerobic Digestion	RES=0.315	The residual fraction of the biomass, consisting of ash, alkali metals and lignin. Values obtained from proximate analysis, ch.2.	R.S.Kempegowda 2013
CH4OUT	Calculated methane fraction in biogas output	CH4YIELD=0.543	Theoretical Yield value obtained from literature.	M.C. Bjune 2009
CO2OUT	Calculated carbon dioxide fraction in biogas output	CO2YIELD=0.502	Theoretical Yield value obtained from literature.	M.C. Bjune 2009
NH3OUT	Calculated ammonia fraction in biogas output	NH3YIELD=0.0275	Theoretical Yield value obtained from literature.	M.C. Bjune 2009
H2SOUT	Calculated hydrogen sulphide in biogas output	H2SYIELD=0.0275	Theoretical Yield value obtained from literature.	M.C. Bjune 2009
RESID	Calculated residue fraction of incoming biomass	VS=0.66	The amount of volatile matter contained in biomass, based on proximate analysis (VM+moisture), ch.2.	R.S.Kempegowda 2013

Table II-9: Variable names and descriptions, Biogas Calculator.

Variable Name	Variable Type	Flow Name	Calculator
BIOMAS	Import	GS07BMAS	
CH4OUT	Export	GS08BMAS	CH4OUT=BIOMAS*VS*CH4YIELD
CO2OUT	Export	GS08BMAS	CO2OUT=BIOMAS*VS*CO2YIELD
NH3OUT	Export	GS08BMAS	NH3OUT=BIOMAS*VS*NH3YIELD
H2SOUT	Export	GS07BMAS	H2SOUT=BIOMAS*VS*H2SYIELD
RESID	Export	GS09RESD	RESID=BIOMAS*RES

Table II-10: Biogas Calculations.

III. Detailed Flow Information

Mass Flows

Area A100 SCENARIO 1	Input		Output		
Flow	PL00BMAS	PL81STM	PL06BMAS	PL84STM	PL92WAT
T (°C)	25	130	90	120	120
P (bar)	1.01	2.03	1.01	1.87	1.87
Mass flow (ton/day)	873.34	1310.00	727.78	1310.00	145.56
Area A100 SCENARIO 2	Input		Output		
Flow	PL00BMAS	PL81STM	PL06BMAS	PL84STM	PL92WAT
T (°C)	25	130	90	120	120
P (bar)	1.01	2.03	1.01	1.87	1.87
Mass flow (ton/day)	873.34	1310.00	727.78	1310.00	145.56

Table III-1: Detailed Mass Flow Information, Aera A100 Biomass Pretreatment

Area A200 SCENARIO 1	Input		Output		
Flow	PL06BMAS	-	PL21BGAS	PL22RESD	PL22RESD
T (°C)	90	-	30	30	-
P (bar)	1.01	-	1.01	1.01	-
Mass flow (ton/day)	727.78	-	493.54	279.10	234.24
Area A200 SCENARIO 2	Input			Output	
Flow	PL06BMAS	PL90OXYG	PL90STM	PL21SYNG	PL22CHAR
T (°C)	90	149	200	861	861
P (bar)	1.01	26	28	28	28
Mass flow (ton/day)	727.78	0.00	300.00	1027.97	0.19

Table III-2: Detailed Mass Flow Information, Area A200 Biomass-to-gas conversion

Area A300 SCENARIO 1	Input		Output		
Flow	PL21BGAS	PL22STM	PL32SYNG	PL33IMPU	-
T (°C)	30	130	225	-	-
P (bar)	1.01	2.03	2.80	-	-
Mass flow (ton/day)	493.54	332.64	826.22	0.00	-
Area A300 SCENARIO 2	Input		Output		
Flow	PL21SYNG	-	PL32SYNG	PL33IMPU	-
T (°C)	861	-	200	200	-
P (bar)	28	-	28	28	-
Mass flow (ton/day)	1027.97	-	922.69	105.28	-

Table III-3: Detailed Mass Flow Information, Area A300 Gas Conditioning Step 1

Area A400 SCENARIO 1	Input		Output		
Flow	PL32SYNG	PL85STM	PL41SYNG	PL42AGAS	-
T (°C)	225	200	1846	1846	-
P (bar)	2.80	10	20	20	-
Mass flow (ton/day)	826.22	342.42	644.39	524.26	-
Area A400 SCENARIO 2	Input		Output		
Flow	PL32SYNG	PL85STM	PL41SYNG	PL42AGAS	-
T (°C)	200	200	76	76	-
P (bar)	28	10	20	20	-
Mass flow (ton/day)	922.69	47.33	296.10	673.92	-

Table III-4: Detailed Mass Flow Information, Area A400 Gas conditioning Step 2

Area A300 SCENARIO 1	Input		Output		
Flow	PL41SYNG	-	PL53FTRO	PL52FGAS	PL93WAT
T (°C)	1846	-	35	35	-
P (bar)	20	-	22.9	23.6	-
Mass flow (ton/day)	644.39	-	137.67	323.30	183.42
Area A300 SCENARIO 2	Input		Output		
Flow	PL41SYNG	-	PL53FTRO	PL52FGAS	PL93WAT
T (°C)	76	-	35	35	-
P (bar)	20	-	22.9	23.6	-
Mass flow (ton/day)	296.10	-	53.12	169.67	73.31

Table III-5: Detailed Mass Flow Information, Area A500 Fischer-Tropsch Synthesis

Energy Flows

Area A100 SCENARIO 1	Input		Output		
Flow	PL00BMAS	PL81STM	PL06BMAS	PL84STM	PL92WAT
T (°C)	25	130	90	120	120
P (bar)	1.01	2.03	1.01	1.87	1.87
Energy flow (MW)	150	1064	134	1064	16
Area A100 SCENARIO 2	Input		Output		
Flow	PL00BMAS	PL81STM	PL06BMAS	PL84STM	PL92WAT
T (°C)	25	130	90	120	120
P (bar)	1.01	2.03	1.01	1.87	1.87
Energy flow (MW)	150	1064	134	1064	16

III-6: Detailed Energy Flow Information, Area A100 Biomass Pretreatment

Area A200 SCENARIO 1	Input	Output			
Flow	PL06BMAS	PL21BGAS	PL22RESD	-	-
T (°C)	90	30	30	-	-
P (bar)	1.01	1.01	1.01	-	-
Energy flow (MW)	134	146	47	-	-
Area A200 SCENARIO 2	Input			Output	
Flow	PL06BMAS	PL90OXYG	PL90STM	PL21SYNG	PL22CHAR
T (°C)	90	149	200	861	-
P (bar)	1.01	26	28	28	-
Energy flow (MW)	134	0	244	146	0.1

Table III-7: Detailed Energy Flow Information, Area A200 Biomass-to-gas Conversion

Area A300 SCENARIO 1	Input		Output		
Flow	PL21BGAS	PL22STM	PL32SYNG	PL33IMPU	-
T (°C)	30	130	225	-	-
P (bar)	1.01	2.03	2.80	-	-
Energy flow (MW)	146	270	216	-	-
Area A300 SCENARIO 2	Input		Output		
Flow	PL21SYNG	-	PL32SYNG	PL33IMPU	-
T (°C)	861	-	200	200	-
P (bar)	28	-	28	28	-
Energy flow (MW)	146	-	105	40	-

Table III-8: Detailed Energy Flow Information, Area A300 Gas Conditioning Step 1

Area A400 SCENARIO 1	Input		Output		
Flow	PL32SYNG	PL85STM	PL41SYNG	PL42AGAS	-
T (°C)	225	200	1846	1846	-
P (bar)	2.80	10	20	20	-
Energy flow (MW)	216	278	208	5	-
Area A400 SCENARIO 2	Input		Output		
Flow	PL32SYNG	PL85STM	PL41SYNG	PL42AGAS	-
T (°C)	200	200	76	76	-
P (bar)	28	10	20	20	-
Energy flow (MW)	105	38	104	0.23	-

Table III-9: Detailed Energy Flow Information, Area A400 Gas Conditioning Step 2

Area A500 SCENARIO 1	Input		Output		
Flow	PL41SYNG	-	PL53FTRO	PL52FGAS	-
T (°C)	1846	-	35	35	-
P (bar)	20	-	22.9	23.6	-
Energy flow (MW)	208	-	76	-	-
Area A500 SCENARIO 2	Input		Output		
Flow	PL41SYNG	-	PL53FTRO	PL52FGAS	-
T (°C)	76	-	35	35	-
P (bar)	20	-	22.9	23.6	-
Energy flow (MW)	104	-	41	-	-

Table III-10: Detailed Energy Flow Information, Area A500 Fischer-Tropsch Synthesis

IV. Feed to Fuel, Feed to loss Calculations

Mass Flow

In the following sections the mass balance evaluations for the two plants are given in detail. The data is evaluated by identifying the percentage of mass flow input that is converted to each of the output flows for each of the processes 1 to 5. The percentages are denoted by

$$M_{ijn}, \qquad \textbf{(IV-1)}$$

where the subscript "i" represent each of the plant processes 1 to 5 where 1 is biomass pretreatment, 2 is biomass-to-gas conversion process, 3 is gas conditioning step one, 4 is gas conditioning step two and 5 is the gas-to-liquid conversion process. The subscript "j" represents the plant, 1 is the biochemical plant and 2 is the thermochemical plant. Subscript "n" represents the output flow that is evaluated. The calculated data are presented in Table IV-1 below. The following sections contain the equations used to obtain the result.

Process	M_{ijn}	Feed To Fuel [%] Scenario1	Feed To Fuel [%] Scenario 2	Feed To Loss [%] Scenario1	Feed To Loss [%] Scenario 2	Equation
A100 Biomass Pretreatm.	M_{11BMAS}	83.33				IV-2
	M_{12BMAS}		83.33			IV-2
	M_{11WAT}			16.67		IV-3
	M_{12WAT}				16.67	IV-3
A200: Biomass to Gas	M_{21BGAS}	67.81				IV-6
	M_{22PGAS}		100.00			IV-9
	M_{21RESD}			32.19		IV-7
	M_{22CHAR}				0.01	IV-10
A300: Gas Cond. Step 1	M_{31BGAS}	100.00				IV-11
	M_{32PGAS}		89.76			IV-13
	M_{31IMPU}			0.00		IV-12
	M_{32IMPU}				10.24	IV-14
A400: Cond. Area Gas Steap 2	M_{41SYNG}	55.14				IV-15
	M_{42SYNG}		30.53			IV-17
	M_{41IMPU}			44.86		IV-16
	M_{42IMPU}				69.47	IV-18
Area A500: Fischer-Tropsch Synthesis	M_{51FTRO}	21.36				IV-19
	M_{52FTRO}		17.94			IV-22
	M_{51FGAS}			50.17		IV-20
	M_{51WAT}			28.46		IV-21
	M_{52FGAS}				57.30	IV-23
	M_{52WAT}				24.76	IV-24

Table IV-1: Feed-to-Fuel, Feed-to-Loss for Mass Flows

Area A100: Biomass Pretreatment

The mass flow data in Table III-1 show that 83 per cent of the raw biomass input is upgraded to dry biomass output as calculated by equation (IV-2):

$$M_{11BMAS} = M_{12BMAS} = \frac{Biomass\ Output}{Biomass\ Input} = \frac{PL06BMAS}{PL00BMAS} = \frac{727.78\frac{ton}{day}}{873.34\frac{ton}{day}} * 100 = 83.33\%. \quad \textbf{(IV-2)}$$

To maintain mass balance, 16.67% of the raw biomass input must be lost to the surroundings. It is suggested that the removal consist of moisture and this can be verified by analyzing the water vapor output flow:

$$M_{11WAT} = M_{12WAT} = \frac{Extracted\ Water\ Output}{Biomass\ Input} = \frac{PL92WAT}{PL00BMAS} = \frac{145.56\frac{ton}{day}}{873.34\frac{ton}{day}} * 100 = 16.67\%. \quad \textbf{(IV-3)}$$

From equation (IV-3) it is concluded that all mass extracted from the biomass is leaving the pretreatment process as water vapor. Thus, the steam input and output mass flows must be unaffected as verified by equation (IV-4):

$$M_{11STM} = M_{12STM} = \frac{Steam\ Output}{Steam\ Input} = \frac{PL84STM}{PL81STM} = \frac{1310\frac{ton}{day}}{1310\frac{ton}{day}} * 100 = 100\%. \quad \textbf{(IV-4)}$$

Area A200: Biomass-to-gas Conversion

Note from Table III-2 that the mass flow does not balance for the biochemical plant because the total mass output is larger than the mass flow input. The percentage difference is calculated by equation (IV-4).

$$M_{21TOT} = \frac{Total\ Output\ flow}{Total\ Input\ flow} = \frac{PL21BGAS + PL22RESD}{PL06BMAS} = \frac{(493.54 + 279.10)\frac{ton}{day}}{727.78\frac{ton}{day}} * 100 = 106.16\%. \quad \textbf{(IV-5)}$$

Equation (IV-4) indicate that the output mass flows is 6.16% larger than input mass flows. This is an error that must be accounted for in the analysis of both mass and energy flows. The error can be a result of a calculation error in the BIOGAS calculator (To adjust for the error, the digester residue flow is adjusted down to 234.24 ton/day as indicated by the red shading in Table III-2. The biogas

output is assumed to be correct. Put this way, the error does not affect the processes downstream of the anaerobic digester, and there is no need to account for the error in downstream processes.

With the corrected value for digester residue, the biomass-to-gas conversion can be expressed in per cent by equation (IV-6):

$$M_{21BGAS=}\frac{Biogas\ Output}{Biomass\ Input}=\frac{PL21BGAS}{PL06BMAS}=\frac{493.54\frac{ton}{day}}{727.78\frac{ton}{day}}*100=67.81\%. \qquad \textbf{(IV-6)}$$

Equation (IV-6) indicate that 67.81% of the biomass is converted to biogas. The rest leaves the process as a digester residue as verified by equation (IV-7):

$$M_{21RESD=}\frac{Digester\ Residue\ Output}{Biomass\ Input}=\frac{PL22RESD}{PL06BMAS}=\frac{234.24\frac{ton}{day}}{727.78\frac{ton}{day}}*100 \qquad \textbf{(IV-7)}$$
$$=32.19\%.$$

Equation (IV-7) verify that 32.19% of the biomass leaves the anaerobic digester as a digester residue. To check for errors in the thermochemical plant, the mass balance is calculated by equation (IV-8).

$$M_{22}=\frac{Total\ Mass\ Output}{Total\ Mass\ Input}=\frac{(PL21SYNG+PL22CHAR)}{(PL06BMAS+PL90OXYG+PL90STM)}$$
$$=\frac{(1027.97+0.19)\frac{ton}{day}}{(727.78+0.00+300.00)\frac{ton}{day}}*100=100.04\% \qquad \textbf{(IV-8)}$$

Equation (IV-8) verifies that the output mass flows are 0.04% larger than the mass flow input. This is a small error and it does not affect the results significantly. Therefore it is neglected in this analysis.

The product gas output as a percentage of total mass input is calculated in equation (IV-9):

$$M_{22PGAS} = \frac{Product\ Gas\ Output}{Biomass + Oxidation\ Agent\ Input} = \frac{PL21SYNG}{PL06BMAS + PLOXYG + PL90STM} = \frac{1027.97\ \frac{ton}{day}}{(727.78 + 0.00 + 300.00)\frac{ton}{day}} * 100 = 100.00\%. \quad \textbf{(IV-9)}$$

Equation (IV-9) verifies that 100.00% of the mass input is converted to product gas output. The percentage of char residue is given by equation (IV-10):

$$M_{22CHAR} = \frac{Char\ Output}{Biomass + Oxidation\ Agent\ Input} = \frac{PL22CHAR}{PL06BMAS + PLOXYG + PL90STM} = \frac{0.19\ \frac{ton}{day}}{(727.78 + 0.00 + 300.00)\frac{ton}{day}} * 100 = 0.01\%. \quad \textbf{(IV-10)}$$

Equations (IV-9) and (IV-10) show that the conversion of gasification process inputs to product gas is 100%, and that the gasification residue, of which consist of char is almost neglected. However the char flow is not zero, and is thus included in the ESankey-diagram in figure 6-1, chapter 6

Area A300: Gas Conditioning Step 1

The mass flow data for the first gas conditioning step is presented in Table III-3. For the biochemical plant, the product gas output flow equals 100% of total raw biogas and steam input as calculated by equation
(IV-11):

$$M_{31BGAS} = \frac{Syngas\ Output}{(Raw\ Biogas\ Input + Steam\ Input)} = \frac{PL32SYNG}{(PL21BGAS + PL22STM)} = \frac{826.22\frac{ton}{day}}{(493.54 + 332.64)\frac{ton}{day}} * 100 = 100\%. \quad \textbf{(IV-11)}$$

Equation

(IV-11) verifies that all mass input to the methane reforming process is conserved in the output syngas, and no mass is lost in the process, expressed by (IV-12):

$$M_{31IMPU} = 0 \qquad \textbf{(IV-12)}$$

For the thermochemical plant, the product gas output measured as a percentage of the mass input is given by equation (IV-13):

$$M_{32PGAS} = \frac{Product\ Gas\ Output}{Raw\ Product\ Gas\ Input} = \frac{PL32SYNG}{PL21SYNG} = \frac{922.69\frac{ton}{day}}{1027.97\frac{ton}{day}} * 100 = 89.76\%. \qquad \textbf{(IV-13)}$$

Equation (IV-13) verifies that 87.76% of the mass input to the filter is conserved to product gas. The gas impurities output mass flow as a percentage of total input is calculated by equation (IV-14):

$$M_{32IMPU} = \frac{Gas\ Impurities\ Output}{Raw\ Product\ Gas\ Input} = \frac{PL33IMPU}{PL21SYNG} = \frac{105.28\frac{ton}{day}}{1027.97\frac{ton}{day}} * 100 = 10.24\%. \qquad \textbf{(IV-14)}$$

Equation (IV-14) verifies that the remaining 10.24% of the mass flow input to the gas cleaning filter is removed from the gas as an impurity residue.

Area A400: Gas Conditioning Step 2

The mass flow data are presented in Table III-4. The percentage of mass flow conversion to syngas and gas impurities for the biochemical process are calculated by equations (IV-15) and (IV-16) below.

$$M_{41SYNG} = \frac{Syngas\ Output}{(Raw\ Syngas\ Input + Steam\ Input)} = \frac{PL41SYNG}{(PL32SYNG + PL85STM)} = \frac{644.39\frac{ton}{day}}{(826.22 + 342.42)\frac{ton}{day}} * 100 = 55.14\%. \qquad \textbf{(IV-15)}$$

Equation (IV-15) verify that 55.14% of the mass input to the gas conditioning process is conserved in the syngas output. The percentage of gas impurities is calculated by equation (IV-16):

$$M_{41IMPU} = \frac{Gas\ Impurities\ Output}{(Raw\ Syngas\ Input + Steam\ Input)}$$
$$= \frac{PL42AGAS}{(PL32SYNG + PL85STM)} = \frac{524.26\frac{ton}{day}}{(826.22 + 342.42)\frac{ton}{day}} * 100 \quad \textbf{(IV-16)}$$
$$= 44.86\%.$$

Equation (IV-16) verify that 44.86% of the mass input to the gas conditioning process is conserved in the gas impurities removed from the syngas. The equations (IV-15) and (IV-16) show that mass balance is conserved and all mass losses are related to gas impurities.

The percentage of mass flow converted to syngas and gas impurities for the thermochemical process are calculated by equations (IV-17) and (IV-18) below.

$$M_{42SYNG} = \frac{Syngas\ Output}{(Raw\ Product\ Gas\ Input + Steam\ Input)}$$
$$= \frac{PL41SYNG}{(PL32SYNG + PL85STM)} = \frac{296.10\frac{ton}{day}}{(922.69 + 47.33)\frac{ton}{day}} * 100 \quad \textbf{(IV-17)}$$
$$= 30.53\%.$$

Equation (IV-17) verify that 30.53% of the mass flow input is conserved in the syngas output. The resulting mass flow is lost to gas impurities removed from the syngas, as calculated by equation (IV-18).

$$M_{42IMPU} = \frac{Gas\ Impurities\ Output}{(Raw\ Product\ Gas\ Input + Steam\ Input)}$$
$$= \frac{PL42AGAS}{(PL32SYNG + PL85STM)} = \frac{673.92\frac{ton}{day}}{(922.69 + 47.33)\frac{ton}{day}} * 100 \quad \textbf{(IV-18)}$$
$$= 69.47\%.$$

Equation (IV-18) verifies that 69.47% of the mass input is conserved in the gas impurities output flow.

Area A500: Fischer-Tropsch Synthesis

The mass flow data is presented in Table III-5. To evaluate the distribution of Fischer-Tropsch diesel, fuel gases and waste water for the biochemical plant three mass balance equations (IV-19) to (IV-21) is developed. The percentage of FT-diesel is calculated by equation (IV-19).

$$M_{51FTRO} = \frac{Fischer-Tropsch\ Diesel\ Output}{Syngas\ Input} = \frac{PL53FTRO}{PL41SYNG} = \frac{137.67\frac{ton}{day}}{644.39\frac{ton}{day}} * 100 = 21.36\%. \quad \textbf{(IV-19)}$$

Equation (IV-19) verifies that 21.36% of the syngas input to the Fischer-Tropsch synthesis is converted to a liquid biofuel; the Fischer-Tropsch diesel. Thus, only 21.36% of the input mass flow to the Fischer-Tropsch synthesis is turned into a useful biofuel. The percentage of fuel gas is calculated by equation (IV-20).

$$M_{51FGAS} = \frac{Fuel\ Gas\ Output}{Syngas\ Input} = \frac{PL52FGAS}{PL41SYNG} = \frac{323.30\frac{ton}{day}}{644.39\frac{ton}{day}} * 100 = 50.17\%. \quad \textbf{(IV-20)}$$

Equation (IV-20) verifies that 50.17% of the syngas input to the Fischer-Tropsch synthesis is converted to fuel gases. The percentage of waste water is calculated by equation (IV-21).

$$M_{51WAT} = \frac{Waste\ Water\ Output}{Syngas\ Input} = \frac{PL93WAT}{PL41SYNG} = \frac{183.42\frac{ton}{day}}{644.39\frac{ton}{day}} * 100 = 28.46\%. \quad \textbf{(IV-21)}$$

Equation (IV-21) verifies that 28.46% of the syngas input to the Fischer-Tropsch synthesis is converted into waste water. To evaluate the Fischer-Tropsch diesel, fuel gases and waste water for the thermochemical plant three mass balance equations (IV-22) to (IV-24) is developed. The percentage of FT-diesel is calculated in equation (IV-22).

$$M_{52FTRO} = \frac{Fischer-Tropsch\ Diesel\ Output}{Syngas\ Input} = \frac{PL53FTRO}{PL41SYNG} = \frac{53.12\frac{ton}{day}}{296.10\frac{ton}{day}} * 100 = 17.94\%. \quad \textbf{(IV-22)}$$

Equation (IV-22) verifies that 17.94% of the syngas input to the Fischer-Tropsch synthesis is

converted into a liquid biofuel; the Fischer-Tropsch diesel. The percentage of fuel gas is calculated in equation (IV-23).

$$M_{52FGAS} = \frac{Fuel\ Gas\ Output}{Syngas\ Input} = \frac{PL52FGAS}{PL41SYNG} = \frac{169.67\,\frac{ton}{day}}{296.10\,\frac{ton}{day}} * 100 = 57.30\%. \quad \textbf{(IV-23)}$$

Equation (IV-23) verifies that 57.30% of the syngas input to the Fischer-Tropsch synthesis is converted to fuel gases. The percentage of waste water is calculated in equation (IV-24).

$$M_{52WAT} = \frac{Waste\ Water\ Output}{Syngas\ Input} = \frac{PL93WAT}{PL41SYNG} = \frac{73.31\,\frac{ton}{day}}{296.10\,\frac{ton}{day}} * 100 \quad \textbf{(IV-24)}$$
$$= 24.76\%.$$

Equation (IV-24) verifies that 24.76% of the syngas input to the Fischer-Tropsch synthesis is converted to waste waters.

Energy Flow

To this point, both mass flows and relevant heating values have been collected from simulations and calculations. In this chapter the results obtained are combined to find the energy flows related to the two scenarios. Energy flow number i is determined by applying one of the following equations (IV-25) to (IV-26):

$$E_i = m_i HV_{i,} \qquad \textbf{(IV-25)}$$

where E_i represents energy flow number i measured in MW, m_i represent mass flow number i measured in (kg/s) and HV_i represents the lower heating value of mass flow i measured in MJ/kg. The steam flows are not calculated by heating value. Instead, a steam-to-energy coefficient obtained from K. Panther et.al is being used (K. Panther, 2006). The energy flow for steam is thus calculated by equation (IV-26):

$$E_{i,steam} = m_i e_{i,} \qquad \textbf{(IV-26)}$$

where $E_{i,steam}$ represent the energy content of steam mass flow i, measured in MW, m_i represent mass flow i measured in kg/s and e_i represent the steam-to-energy coefficient measured in MJ/kg. The calculations are performed sequentially for each of the five plant processes. In Table IV-2, each row is devoted to the energy content calculation of one flow. The table contains all information necessary to perform the calculations given in equations (IV-25) and (IV-26) presented above. Column one lists the process area the calculation applies to, which is area A100. The equation number i=1-5 lists the calculations performed on each flow i related to area A100. The scenario is given by j=1,2 where j=1 refers to scenario 1 and j=2 refers to scenario 2. Since the energy calculations are equal for the special case of area A100 j=12 in Table IV-2. Column two lists the respective flow names for each flow in area A100. Column three and four lists the mass flows in ton/day and kg/s respectively. The mass flows in column three is obtained from results from mass flow calculations. To calculate the heating values the mass flows must be expressed in kg/s as derived by the following equation (IV-27):

$$m_i \left[\frac{kg}{s}\right] = M_i \left[\frac{ton}{day}\right] \frac{1000kg}{ton} \frac{day}{24h} \frac{h}{3600s}, \qquad \textbf{(IV-27)}$$

Where m_i represents mass flow number i in kg/s. M_i represent mass flow i in ton/day. Column five lists the mass flow heating values for flow i on a lover heating value basis, measured in MJ/kg. The heating values are obtained from chapter 6.2. Column six lists the theoretical energy-to-steam ratio

e_i for flow I measured in MJ/kg. Recall from the introduction to this sub-chapter that the energy-to-steam ratio is obtained from literature. Column seven lists the energy flow calculation for energy flow i.

Area-ij	Flow	Mass flow m_i		Heating value	energy-to-steam ratio: e_i	Calculation	Energy Flow E_i
		[ton/day]	[kg/s]	HV_i [MJ/kg]	[MJ/kg]		[MW]
A100-112	PL00BMAS	873.34	10.11	14.83 (ref)	-	$E_1=m_1*HV_1$	150
A100-212	PL81STM	1310.00	15.16	-	70.2 (K.Panther, 2006)	$E_2=m_2*e_2$	1064.38
A100-312	PL06BMAS	727.78	8.42	15.88		$HV_3=E_3/m_3$	133.76(simulation)
A100-412	PL84STM	1310.00	15.16	-	70.2(K.Panther, 2006)	$E_4=E_2$	1064.38
A100-512	PL92WAT	145.56	1.68	-	-	$E_5=(E_1+E_2)-(E_3+E_4)$	16.24

Table IV-2: Energy Flow Calculations based on Mass Flow and Heating Values, area A100 Biomass Pretreatment.

For energy flow E_1 the value is obtained by taking the product of the respective heating value and mass flow in kg/s. For the steam flows in row 2 and 4, energy flow values are obtained by taking the product of the energy-to-steam ratio and the mass flow in kg/s. Energy flow E_3 is obtained from simulations, and the heating value is calculated by dividing the energy flow by the mass flow in kg/s. The last energy flow E_5, row 5 is obtained by the energy conservation principle stating that no energy can be formed or disappear in the process, meaning that total energy input must equal total energy output. Column eight lists the resulting energy flow in MW.

Area-ij	Flow	Mass flow m_i		Heating value	energy-to-steam ratio: e_i	Calculation	Energy Flow E_i
		[ton/day]	[kg/s]	HV_i [MJ/kg]	[MJ/kg]		[MW]
A200-61	PL06BMAS	727.78	8.42	15.88	-	$E_6=M_6*HV_6$	133.76
A200-71	PL21BGAS	493.54	5.71	25.6	-	$E_7=M_7*HV_7$	146.00
A200-81	PL22RESD	279.10	3.23	14.56	-	$E_8=M_8*HV_8$	47.03
A200-92	PL06BMAS	727.78	8.42	15.88	-	$HV_9=E_9/M_9$	133.76(simulation)
A200-102	PL90OXYG	0.00	0.00	-	-	-	0.00
A200-112	PL90STM	300.00	3.47	-	70.2(K.Panther, 2006)	$E_{11}=M_{11}*e_{11}$	243.75
A200-122	PL21SYNG	1027.97	11.90	12.20	-	$E12=M_{12}*HV_{12}$	145.15
A200-132	PL22CHAR	0.19	0.02	-	-	$E_{13}=(E_9+E_{10}+E_{11})-E_{12}$	0.10

Table IV-3: Energy Flow Calculations based on Mass Flow and Heating Values, area A200 Anaerobic Digestion/Gasification.

The rows in Table IV-3 represent the energy flows calculations for the biomass-to-gas conversion processes for both scenarios. Rows 2 to 4 represents scenario 1 and rows 5 to 9 represents scenario 2. Energy flows E_6-E_8 and E_{12} are obtained by taking the product of the respective heating values in MJ/kg and mass flows in kg/s. Energy flow E_9 is obtained directly from simulation data, and the respective heating value HV_9 is obtained by dividing the energy flow by the mass flow in kg/s. Energy flow E_{11} is obtained by taking the product of the mass flow in kg/s and the energy-to-steam ratio in MJ/kg. Energy flow E_{13} is obtained from conversation of energy.

Area-ij	Flow	Mass flow m_i		Heating value	energy-to-steam ratio: e_i	Calculation	Energy Flow E_i
		[ton/day]	[kg/s]	HV_i [MJ/kg]	[MJ/kg]		[MW]
A300-141	PL21BGAS	493.54	5.71	25.6	-	$E_{14}=M_{14}*HV_{14}$	146.00
A300-151	PL32SYNG	826.22	9.56	22.58	-	$E_{15}=M_{15}*HV_{15}$	215.93
A300-161	PL33IMPU	0.00	0.00	-	-	$E_{16}=M_{16}*HV_{16}$	0.00
A300-171	PL22STM	332.64	3.85	-	70.2(K.Panther, 2006)	$E_{17}=M_{17}*e_{17}$	270.27
A300-182	PL21SYNG	1027.97	11.90	12.20	-	$E_{18}=M_{18}*HV_{18}$	145.00
A300-192	PL32SYNG	922.69	10.68	9.86	-	$E_{19}=M_{19}*HV_{19}$	105.29
A300-202	PL33IMPU	105.28	1.22	32.74	-	$E_{20}=M_{20}*HV_{20}$	39.90

Table IV-4: Energy Flow Calculations based on Mass Flow and Heating Values, area A300 Methane Reforming/Gas Filtering.

Row 2 to 4 contain energy flow calculations for all flows relevant to the methane reforming of scenario 1 and row 5 to 8 contain the respective calculations for the gas filtration of scenario 2. Energy flows E_{14}-E_{16} and E_{18}-E_{20} are obtained by taking the product of the respective heating values in MJ/kg and mass flows in kg/s. Energy flow E_{17} is obtained by taking the product of the mass flow in kg/s and the energy-to-steam ratio in MJ/kg.

Area-ij	Flow	Mass flow m_i		Heating value	energy-to-steam ratio: e_i	Calculation	Energy Flow E_i
		[ton/day]	[kg/s]	HV_i [MJ/kg]	[MJ/kg]		[MW]
A400-211	PL32SYNG	826.22	9.56	22.58	-	$E_{21}=M_{21}*HV_{21}$	215.93
A400-221	PL85STM	342.42	3.96	-	70.2(K.Panther, 2006)	$E_{22}=M_{22}*e_{22}$	278.22
A400-231	PL41SYNG	644.39	7.46	27.85	-	$E_{23}=M_{23}*HV_{23}$	207.71
A400-241	PL42AGAS	524.26	6.07	0.85	-	$E_{24}=M_{24}*HV_{24}$	5.16
A400-252	PL32SYNG	922.69	10.68	9.86	-	$E_{25}=M_{25}*HV_{25}$	105.30
A400-262	PL85STM	47.33	0.55	-	70.2(K.Panther, 2006)	$E_{26}=M_{26}*e_{26}$	38.46
A400-272	PL41SYNG	296.10	3.43	30.31	-	$E_{27}=M_{27}*HV_{27}$	103.88
A400-282	PL42AGAS	673.92	7.80	0.03	-	$E_{28}=M_{28}*HV_{28}$	0.23

Table IV-5: Energy Flow Calculations based on Mass Flow and Heating Values, area A400 Water-gas-shift and Membrane Separation.

Rows 2 to 5 represent the energy flow calculations for scenario 1 whereas rows 6 to 9 represent the energy flows for scenario 2. Table IV-5 follows the same structure as Table IV-2. Energy flows E_{21}, E_{23}-E_{25} and E_{27}-E_{28} are obtained by taking the product of the respective heating values in MJ/kg and mass flows in kg/s. Energy flow E_{22} and E_{26} is obtained by taking the product of the mass flow in kg/s and the energy-to-steam ratio in MJ/kg.

Area-ij	Flow	Mass flow m_i		Heating value	energy-to-steam ratio: e_i	Calculation	Energy Flow E_i
		[ton/day]	[kg/s]	HV_i [MJ/kg]	[MJ/kg]		[MW]
A500-291	PL41SYNG	644.39	7.46	27.85	-	$E_{29}=M_{29}*HV_{29}$	207.71
A500-301	PL53FTRO	137.68	1.59	47.89	-	$HV_{30}=E_{30}/M_{30}$	76.31 (simulation)
A500-311	PL52FGAS	323.30	3.74	-	-	$E_{31}=M_{31}*HV_{31}$	-
A500-322	PL41SYNG	296.10	3.43	30.31	-	$E_{32}=M_{32}*HV_{32}$	103.88
A500-332	PL53FTRO	51.12	0.61	66.34	-	$HV_{33}=E_{33}/M_{33}$	40.79 (simulation)
A500-342	PL52FGAS	169.671	1.96	-	-	$E_{34}=M_{34}*HV_{34}$	-

Table IV-6: Energy Flow Calculations based on Mass Flow and Heating Values, area A500 Fischer-Tropsch Synthesis.

Rows 2 to 4 represent energy flow calculations for scenario 1 whereas rows 5 to 7 represent scenario 2. Energy flows E_{29},$E_{31,}$ E_{32} and E_{34} are obtained by taking the product of the respective heating values in MJ/kg and mass flows in kg/s. Energy flow E_{30} and E_{33} are obtained directly from simulation data, and the respective heating values are obtained by dividing the energy flow by the mass flow in kg/s.

In the following sections the energy flow calculations for the two scenarios are given in detail. The data is evaluated by calculating the energy utility process by process for both scenarios. The energy utilities are denoted by expression (IV-28):

$$E_{ijn}, \qquad \textbf{(IV-28)}$$

where the subscript "i" represent each of the plant processes 1 to 5 where 1 is biomass pretreatment, 2 is biomass-to-gas conversion process, 3 is gas conditioning step one, 4 is gas conditioning step two and 5 is the gas-to-liquid conversion process. The subscript "j" represents the plant, 1 is the biochemical plant and 2 is the thermochemical plant. Subscript "n" represents the output flow that is evaluated, expressed by flow name.

Process	E_{ijn}	Feed To Fuel [%] Scenario1	Feed To Fuel [%] Scenario 2	Feed To Loss [%] Scenario1	Feed To Loss [%] Scenario 2	Equation
A100 Biomass Pretreatm.	E_{11BMAS}	89.33				IV-29
	E_{12BMAS}		89.33			IV-29
	E_{11WAT}			10.67		IV-30
	E_{12WAT}				10.67	IV-30
A200: Biomass to Gas	E_{21BGAS}	108.96				IV-31
	E_{22PGAS}		38.62			IV-33
	E_{21RESD}			35.07		IV-32
	E_{22CHAR}				0.03	IV-34
A300: Gas Cond. Step 1	E_{31BGAS}	51.92				IV-35
	E_{32PGAS}		71.92			IV-37
	E_{31IMPU}			0.00		IV-36
	E_{32IMPU}				0.00	IV-36
Area A400: Gas Cond. Steap 2	E_{41SYNG}	42.11				IV-39
	E_{42SYNG}		72.73			IV-41
	E_{41IMPU}			1.01		IV-40
	E_{42IMPU}				0.16	IV-42
Area A500: Fischer-Tropsch Synthesis	E_{51FUEL}	36.54				IV-43
	E_{52FUEL}		39.42			IV-44
	E_{51EFF}	51				IV-45
	E_{52EFF}		27			IV-46

Table IV-7: Feed-to-Fuel and Feed-to-Loss ratios, energy flow.

The energy utility for the biomass pretreatment process is obtained by equation (IV-29):

$$E_{11BMAS} = E_{12BMAS} = \frac{Biomass\ Output}{Biomass\ Input} = \frac{PL06BMAS}{PL00BMAS} = \frac{134\ MW}{150\ MW} * 100 = 89.33\%. \quad \textbf{(IV-29)}$$

Equation (IV-29) verifies that 89.33% of the energy in the raw biomass feedstock is retained in the pretreated biomass. The energy loss is related to the extracted water and is calculated by equation (IV-30):

$$E_{11WAT} = E_{12WAT} = \frac{Water\ Output}{Biomass\ Input} = \frac{PL92WAT}{PL00BMAS} = \frac{16\ MW}{150\ MW} * 100 = 10.67\%. \quad \textbf{(IV-30)}$$

Equation (IV-30) verifies that 10.67% of the energy contained in the biomass is lost with waste water extracted from the biomass by drying in both plants.

The energy utility for scenario 1 is given by equation (IV-31):

$$E_{21BGAS} = \frac{Biogas\ Output}{Biomass\ Input} = \frac{PL21BGAS}{PL06BMAS} = \frac{146\ MW}{134\ MW} * 100 = 108.96\%, \qquad \textbf{(IV-31)}$$

which indicate that the energy content of the biogas output is 8.96% larger than the biomass input. This makes sense in terms of heating values. The biogas heating value equals 25.6 MJ/kg whereas the biomass heating value is 15.88 MJ/kg. The biogas heating value is larger because of its composition and is a topic relevant for the discussion in chapter 7. The energy content in the digester residue is expressed by equation (IV-32):

$$E_{21RESD} = \frac{Residue\ Output}{Biomass\ Input} = \frac{PL22CHAR}{PL06BMAS} = \frac{0.1\ MW}{134\ MW} * 100 = 35.07\%, \qquad \textbf{(IV-32)}$$

which indicate that only 35.07% of the energy input is lost to the residue. The energy utility for scenario 2 is given by equation (IV-33):

$$E_{22PGAS} = \frac{Product\ Gas\ Output}{(Biomass\ Input + Oxidation\ Agent)} = \frac{PL21SYNG}{(PL06BMAS + PL90OXYG + PL90STM)} = \frac{146\ MW}{(134 + 0 + 244)\ MW} * 100 = 38.62\%. \qquad \textbf{(IV-33)}$$

Equation (IV-33) shows that 38.62% of the energy input is conserved in the output product gas. The energy loss related to the char residue in scenario 2 is given by equation (IV-34):

$$E_{22CHAR} = \frac{Char\ Output}{(Biomass\ Input + Oxidation\ Agent)} = \frac{PL22CHAR}{(PL06BMAS + PL90OXYG + PL90STM)} = \frac{0.1\ MW}{(134 + 0 + 244)MW} * 100 = 0.03\%. \qquad \textbf{(IV-34)}$$

Equation (IV-34) verifies that 0.03% of the energy contained in the biomass and oxidation agent input is lost to char residues, which is a small loss reflecting the small loss in terms of mass for the same flow as presented in chapter 6.1.

The energy utility for the methane reforming scenario 1 is given by equation (IV-35):

$$E_{31BGAS} = \frac{Raw\ Syngas\ Output}{(Raw\ Biogas\ Input + Steam\ Input)} = \frac{PL32SYNG}{(PL21BGAS + PL22STM)} = \frac{216\ MW}{(146 + 270)MW} * 100 = 51.92\% \quad \textbf{(IV-35)}$$

Equation (IV-35) verifies that 51.92% of the energy input to the methane reforming is conserved in the syngas output. It follows from equation (IV-12) that:

$$M_{31IMPU} = 0 \rightarrow E_{32IMPU} = 0. \quad \textbf{(IV-36)}$$

Equation (IV-36) verifies that there is no energy loss related to combustible energy for the methane reformation. However, to sustain conservation of energy, the 48.08% of energy that is not conserved in the raw syngas output is assumed to consist of excess heat forming a thermal heat output flow.

The energy utility for the gas filtration in scenario 2 is calculated by equation (IV-37):

$$E_{32PGAS} = \frac{Product\ Gas\ Output}{Raw\ Product\ Gas\ Input} = \frac{PL32SYNG}{PL21SYNG} = \frac{105\ MW}{146\ MW} * 100 = 71.92\%. \quad \textbf{(IV-37)}$$

Equation (IV-37) verifies that the energy content in the fuel output equals 71.92% of the energy in the raw product gas input. The energy loss is related to the ash and char removal as indicated by equation (IV-38):

$$E_{32IMPU} = \frac{Gas\ Impurities\ Output}{Raw\ Product\ Gas\ Input} = \frac{PL33IMPU}{PL21SYNG} = \frac{40\ MW}{146\ MW} * 100 = 27.40\%. \quad \textbf{(IV-38)}$$

Equation (IV-38) verifies that 27.40% of the energy input is lost to ash, char and soot residual.

The energy utlity for scenario 1 is calculated by equation (IV-39):

$$E_{41SYNG} = \frac{Syngas\ Output}{Raw\ Syngas\ Input + Steam\ Input} = \frac{PL41SYNG}{(PL32SYNG + PL85STM)} = \frac{208\ MW}{(216 + 278)MW} * 100 = 42.11\% \quad \textbf{(IV-39)}$$

Equation (IV-39) verifies that 42.11% of the total energy input to the gas conditioning is conserved in the syngas output. The energy loss related to gas impurities extracted from the syngas in scenario 1 is calculated by equation (IV-40):

$$E_{41IMPU} = \frac{Gas\ impurities\ Output}{Raw\ Syngas\ Input + Steam\ Input} = \frac{PL42AGAS}{(PL32SYNG + PL85STM)} = \frac{5\ MW}{(216 + 278)MW} * 100 = 1.01\% \quad \textbf{(IV-40)}$$

Equation (IV-40) verifies that 1.01% of the total energy input to the gas conditioning is conserved in the gas impurities extracted from the syngas. Thus, based on conservation of energy, an energy loss equal to 56.88% is not accounted for in the analysis. The energy loss is assumed to consist of excess heat from the gas conditioning processes, which is an assumption that will be evaluated further in chapter 7.

The energy utility for scenario 2 is calculated by equation (IV-41):

$$E_{42SYNG} = \frac{Syngas\ Output}{Raw\ Product\ Gas\ \ Input + Steam\ Input} = \frac{PL41SYNG}{(PL32SYNG + PL85STM)} = \frac{104\ MW}{(105+38)MW} * 100 = 72.73\% \quad \textbf{(IV-41)}$$

Equation (IV-41) verifies that 72.73% of total energy input to the gas conditioning is conserved in the syngas output. The energy loss related to gas impurities extracted from the syngas in scenario 2 is calculated by equation (IV-42):

$$E_{42IMPU} = \frac{Gas\ impurities\ Output}{Raw\ Product\ Gas\ Input + Steam\ Input} = \frac{PL42AGAS}{(PL32SYNG + PL85STM)} = \frac{0.23\ MW}{(105+38)MW} * 100 = 0.16\% \quad \textbf{(IV-42)}$$

Equation (IV-42) verifies that 0.16% of the total energy input to the gas conditioning is conserved in the gas impurities extracted from the syngas. Thus, based on conservation of energy, an energy loss equal to 27.11% is not accounted for in the analysis. The energy loss is assumed to consist of excess heat from the gas conditioning processes which is an assumption that will be further investigated in chapter 7.

In scenario 1, the energy utility for the Fischer-Tropsch synthesis is calculated by equation (IV-43).

$$E_{51FUEL} = \frac{FT - diesel\ Output}{Syngas\ Input} = \frac{PL53FTRO}{PL41SYNG} = \frac{76\ MW}{208\ MW} * 100 = 36.54\%. \quad \textbf{(IV-43)}$$

Equation (IV-43) verifies that 36.54% of the energy input to the Fischer-Tropsch synthesis is conserved in the Fischer-Tropsch diesel product. In scenario 2, the energy utility for the Fischer-Tropsch synthesis is calculated by equation (IV-44).

$$E_{52FUEL} = \frac{FT - diesel\ Output}{Syngas\ Input} = \frac{PL53FTRO}{PL41SYNG} = \frac{41\ MW}{104\ MW} * 100 = 39.42\%. \quad \textbf{(IV-44)}$$

Equation (IV-44) verifies that 39.42% of the energy input to the Fischer-Tropsch synthesis is conserved in the Fischer-Tropsch diesel product. Compared to scenario 1, scenario 2 performs the most energy efficient process. The fuel efficiency for the total plant in scenario 1 is calculated by

dividing the energy content of the Fischer-Tropsch diesel with the energy content of the biomass feedstock, expressed by equation (IV-45)

.

$$E_{51EFF} = \frac{FT - diesel\ Output}{Biomass\ Input} = \frac{PL53FTRO}{PL00BMAS} = \frac{76MW}{150MW} = 0.51 \qquad \textbf{(IV-45)}$$

Equation (IV-45) verifies that the fuel efficiency for scenario 1, the biochemical plant is 0.51 which means that 51% of the energy input into the plant by biomass is converted to useful biofuel energy output. The fuel efficiency for the total plant in scenario 2 is calculated by equation (IV-46).

$$E_{52EFF} = \frac{FT - diesel\ Output}{Biomass\ Input} = \frac{PL53FTRO}{PL00BMAS} = \frac{41MW}{150MW} = 0.27 \qquad \textbf{(IV-46)}$$

Equation (IV-45) verifies that the fuel efficiency for scenario 2, the thermochemical plant is 0.27, which means that 27% of the energy input into the plant by biomass is converted to useful biofuel energy output. The fuel efficiency for the biochemical plant is 0.51, which is 53% higher than the efficiency obtained for the thermochemical plant.